

■ Polycyclic Aromatic Hydrocarbons

Facile Synthetic Approach to a Large Variety of Soluble Diarenoperylenes

Gang Zhang,^[a, b] Frank Rominger,^[a] Ute Zschieschang,^[c] Hagen Klauk,^[c] and Michael Mastalerz^{*[a]}

Abstract: Fused, extended π -systems such as larger acenes and heteroacenes are interesting compounds for organic thin-film transistors (TFTs). The larger the number of linearly cata-fused rings, the lower the stability of the acenes. By peri-fusion of additional rings, the stabilities can significantly be increased. Here we present a facile approach to use a diborylated dihydroanthracene as precursor to get diareno-fused perylenes in just two steps in high yields. The compounds show pronounced packing in the crystalline states by π -stacking. Promising candidates have been used to fabricate *p*-channel TFTs by vacuum sublimation showing field-effect mobilities up to $0.12 \text{ cm}^2 \text{V}^{-1} \text{s}^{-1}$.

The larger acenes and heteroacenes are fascinating synthetic targets due to their promising properties as organic semiconductors.^[1] Pure non-substituted acenes as well as heteroacenes with more than six linearly fused aromatic six-membered rings are not stable under normal conditions (air, room temperature) and undergo oxidations with singlet-oxygen or dimerization reactions.^[1g, 2] In contrast, peri-fused extended aromatics, such as pyrene, perylene or coronene derivatives are chemically more stable,^[3] which can be simply explained by the heuristic Clar's rule that more isolated Robinson sextets can be drawn.^[4] Recently, some compounds have been introduced, in which peri-fused systems show a higher stability in comparison to the parent acene and additionally good performances as semiconducting layers for organic field-effect transistors. For instance, bisindeno-annulated pentacenes with 5-membered peri-fused rings have been synthetically achieved by two dif-

ferent routes.^[5] One strategy started from octahydro dibromopentacene, giving the products in three steps.^[5a] Independently, the same backbone has been constructed in a two-step approach from pentacenequinone in good yields.^[5b] For one of the peri-fused compounds a field-effect mobility of $0.06 \text{ cm}^2 \text{V}^{-1} \text{s}^{-1}$ was measured in *p*-channel TFTs.^[5b, 6] Other examples are phenylenetetracene, a 2D-fused π -system based on tetracene, giving hole mobilities of $0.01 \text{ cm}^2 \text{V}^{-1} \text{s}^{-1}$,^[7] or dibenzorubicene with hole mobilities of $1.0 \text{ cm}^2 \text{V}^{-1} \text{s}^{-1}$.^[8] There are also a few acene systems stabilized with six-membered fused rings described as materials for organic TFTs. For instance, Per-epichka et al. described two isomeric dibenzoperylenes, where one is an insulator and the other one shows electron mobilities of $0.04 \text{ cm}^2 \text{V}^{-1} \text{s}^{-1}$ and a hole mobility of $0.002 \text{ cm}^2 \text{V}^{-1} \text{s}^{-1}$.^[9] Miao et al. revisited zethrenes as *p*-channel semiconductors, reporting hole mobilities of $0.01\text{--}0.05 \text{ cm}^2 \text{V}^{-1} \text{s}^{-1}$.^[10] The most striking example of a peri-fused system as a semiconducting material is probably the so-called bistetracene, for which a field-effect mobility of $6.1 \text{ cm}^2 \text{V}^{-1} \text{s}^{-1}$ and on/off ratios as large as 10^7 have been reported.^[11] For the bistetracene, two aromatic sextets can be drawn, giving a hint to its chemical stability that was later also confirmed by more sophisticated DFT calculations.^[12, 13] Closely related to this, one class of smaller peri-condensed systems that contain pentacene (**A**) or heptacene (**B**) backbones within the scaffold are dibenzoperylene **C** and dinaphthoperylene **D** (see Figure 1). In contrast to the pure acenes **A** and **B**, four Robinson sextets can be drawn for **C** and **D**, which corresponds to a higher chemical stability. Since perylene backbones are known to be, as a molecular part of perylenediimides, chemically and thermally very stable and exhibit excellent performance as electron acceptors,^[14] we were interested in soluble derivatives of **C** and **D** as potential electron-donating molecules for hole-transporting organic semiconductors.^[15] Interestingly, unsubstituted **C** was synthesized by Clar already in 1932 by treating 9-bromophenanthrene with AlCl_3 in benzene or by adding bromine and AlCl_3 to a benzene solution of phenanthrene, although in this original paper the structure was unfortunately not correctly assigned.^[16] After recrystallization the yields were about 5%.^[16] The dinaphthoperylene **D** was synthesized in 13% yield by a thermally conducted Elbs reaction from a dibenzoylperylene precursor.^[17]

Here we present a facile two-step route to soluble arene- and heteroarene-fused perylenes and their use as semiconductors in organic TFTs. The synthetic strategy is related to our recent approach to π -extended truxenes^[18] and starts with

[a] Prof. Dr. G. Zhang, Dr. F. Rominger, Prof. Dr. M. Mastalerz
Organisch-Chemisches Institut, Ruprecht-Karls-Universität Heidelberg
Im Neuenheimer Feld 273, 69120 Heidelberg (Germany)
E-mail: michael.mastalerz@oci.uni-heidelberg.de

[b] Prof. Dr. G. Zhang
present address: College of Chemical Engineering,
Nanjing Forestry University, 210037
Nanjing, (P. R. China)

[c] Dr. U. Zschieschang, Dr. H. Klauk
Max Planck Institute for Solid State Research
Heisenbergstr. 1, 70569 Stuttgart (Germany)

Supporting Information containing full experimental details, NMR, UV/Vis and fluorescence spectroscopy data, cyclovoltammograms, single-crystal data including CCDC numbers, and TFT characteristics can be found under: <http://dx.doi.org/10.1002/chem.201603336>.

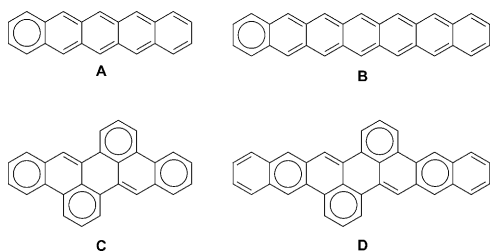
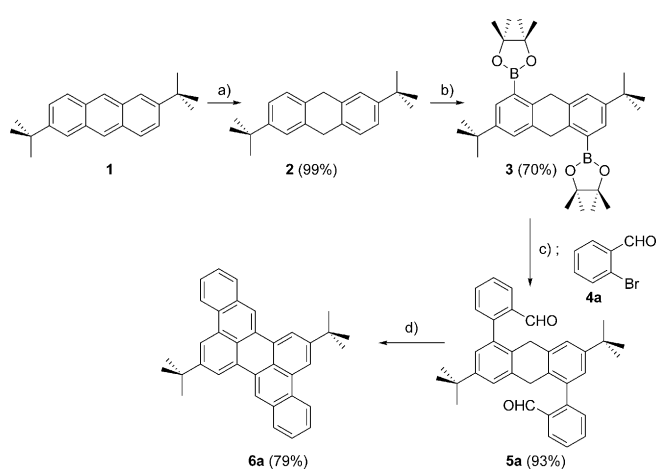


Figure 1. Comparison of pentacene (**A**), heptacene (**B**) and their peri-fused dibenzocoronene analogues **C** and **D** according to Clar's sextet rule.

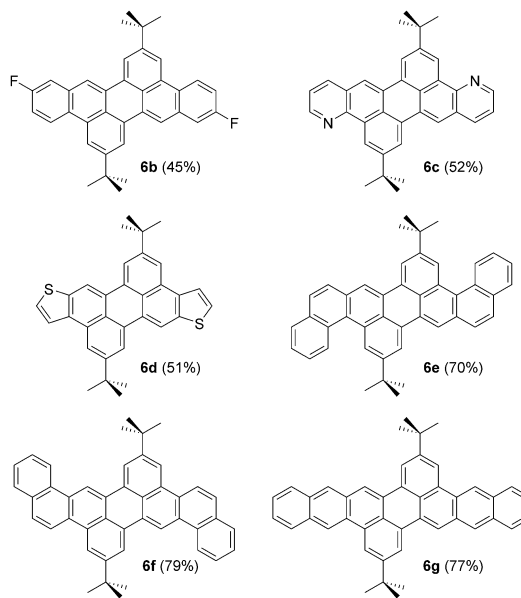
a Birch reduction of 2,7-di-*tert*-butylanthracene **1**^[19] in the 9- and 10-position with sodium in *t*BuOH and THF, giving dihydroanthracene **2** in quantitative yield (Scheme 1). Ir-catalyzed borylation under CH-activation with TMPhen as ligand gave regioselectively diborylated compound **3** in 70% yield.^[20] The structure has been confirmed by single-crystal X-ray diffraction (see Supporting Information). The diborylated compound was subsequently used in a palladium-catalyzed Suzuki–Miyaura cross-coupling reaction with bromobenzaldehyde **4a**, giving **5a** in 93% yield. After treatment with potassium *tert*-butoxide, the dibenzocoronene **6a** was achieved as the two-fold condensation product in 79% yield.



Scheme 1. Synthesis of bis-*tert*-butyl dibenzocoronene **6a**. a) Na, *t*BuOH, r.t., 6 h; b) [Ir(COD)OMe]₂; TMPhen (3,4,7,8-tetramethyl-9,10-phenanthroline), B₂pin₂, THF, 85 °C, 48 h; c) Pd₂dba₃, *t*Bu₃PHBF₄, THF, K₂CO₃ aq., 80 °C, 16 h; d) *KOTBu*, THF, 60 °C, 16 h.

Please note that the overall yield of this four-step approach is >50%, which is significantly higher than that of the original route using phenanthrene dimerisation.^[16] Perylene **6a** is soluble in organic solvents, allowing a full spectroscopic characterization (see discussion below). In a similar fashion, diboronic ester **3** can be reacted in the same two-step sequence with other bromoarenes with an aldehyde function in the *ortho*-position to give, for example, difluoro compound **6b** in high yield (45%). Furthermore, the approach also allows the introduction of heterocyclic aromatic rings, such as in dipyridino perylene **6c** (52%) and dithieno perylene **6d** (51%). Larger

linear as well as angular cata-condensed compounds **6e–6g** were easily accessible in high yields >70% (over two steps) (Scheme 2).



Scheme 2. Cata-condensed diarenoperylenes **6b–6g**. In parentheses the combined yields are given for the two-step reaction starting from diborylated dihydroanthracene **3**.

All compounds were investigated by absorption and emission spectroscopy (Figure 2 and Table 1) as well as by cyclic voltammetry (see Table 1 and the Supporting Information). Frontier molecular orbital levels were calculated by DFT methods (see Table 1 and Supporting Information). The absorption spectra of **6a–6c** are very similar with maximum absorption peaks at $\lambda_{\text{max}}=434$, 433, and 432 nm for the $\pi-\pi^*$ transitions. Although the energy gap between HOMOs and LUMOs of these compounds are very close, energies of all frontier orbitals of **6b** are 0.1 eV lower than for **6a** due to the attached electron-withdrawing fluoro substituents. For the *N*-heterocyclic **6c**, the absolute values are even somewhat lower. In comparison, the maximum absorption of dithieno compound **6d** is bathochromically shifted about 30 nm to $\lambda_{\text{max}}=461$ nm and the frontier orbital energies ($E_{\text{LUMO}}=-2.65$ and $E_{\text{HOMO}}=-5.12$ eV) are slightly higher in comparison to those of **6a**. For **6e** and **6f**, absorption maxima are shifted to $\lambda_{\text{max}}=471$ and $\lambda_{\text{max}}=467$ nm, whereas the maximum absorption of isomer **6g** appears at lower wavelengths at $\lambda_{\text{max}}=445$ nm. For all naphto-perylenes the band gap is decreased and the LUMO energy levels are about 0.1 eV lower and the HOMO levels are about 0.1 eV higher for **6e** and **6f** than for **6a**. All compounds are fluorescent and with the exception of **6d**, **6e** and **6g**, the quantum yields are between $\Phi=63$ and 68%.

High-quality X-ray crystal structures have been obtained for all compounds, allowing a detailed analysis in the solid state to get further insights to bond characters, conjugation and aromaticity (Figure 3, for crystallographic details, see the Sup-

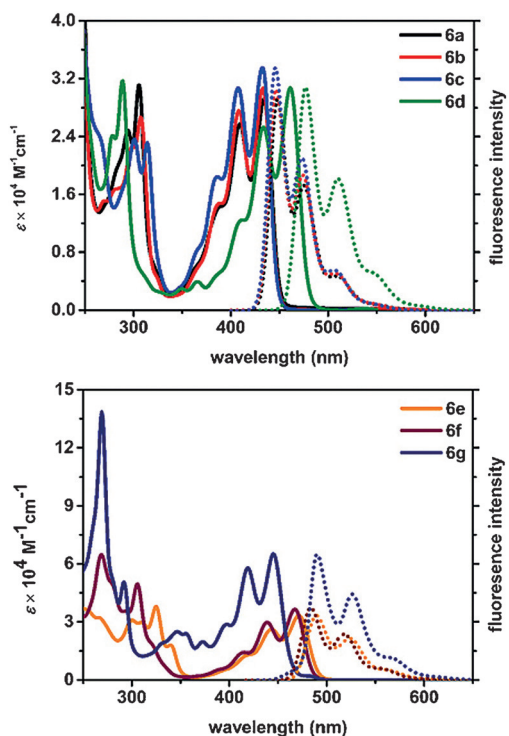


Figure 2. Absorption and emission spectra in chloroform (solid lines: absorption; dotted lines: emission).

porting Information). It is worth mentioning that for the unsubstituted dibenzoperylene **C**, crystal structures were published in 1959 by Lipscomb et al.^[21] Most interestingly, the shortest C–C bond in **6a** is with $d=1.357\text{ \AA}$ located in the perylene backbone (α and κ edges), suggesting that this one has the largest olefin character. This differs from the reported data from Lipscomb et al., who reported a distance of $d=1.41\text{ \AA}$ for the analogous bond in the unsubstituted dibenzoperylene **C**, which is significantly longer.^[21] If this short bond is compared with all other bond lengths, the structure can be best described according to Clar with four aromatic sextets, such as depicted for compound **C** (Figure 1). Similar relative bond lengths are found for the difluoro compound **6b** (see Supporting Information) and the dipyridino compound **6c**. In dithieno compound **6d**, the shortest bond ($d=1.34\text{ \AA}$) is found between positions 2 and 3 of the thiophene ring. The bond lengths of the linearly cata-condensed dinaphthoperylene **6g**

again agrees best with a structure with four aromatic sextets as depicted for the scaffold **D**. Dinaphthoperylene **6e** has in contrast to all other herein-discussed compounds a contorted π -surface, because the angular cata-condensed naphthalene unit generates a fjord region. Compound **6f** is the only one that is not centrosymmetric in the crystal and it is hard to assign aromatic sextets for more than one six-membered ring. For all compounds, the internal C–C-bonds (marked red) are with $d=1.46\text{--}1.48\text{ \AA}$ relatively long, which is consistent with those bond lengths of other perylene compounds and reveal that the electron density in the center of the molecule is minimum.^[22] Pronounced π -stacking can be observed in all cases in the crystalline state. For **6a**, **6b**, **6e** and **6f**, a herringbone-type arrangement of the molecules is observed, whereas **6c**, **6d** and **6g** are packing in a brickwork-type fashion. For all structures, except for **6e** a close contact of parallel arranged π -planes is observed (shortest $d_{\pi-\pi}=3.32\text{ \AA}$ (**6a**), 3.38 \AA (**6b**), 3.24 \AA (**6c**), 3.48 \AA (**6d**), 3.22 \AA (**6f**), 3.31 \AA (**6g**)).

The calculated HOMO levels of **6a** and **6d**–**6g** are between $E_{\text{HOMO}}=-5.10$ and -5.22 eV and are in the range of typical hole-transporting organic semiconductors.^[23] Based on the packing in the crystalline states, **6a**, **6d**, **6f**, and **6g** have been considered as promising candidates for *p*-channel TFTs. To investigate the charge-transport properties of these materials, bottom-gate, top-contact TFTs have been fabricated and characterized in air. The TFTs were fabricated on doped silicon substrates with a gate dielectric composed of 100 nm thick, thermally grown SiO_2 , 8 nm thick atomic-layer-deposited Al_2O_3 , and either an alkyl- or a fluoroalkyl phosphonic acid self-assembled monolayer.^[24] Semiconductor layers with a thickness of 30 nm were deposited by thermal sublimation in vacuum at an elevated substrate temperature to optimize the thin-film morphology of the semiconductor. (For details on TFT fabrication and current–voltage characteristics, see the Supporting Information). TFTs based on **6a** have field-effect mobilities up to $0.012\text{ cm}^2\text{ V}^{-1}\text{ s}^{-1}$. A slightly larger mobility of $0.014\text{ cm}^2\text{ V}^{-1}\text{ s}^{-1}$ was measured for TFTs based on the thieno compound **6d**. The compounds with the larger π -system have been expected to be better semiconductors than **6a** and **6d**. Indeed, TFTs based on **6g** have field-effect mobilities up to $0.08\text{ cm}^2\text{ V}^{-1}\text{ s}^{-1}$, and for the angular cata-condensed compound **6f**, a mobility of $0.12\text{ cm}^2\text{ V}^{-1}\text{ s}^{-1}$ has been measured. The on/off current ratio of these TFTs is around 10^5 . It is worth mentioning that the best-performing compound shows the

Table 1. Summary of photophysical and electrochemical characterization of compounds **6a**–**6g**.

Compd.	λ_{max} ($\lg \epsilon$) [nm] ^[a]	λ_{em} (λ_{ex}) [nm] ^[a]	Φ [%] ^[a]	$E_{\text{g, opt}}$ [eV] ^[b]	$E_{\text{g,CV}}$ [eV] ^[c]	E_{LUMO} [eV] ^[d]	E_{HOMO} [eV] ^[e]	$E_{\text{LUMO,cal}}$ [eV] ^[f]	$E_{\text{HOMO,cal}}$ [eV] ^[f]
6a	434 (4.47)	448 (434)	68 ± 2	2.75	2.68	-2.59	-5.27	-2.15	-5.22
6b	433 (4.48)	447 (433)	67	2.75	2.68	-2.69	-5.37	-2.38	-5.47
6c	432 (4.52)	446 (432)	67 ± 1	2.75	2.64	-2.76	-5.40	-2.30	-5.37
6d	461 (4.49)	477 (461)	24	2.59	2.47	-2.65	-5.12	-2.25	-5.10
6e	471 (4.52)	490 (471)	36 ± 1	2.51	2.47	-2.69	-5.16	-2.31	-5.14
6f	467 (4.56)	484 (467)	63 ± 1	2.55	2.46	-2.68	-5.14	-2.28	-5.15
6g	445 (4.81)	491 (445)	18	2.50	2.54	-2.61	-5.15	-2.25	-5.18

[a] Measured in CHCl_3 at room temperature. [b] Estimated from absorption onset. [c] Calculated from CV measurements. [d] $E_{\text{LUMO}} = -(E_{\text{onset red}} + 4.8\text{ eV})$.
[e] $E_{\text{HOMO}} = -(E_{\text{onset ox}} + 4.8\text{ eV})$. [f] Calculated at the B3LYP/6-311+G** level.

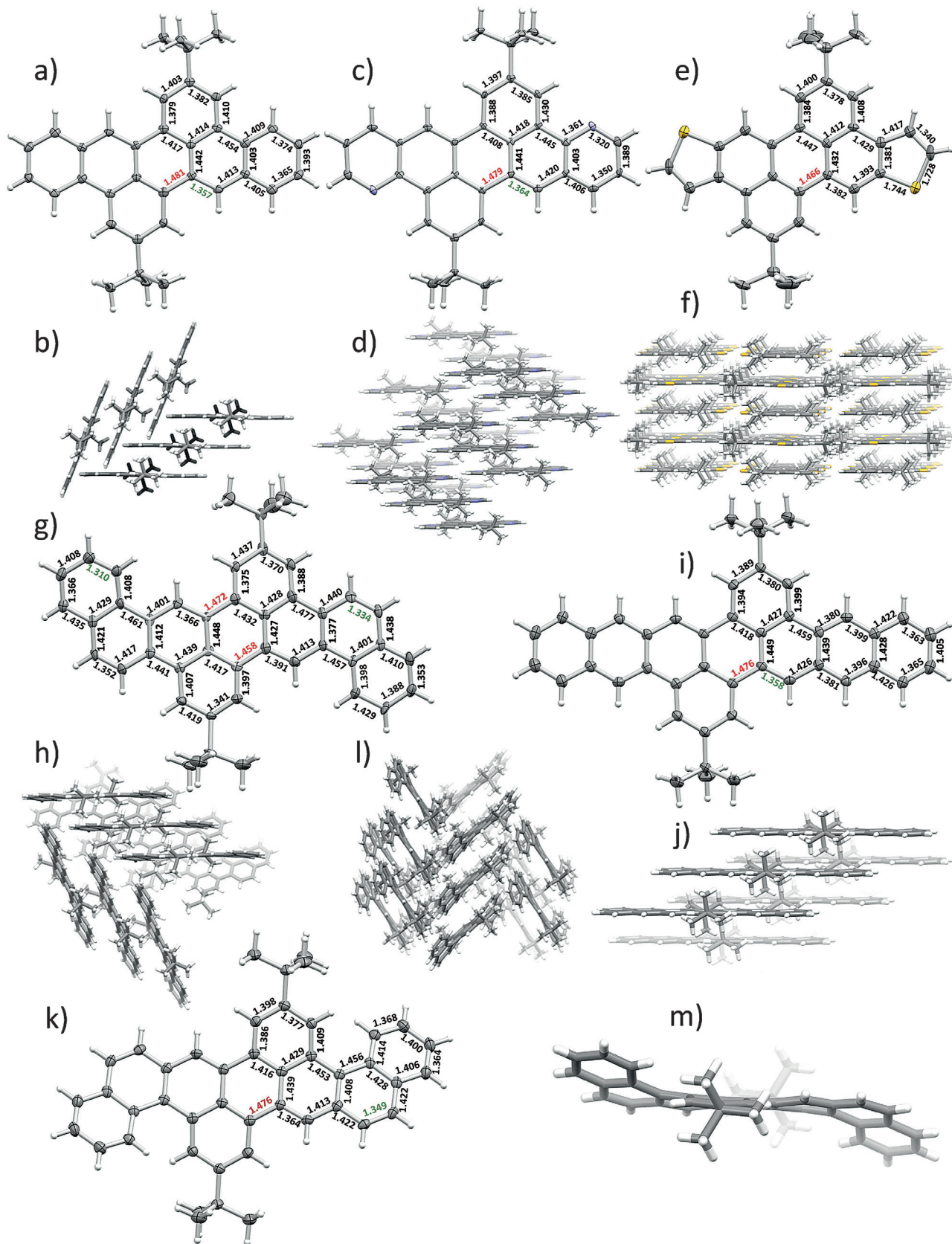


Figure 3. Single crystal structures of **6a** (a and b), **6c** (c and d), **6d** (e and f), **6e** (k, l and m), **6f** (g and h) and **6g** (i and j). For structure of **6b**, see Supporting information. Bond lengths are given in Å. ORTEP plots are at the 50% probability. For detailed crystallographic data, see the Supporting Information.

closes contacts between π -planes in the crystal structure, giving a hint that the arrangement has a large impact on the device characteristics, although it is not clear yet, whether the arrangement of the molecules in the semiconducting monolayer is related to the one in the single crystalline state.

These first results demonstrate that at least some members of this class of compounds, which were mentioned as early as 1932, show promise for applications in organic electronic devices, even though the field-effect mobilities we have achieved so far are not as high as those of some other discrete organic molecules, such as pentacene,^[25] TIPS-pentacene,^[26] rubrene^[27] or dinaphtho[2,3-*b*:2',3'-*f*]-thieno[3,2-*b*]thiophene (DNTT).^[28] However, it should be kept in mind that the device preparation and thin-film morphology play a crucial role and total numbers for measured mobilities for the same organic semiconductor can vary largely; for example, the mobility for TIPS-pentacene has been improved from initially $0.4 \text{ cm}^2 \text{V}^{-1} \text{s}^{-1}$ to $11 \text{ cm}^2 \text{V}^{-1} \text{s}^{-1}$ over time.^[26,29,30]

In summary, we have provided the synthetic access by a facile two-step approach to a large variety of soluble bisareneperylene in good yields. First TFTs with these materials gave promising device characteristics with charge-carrier field-effect mobilities of up to $0.12 \text{ cm}^2 \text{V}^{-1} \text{s}^{-1}$ and on/off ratios of 5×10^5 . Since all new compounds are soluble in organic solvents and tend to form single crystals, we will alternatively build devices by depositing the molecules from solution and also grow larger single crystals to make single-crystal organic field-effect transistors (SC—OFETs), which usually show much better performance than thin-film transistors. Furthermore, the two-step approach provides a quick access to a large library of new derivatives of this class, so that substitution patterns as well as positions and numbers of heteroatoms can be adjusted in order to fine-tune molecular properties, such as the frontier molecular orbital levels, to study the impact of supramolecular aggregation on the charge transport.

Acknowledgements

M.M. and G.Z. thank the Ruprecht-Karls-University for funding this project (FRONTIER project ZUK 49/2) in the frame of excellence initiative II. We thank M. Hagel at the Max Planck Institute for Solid State Research for expert technical assistance.

Keywords: heterocycles • organic thin film transistors • perylenes • polycyclic aromatic hydrocarbons • synthesis

- [1] For reviews, see: a) J. E. Anthony, *Chem. Rev.* **2006**, *106*, 5028–5048; b) J. E. Anthony, *Angew. Chem. Int. Ed.* **2008**, *47*, 452–483; *Angew. Chem.* **2008**, *120*, 460–492; c) H. F. Bettinger, C. Tönshoff, *Chem. Rec.* **2015**, *15*, 364–369; d) Q. Ye, C. Chi, *Chem. Mater.* **2014**, *26*, 4046–4056; e) S. S. Zade, M. Bendikov, *Angew. Chem. Int. Ed.* **2010**, *49*, 4012–4015; *Angew. Chem.* **2010**, *122*, 4104–4107; f) U. H. F. Bunz, *Acc. Chem. Res.* **2015**, *48*, 1676–1686; g) U. H. F. Bunz, J. U. Engelhart, B. D. Lindner, M. Schaffroth, *Angew. Chem. Int. Ed.* **2013**, *52*, 3810–3821; *Angew. Chem.* **2013**, *125*, 3898–3910; for examples of larger acenes and heterocacenes, see: h) B. D. Lindner, J. U. Engelhart, O. Tverskoy, A. L. Appleton, F. Rominger, A. Peters, H.-J. Himmel, U. H. F. Bunz, *Angew. Chem. Int. Ed.* **2011**, *50*, 8588–8591; *Angew. Chem.* **2011**, *123*, 8747–8750; i) M. Watanabe, Y. J.

Chang, S.-W. Liu, T.-H. Chao, K. Goto, M. M. Islam, C.-H. Yuan, Y.-T. Tao, T. Shimmyozu, T. J. Chow, *Nat. Chem.* **2012**, *4*, 574–578; j) M. M. Payne, S. R. Parkin, J. E. Anthony, *J. Am. Chem. Soc.* **2005**, *127*, 8028–8029; k) M. M. Payne, S. A. Odom, S. R. Parkin, J. E. Anthony, *Org. Lett.* **2004**, *6*, 3325–3328; l) M. J. Bruzek, J. E. Anthony, *Org. Lett.* **2014**, *16*, 3608–3610; m) J. U. Engelhart, O. Tverskoy, U. H. F. Bunz, *J. Am. Chem. Soc.* **2014**, *136*, 15166–15169; n) J. Li, Q. Zhang, *ACS Appl. Mater. Interfaces* **2015**, *7*, 28049–28062; o) J. U. Engelhart, B. D. Lindner, M. Schaffroth, D. Schrempp, O. Tverskoy, U. H. F. Bunz, *Chem. Eur. J.* **2015**, *21*, 8121–8129; p) B. Purushothaman, M. Bruzek, S. R. Parkin, A.-F. Miller, J. E. Anthony, *Angew. Chem. Int. Ed.* **2011**, *50*, 7013–7017; *Angew. Chem.* **2011**, *123*, 7151–7155; q) B. Gao, M. Wang, Y. Cheng, L. Wang, X. Jing, F. Wang, *J. Am. Chem. Soc.* **2008**, *130*, 8297–8306; r) I. Kaur, M. Jazdzyk, N. N. Stein, P. Prusevich, G. P. Miller, *J. Am. Chem. Soc.* **2010**, *132*, 1261–1263; s) Q. Miao, *Adv. Mater.* **2014**, *26*, 5541–5549; t) Z. Liang, Q. Tang, R. Mao, D. Liu, J. Xu, Q. Miao, *Adv. Mater.* **2011**, *23*, 5514–5518; u) Z. Liang, Q. Tang, J. Xu, Q. Miao, *Adv. Mater.* **2011**, *23*, 1535–1539; v) D. Liu, X. Xu, Y. Su, Z. He, J. Xu, Q. Miao, *Angew. Chem. Int. Ed.* **2013**, *52*, 6222–6227; *Angew. Chem.* **2013**, *125*, 6342–6347.

- [2] a) R. Mondal, B. K. Shah, D. C. Neckers, *J. Am. Chem. Soc.* **2006**, *128*, 9612–9613; b) H. F. Bettinger, R. Mondal, D. C. Neckers, *Chem. Commun.* **2007**, *5209*–5211; c) R. Mondal, C. Tönshoff, D. Khon, D. C. Neckers, H. F. Bettinger, *J. Am. Chem. Soc.* **2009**, *131*, 14281–14289; d) C. Tönshoff, H. F. Bettinger, *Angew. Chem. Int. Ed.* **2010**, *49*, 4125–4128; *Angew. Chem.* **2010**, *122*, 4219–4222; e) R. Einholz, H. F. Bettinger, *Angew. Chem. Int. Ed.* **2013**, *52*, 9818–9820; *Angew. Chem.* **2013**, *125*, 10000–10003.
- [3] a) A. H. Endres, M. Schaffroth, F. Paulus, H. Reiss, H. Wadeppohl, F. Rominger, R. Krämer, U. H. F. Bunz, *J. Am. Chem. Soc.* **2016**, *138*, 1792–1795; b) B. Kohl, F. Rominger, M. Mastalerz, *Angew. Chem. Int. Ed.* **2015**, *54*, 6051–6056; *Angew. Chem.* **2015**, *127*, 6149–6154; c) D. Chun, Y. Cheng, F. Wudl, *Angew. Chem. Int. Ed.* **2008**, *47*, 8380–8385; *Angew. Chem.* **2008**, *120*, 8508–8513; d) J. Xiao, H. M. Duong, Y. Liu, W. Shi, L. Ji, G. Li, S. Li, X.-W. Liu, J. Ma, F. Wudl, Q. Zhang, *Angew. Chem. Int. Ed.* **2012**, *51*, 6094–6098; *Angew. Chem.* **2012**, *124*, 6198–6202; e) Z. Wang, J. Miao, G. Long, P. Gu, J. Li, N. Aratani, H. Yamada, B. Liu, Q. Zhang, *Chem. Asian J.* **2016**, *11*, 482–485.
- [4] E. Clar, *The Aromatic Sextet*, Wiley, New York, **1972**.
- [5] a) S. R. Bheemireddy, P. C. Ubaldo, P. W. Rose, A. D. Finke, J. Zhuang, L. Wang, K. N. Plunkett, *Angew. Chem. Int. Ed.* **2015**, *54*, 15762–15766; *Angew. Chem.* **2015**, *127*, 15988–15992; b) A. Naibi Lakshminarayana, J. Chang, J. Luo, B. Zheng, K.-W. Huang, C. Chi, *Chem. Commun.* **2015**, *51*, 3604–3607; c) G. Dai, J. Chang, J. Luo, S. Dong, N. Aratani, B. Zheng, K.-W. Huang, H. Yamada, C. Chi, *Angew. Chem. Int. Ed.* **2016**, *55*, 2693–2696; *Angew. Chem.* **2016**, *128*, 2743–2746.
- [6] H. Xia, D. Liu, X. Xu, Q. Miao, *Chem. Commun.* **2013**, *49*, 4301–4303.
- [7] T. Wombacher, A. Gassmann, S. Foro, H. von Seggern, J. J. Schneider, *Angew. Chem. Int. Ed.* **2016**, *55*, 6041–6046.
- [8] X. Gu, X. Xu, H. Li, Z. Liu, Q. Miao, *J. Am. Chem. Soc.* **2015**, *137*, 16203–16208.
- [9] M. R. Rao, H. T. Black, D. F. Perepichka, *Org. Lett.* **2015**, *17*, 4224–4227.
- [10] L. Shan, Z. Liang, X. Xu, Q. Tang, Q. Miao, *Chem. Sci.* **2013**, *4*, 3294–3297.
- [11] a) L. Zhang, A. Fonari, Y. Liu, A.-L. M. Hoyt, H. Lee, D. Granger, S. Parkin, T. P. Russell, J. E. Anthony, J.-L. Brédas, V. Coropceanu, A. L. Briseno, *J. Am. Chem. Soc.* **2014**, *136*, 9248–9251; b) L. A. Stevens, K. P. Goetz, A. Fonari, Y. Shu, R. M. Williamson, J.-L. Brédas, V. Coropceanu, O. D. Jurchescu, G. E. Collis, *Chem. Mater.* **2015**, *27*, 112–118.
- [12] Y. Cao, Y. Liang, L. Zhang, S. Osuna, A.-L. M. Hoyt, A. L. Briseno, K. N. Houk, *J. Am. Chem. Soc.* **2014**, *136*, 10743–10751.
- [13] The scaffold of the bistetracene has former also be called dinaphthopyrene. See: E. Clar, *J. Chem. Soc.* **1949**, 2013–2016.
- [14] See for instance a) F. Würthner, M. Stolte, *Chem. Commun.* **2011**, *47*, 5109–5115; b) R. Schmidt, J. H. Oh, Y.-S. Sun, M. Deppisch, A.-M. Krause, K. Radacki, H. Braunschweig, M. Könemann, P. Erk, Z. Bao, F. Würthner, *J. Am. Chem. Soc.* **2009**, *131*, 6215–6228.
- [15] H. Klauk, *Chem. Soc. Rev.* **2010**, *39*, 2643–2666.
- [16] E. Clar, *Ber. Dtsch. Chem. Ges.* **1932**, *65*, 846–859.
- [17] E. Clar, C. T. Ironside, M. Zander, *Tetrahedron* **1966**, *22*, 3527–3533.
- [18] G. Zhang, F. Rominger, M. Mastalerz, *Chem. Eur. J.* **2016**, *22*, 3084–3093.

- [19] J.-F. Lee, Y.-C. Chen, J.-T. S. Lin, C.-C. Wu, C.-Y. Chen, C.-A. Dai, C.-Y. Chao, H.-L. Chen, W.-B. Liau, *Tetrahedron* **2011**, *67*, 1696–1702.
- [20] a) T. Ishiyama, J. Takagi, K. Ishida, N. Miyaura, N. R. Anastasi, J. F. Hartwig, *J. Am. Chem. Soc.* **2002**, *124*, 390–391; b) I. A. I. Mkhaldid, J. H. Barnard, T. B. Marder, J. M. Murphy, J. F. Hartwig, *Chem. Rev.* **2010**, *110*, 890–931; c) S. M. Preshlock, B. Ghaffari, P. E. Maligres, S. W. Kraska, R. E. Maleczka, M. R. Smith, *J. Am. Chem. Soc.* **2013**, *135*, 7572–7582.
- [21] W. N. Lipscomb, J. M. Robertson, M. G. Rossmann, *J. Chem. Soc.* **1959**, 2601–2607.
- [22] a) T. K. Dickens, R. B. Mallion, *J. Phys. Chem. A* **2011**, *115*, 351–356; b) T. K. Dickens, R. B. Mallion, *J. Phys. Chem. A* **2015**, *119*, 5019–5025.
- [23] M. L. Tang, Z. Bao, *Chem. Mater.* **2011**, *23*, 446–455.
- [24] a) R. Hofmockel, U. Zschieschang, U. Kraft, R. Rödel, N. H. Hansen, M. Stolte, F. Würthner, K. Takimiya, K. Kern, J. Pflaum, H. Klauk, *Org. Electron.* **2013**, *14*, 3213–3221; b) U. Kraft, M. Sejfić, M. J. Kang, K. Takimiya, T. Zaki, F. Letzkus, J. N. Burghartz, E. Weber, H. Klauk, *Adv. Mater.* **2015**, *27*, 207–214.
- [25] a) O. D. Jurchescu, M. Popinciuc, B. J. van Wees, T. T. M. Palstra, *Adv. Mater.* **2007**, *19*, 688–692; b) Y. Takeyama, S. Ono, Y. Matsumoto, *Appl. Phys. Lett.* **2012**, *101*, 083303.
- [26] a) G. Giri, E. Verploegen, S. C. B. Mannsfeld, S. Atahan-Evrenk, D. H. Kim, S. Y. Lee, H. A. Becerril, A. Aspuru-Guzik, M. F. Toney, Z. Bao, *Nature* **2011**, *480*, 504–508; b) Y. Diao, B. C. K. Tee, G. Giri, J. Xu, D. H. Kim, H. A. Becerril, R. M. Stoltzenberg, T. H. Lee, G. Xue, S. C. B. Mannsfeld, Z. Bao, *Nat. Mater.* **2013**, *12*, 665–671.
- [27] J. Takeya, M. Yamagishi, Y. Tominari, R. Hirahara, Y. Nakazawa, T. Nishikawa, T. Kawase, T. Shimoda, S. Ogawa, *Appl. Phys. Lett.* **2007**, *90*, 102120.
- [28] M. de Pauli, U. Zschieschang, I. D. Barcelos, H. Klauk, A. Malachias, *Adv. Electron. Mat.* **2016**, *2*, 1500402.
- [29] C. D. Sheraw, T. N. Jackson, D. L. Eaton, J. E. Anthony, *Adv. Mater.* **2003**, *15*, 2009–2011.
- [30] G. Schweicher, Y. Olivier, V. Lemaury, Y. H. Geerts, *Isr. J. Chem.* **2014**, *54*, 595–620.

Received: July 14, 2016

Published online on August 30, 2016

CHEMISTRY

A European Journal

Supporting Information

Facile Synthetic Approach to a Large Variety of Soluble Diarenoperylenes

Gang Zhang,^[a, b] Frank Rominger,^[a] Ute Zschieschang,^[c] Hagen Klauk,^[c] and Michael Mastalerz^{*[a]}

chem_201603336_sm_miscellaneous_information.pdf

Table of Contents

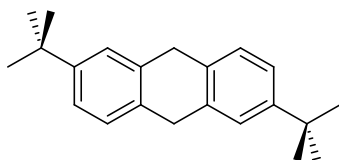
1. General remarks.....	S2
2. Experimental part.....	S2
3. X-ray crystallographic structure determination.....	S14
4. NMR and FT-IR spectra	S20
5. UV/vis and fluorescence spectra	S58
6. DFT calculations	S62
7. Cyclovoltammograms.....	S66
8. OFETs characterization	S70
9. References	S82

1. General Remarks

All reagents and solvents were obtained from Fisher Scientific, Alfa Aesar, Sigma-Aldrich or VWR and were used without further purification unless otherwise noted. For thin layer chromatography silica gel 60 F254 plates from Merck were used and examined under UV-light irradiation (254 nm and 365 nm). Flash column chromatography was performed on silica gel from Sigma-Aldrich (particle size: 0.04-0.063 mm) using petroleum ether, dichloromethane and/or ethyl acetate. Melting points (not corrected) were measured with a Büchi Melting Point B-545. IR-Spectra were recorded on a Bruker Lumos spectrometer on a Ge ATR crystal. NMR spectra were taken on a Bruker 300 (300 MHz) and Bruker Avance 500 (500 MHz). Chemical shifts (δ) are reported in parts per million (ppm) relative to traces of CHCl_3 or tetrachloroethane in the corresponding deuterated solvent. HRMS experiments were carried out on a Fourier Transform Ion Cyclotron Resonance (FTICR) mass spectrometer solariX (Bruker Daltonik GmbH, Bremen, Germany) equipped with a 7.0 T superconducting magnet and interfaced to an Apollo II Dual ESI/MALDI source. Absorption spectra were recorded on a Jasco UV-VIS V-660 or Jasco UV-VIS V-670. Emission spectra were recorded on a Jasco FP-6500. Electrochemical data were obtained in dichloromethane or *o*-dichlorobenzene solution of Bu_4NClO_4 (0.1 M), as indicated. Ferrocene was used as an internal standard. Cyclic voltammograms were obtained using a glassy carbon working electrode, a Pt/Ti counter electrode, and a Ag reference electrode. Elemental Analysis was performed by the Microanalytical Laboratory of the University of Heidelberg using an Elementar Vario EL machine. Crystal structure analysis was accomplished on Bruker APEX II Quazar or on a Bruker APEX I diffractometer with a molybdenum source ($\lambda(\text{MoK}\alpha) = 0.71073 \text{ \AA}$). 2,6-di-tert-butylanthracene (**1**)^{S1}, 1-bromo-2-naphthaldehyde (**4e**)^{S2}, 2-bromo-1-naphthaldehyde (**4f**)^{S2} and 3-bromo-2-naphthaldehyde (**4g**)^{S3} were prepared according to the reported methods.

2. Experimental part

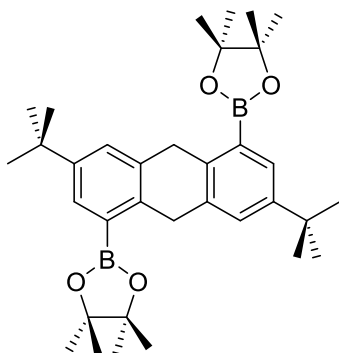
2,6-di-tert-butyl-9,10-dihydroanthracene (**2**)



Freshly cut small pieces of sodium (1.15 g, 50 mmol) were added to a solution of anthracene **1** (5.81 g, 20 mmol) in dry THF (100 mL). $^t\text{BuOH}$ (3.71 g, 50 mmol) in dry THF (10 mL) was added to the suspension. The mixture was stirred at room temperature for 6 hours during which time the suspension became a solution. The unreacted sodium was carefully removed and the reaction solution was diluted with diethyl ether (200 mL). The organic layer was washed with water (3×200 mL) and dried over Na_2SO_4 . After removal of the solvent by rotary evaporation, the dihydroanthracene **2** was obtained as colorless solid (5.80 g, 99%). mp: 141 °C. ^1H NMR (500 MHz, CD_2Cl_2) δ (ppm) = 7.32 (s, 2H), 7.23-7.20 (m, 4H), 3.89 (s, 4H), 1.32 (s, 18H). ^{13}C NMR (125 MHz, CD_2Cl_2) δ (ppm) = 149.3, 137.0, 134.4, 127.2, 124.7, 123.2, 36.3, 34.7, 31.6. FT-IR (ATR) $\tilde{\nu}$ (cm^{-1}) = 2957 (s), 2901 (m), 2865(m), 1614 (w), 1571 (w), 1505 (m), 1472 (m), 1422 (m), 1399 (w), 1361 (m), 1337 (w), 1265 (m), 1199 (m), 1146 (m), 964 (w), 915 (m), 812

(s), 724 (m), 606 (m). Elemental anal. calcd. for C₂₂H₂₈: C 90.35 H 9.65, found: C 90.17 H 9.74. HRMS (EI) (*m/z*): [M]⁺ calcd. for C₂₂H₂₈, 292.21855; found, 292.21676; [M-C₄H₉]⁺ calcd. for C₁₈H₁₉, 235.14813; found, 235.14739.

2,2'-(3,7-di-tert-butyl-9,10-dihydroanthracene-1,5-diyl)bis(4,4,5,5-tetramethyl-1,3,2-dioxaborolane) (3)

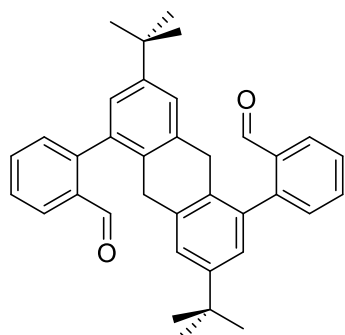


In a glovebox, [Ir(COD)OMe]₂ (20 mg, 0.03 mmol Ir), 3,4,7,8-tetramethylphenanthroline (14 mg, 0.06 mmol) and a small amount of B₂pin₂ (51 mg, 0.20 mmol) were mixed in THF (1 mL) and stirred vigorously until the solution turned brown-red. The catalyst solution was then added to a mixture of dihydroanthracene **2** (292 mg, 1 mmol) and B₂pin₂ (840 mg, 3.30 mmol) in a screw-capped vial. The reaction mixture was stirred at 85 °C for 48 h to give a dark red solution. After cooling down to room temperature, the solvent was removed by rotary evaporation and the crude product was washed with methanol (2×20 mL) to give the product **3** as colorless powder (383 mg, 70%). mp: 265 °C. ¹H NMR (500 MHz, CDCl₃) δ (ppm) = 7.70 (d, *J* = 1.08 Hz, 2H), 7.39 (d, *J* = 1.35 Hz, 2H), 4.24 (s, 4H), 1.40 (s, 24H), 1.35 (s, 18H). ¹³C NMR (125 MHz, CDCl₃) δ (ppm) = 147.5, 140.9, 137.4, 130.3, 127.6, 83.4, 35.8, 34.3, 31.5, 24.9. FT-IR (ATR) ν (cm⁻¹) = 2964 (m), 2908 (w), 2869 (w), 1573 (w), 1458 (m), 1417 (m), 1409 (m), 1367 (s), 1334 (m), 1310 (m), 1254 (m), 1232 (w), 1210 (m), 1167 (s), 1142 (m), 975 (w), 930 (m), 901 (m), 855 (m), 835 (w), 741 (m), 680 (m), 617 (m). Elemental anal. calcd. for C₃₄H₅₀B₂O₄·0.2H₂O: C 74.52 H 9.27, found: C 74.58 H 9.48. HRMS-DART (*m/z*): [M+NH₄]⁺ calcd. for C₃₄H₅₄B₂NO₄, 562.42447; found, 562.42581.

General Procedure (GP1) for the Suzuki Miyaura cross coupling reactions of boronic ester **3 and bromo-aldehyde **4**.**

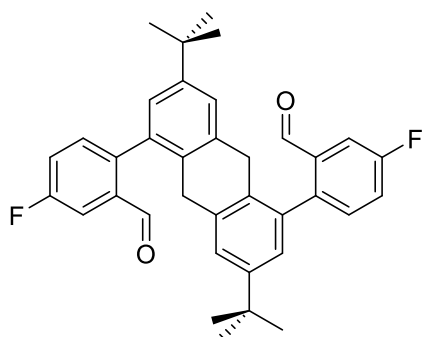
In a screw-capped vial, a mixture of boronic pinacol ester **3**, Pd₂(dba)₃, ¹Bu₃PHBF₄, K₂CO₃ and bromo-aldehyde **4** was dissolved in degassed THF (2 mL) and degassed water (0.5 mL) and heated at 80 °C overnight. After cooling down to room temperature, the mixture was diluted with dichloromethane (50 mL) and washed with water (3×50 mL) and dried over Na₂SO₄. The solvent was removed by rotary evaporation and the crude product was purified by silica gel chromatography to give the product **5**.

2,2'-(3,7-di-tert-butyl-9,10-dihydroanthracene-1,5-diyl)dibenzaldehyde (5a)



According to **GP1**, boronic pinacol ester **3** (163 mg, 0.3 mmol), Pd₂(dba)₃ (14 mg, 0.015 mmol), ^tBu₃PHBF₄ (14 mg, 0.049 mmol), K₂CO₃ (83 mg, 0.6 mmol) and 2-bromo-benzaldehyde **4a** (133 mg, 0.72 mmol) gave after workup and silica gel column chromatography (light petroleum/dichloromethane/ethyl acetate 50:10:1), **5a** (mixture of atropisomers) as colorless solid (140 mg, 93%). mp: 270 °C. ¹H NMR (500 MHz, CDCl₃) δ (ppm) = 9.82 (s, 1H), 9.80 (s, 1H), 8.13 (dd, *J* = 3.0, 1.1 Hz, 1H), 8.12 (dd, *J* = 3.0, 1.1 Hz, 1H), 7.75-7.73 (m, 1H), 7.72-7.70 (m, 1H), 7.59 (t, *J* = 7.6 Hz, 2H), 7.44 (d, *J* = 7.5 Hz, 1H), 7.41 (d, *J* = 7.5 Hz, 1H), 7.17 (t, *J* = 1.7 Hz, 2H), 7.13 (d, *J* = 1.9 Hz, 2H), 3.77-3.66 (m, 4H), 1.28 (s, 18H). ¹³C NMR (125 MHz, CDCl₃) δ (ppm) = 192.48, 192.42, 148.89, 148.87, 145.60, 145.56, 136.65, 136.64, 135.45, 135.41, 134.25, 134.19, 133.77, 133.68, 132.15, 132.11, 131.23, 131.16, 127.89, 127.13, 127.09, 125.69, 125.65, 124.75, 124.74, 34.43, 34.37, 31.34. FT-IR (ATR) $\tilde{\nu}$ (cm⁻¹) = 3059 (w), 3032 (w), 2961 (m), 2905 (w), 2866 (w), 2838 (w), 2748 (w), 1693 (s), 1652 (w), 1597 (s), 1573 (w), 1473 (m), 1421 (w), 1391 (m), 1361 (m), 1292 (w), 1265 (m), 1246 (m), 1196 (m), 1158 (w), 1087 (w), 947 (w), 929 (w), 903 (w), 866 (m), 823 (m), 764 (s), 740 (s), 648 (m), 631(m). Elemental anal. calcd. for C₃₆H₃₆O₂: C 86.36 H 7.25, found: C 86.44 H 7.43. HRMS-MALDI (DCTB) (*m/z*): [M+Na]⁺ calcd. for C₃₆H₃₆NaO₂, 523.26075; found, 523.26195.

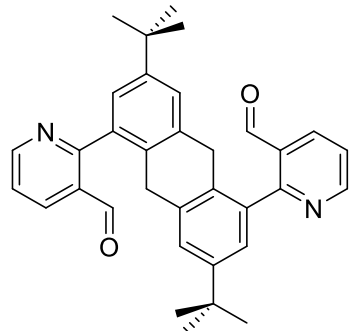
2,2'-(3,7-di-tert-butyl-9,10-dihydroanthracene-1,5-diyl)bis(5-fluorobenzaldehyde) (5b)



According to **GP1**, boronic pinacol ester **3** (163 mg, 0.3 mmol), Pd₂(dba)₃ (14 mg, 0.015 mmol), ^tBu₃PHBF₄ (14 mg, 0.049 mmol), K₂CO₃ (83 mg, 0.6 mmol) and 2-bromo-5-fluorobenzaldehyde **4b** (146 mg, 0.72 mmol) gave after workup and silica gel column chromatography (light petroleum/dichloromethane/ethyl acetate 50:10:1), **5b** as colorless solid

(mixture of atropisomers) (143 mg, 89%). mp: 300 °C. ^1H NMR (500 MHz, CDCl_3) δ (ppm) = 9.73 (d, 1H), 9.72 (d, 1H), 7.80-7.77 (m, 2H), 7.44-7.37 (m, 4H), 7.17 (s, br, 2H), 7.10 (d, J = 1.81 Hz, 2H), 3.73-3.62 (m, 4H), 1.28 (s, 18H). ^{13}C NMR (125 MHz, CDCl_3) δ (ppm) = 191.22 (d, $J_{C,F}$ = 1.7 Hz), 191.16 (d, $J_{C,F}$ = 1.7 Hz), 163.27, 161.28, 149.15, 149.13, 141.44 (d, $J_{C,F}$ = 3.1 Hz), 141.40 (d, $J_{C,F}$ = 3.4 Hz), 136.65, 136.63, 135.86, 135.80, 135.75, 134.49, 134.46, 133.10 (d, $J_{C,F}$ = 7.4 Hz), 133.03 (d, $J_{C,F}$ = 7.4 Hz), 132.28, 132.23, 128.96, 128.39, 125.87, 125.82, 124.97, 124.96, 121.09 (d, J = 9.4 Hz), 120.92 (d, J = 9.3 Hz), 113.39 (d, J = 5.3 Hz), 113.21 (d, J = 5.5 Hz), 34.44, 34.34, 31.32. FT-IR (ATR) $\tilde{\nu}$ (cm^{-1}) = 2957 (m), 2907 (w), 2864 (m), 2756 (w), 1691 (s), 1604 (m), 1579 (w), 1492 (s), 1479 (m), 1460 (m), 1413 (m), 1391 (s), 1362 (w), 1335 (w), 1310 (w), 1290 (w), 1262 (s), 1244 (m), 1214 (m), 1147 (s), 966 (m), 931 (w), 886 (m), 840 (m), 783 (w), 757 (m), 718 (m), 643 (m), 617 (w). Elemental anal. calcd. for $\text{C}_{36}\text{H}_{34}\text{F}_2\text{O}_2$: C 80.57 H 6.39, found: C 80.59 H 6.62. HRMS-MALDI (DCTB) (m/z): [M + Na] $^+$ calcd. for $\text{C}_{36}\text{H}_{34}\text{F}_2\text{NaO}_2$, 559.24191; found, 559.24492.

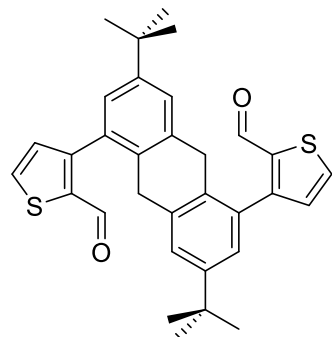
2,2'-(3,7-di-tert-butyl-9,10-dihydroanthracene-1,5-diyl)dinicotinaldehyde (5c)



According to **GP1**, boronic pinacol ester **3** (163 mg, 0.3 mmol), $\text{Pd}_2(\text{dba})_3$ (14 mg, 0.015 mmol), $^t\text{Bu}_3\text{PHBF}_4$ (14 mg, 0.049 mmol), K_2CO_3 (83 mg, 0.6 mmol) and 2-bromonicotinaldehyde **4c** (146 mg, 0.72 mmol) gave after workup and silica gel column chromatography (light petroleum/dichloromethane/ethyl acetate 5:1:1 to 10:5:2) **5c** as colorless solid (mixture of atropisomers) (143 mg, 94%).

mp: 239 °C (dec.). ^1H NMR (500 MHz, CDCl_3) δ (ppm) = 9.84 (s, br, 2H), 8.97 (d, J = 1.8 Hz, 1H), 8.96 (d, J = 1.8 Hz, 1H), 8.41 (d, J = 1.7 Hz, 1H), 8.39 (d, J = 1.7 Hz, 1H), 7.55-7.53 (m, 2H), 7.22 (d, J = 1.7 Hz, 2H), 7.16 (s, br, 2H), 4.03 (s, br, 1H), 3.93 (s, br, 1H), 3.69 (s, br, 2H), 1.27 (s, 18H). ^{13}C NMR (125 MHz, CDCl_3) δ (ppm) = 191.7, 163.2, 153.5, 148.9, 137.1, 135.3, 134.4, 132.4, 130.2, 125.9, 122.8, 34.4, 31.3. FT-IR (ATR) $\tilde{\nu}$ (cm^{-1}) = 3063 (w), 2961 (m), 2905 (w), 2867 (m), 2744 (w), 1692 (s), 1607 (w), 1579 (s), 1562 (m), 1477 (m), 1453 (m), 1436 (m), 1383 (s), 1362 (m), 1262 (m), 1241 (m), 1201 (w), 1182 (w), 1139 (w), 1088 (w), 1056 (w), 927 (w), 890 (w), 828 (m), 790 (m), 739 (w), 669 (w), 646 (m), 625 (m). Elemental anal. calcd. for $\text{C}_{34}\text{H}_{34}\text{N}_2\text{O}_2 \cdot 0.4 \text{ H}_2\text{O}$: C 80.09 N 5.49 H 6.88, found: C 80.17 N 5.30 H 6.85. HRMS-MALDI (DCTB) (m/z): [M + H] $^+$ calcd. for $\text{C}_{34}\text{H}_{35}\text{N}_2\text{O}_2$, 503.26930; found, 503.27065.

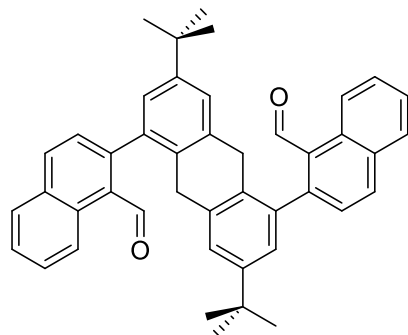
3,3'-(3,7-di-tert-butyl-9,10-dihydroanthracene-1,5-diyl)bis(thiophene-2-carbaldehyde) (5d)



According to **GP1**, boronic pinacol ester **3** (163 mg, 0.3 mmol), Pd₂(dba)₃ (14 mg, 0.015 mmol), ^tBu₃PHBF₄ (14 mg, 0.049 mmol), K₂CO₃ (83 mg, 0.6 mmol) and 3-bromothiophene-2-carbaldehyde **4d** (138 mg, 0.72 mmol) gave after workup and silica gel column chromatography (light petroleum/dichloromethane/ethyl acetate 40:10:1), **5d** as colorless solid (mixture of atropisomers) (142 mg, 92%).

mp: 302 °C (dec.). ¹H NMR (500 MHz, CD₂Cl₂) δ (ppm) = 9.62 (s, 1H), 9.62 (s, 1H), 7.87 (d, J = 1.2 Hz, 1H), 7.86 (d, J = 1.1 Hz, 1H), 7.28 (d, J = 1.9 Hz, 2H), 7.23 (d, J = 4.8 Hz, 2H), 7.21 (d, J = 2.0 Hz, 2H), 3.87 (br s, 2H, CH₂), 3.83 (br s, 2H, CH₂), 1.29 (s, 18H). ¹³C NMR (125 MHz, CD₂Cl₂) δ (ppm) = 184.5, 151.5, 149.5, 139.9, 137.7, 134.1, 132.9, 132.0, 126.2, 125.6, 34.8, 34.7, 31.5. FT-IR (ATR) ν (cm⁻¹) = 3076 (w), 2960 (m), 2867(w), 2840 (w), 2814 (w), 1656 (s), 1604 (w), 1524 (w), 1476 (w), 1458 (w), 1417 (m), 1379 (w), 1358 (m), 1305 (w), 1253 (w), 1209 (m), 1158 (w), 931 (w), 893 (w), 869 (w), 853 (w), 746 (m), 693 (m), 663 (m), 635 (w). Elemental anal. calcd. for C₃₂H₃₂S₂O₂: C 74.94 H 6.29, found: C 74.97 H 6.50. HRMS-MALDI (DCTB) (*m/z*): [M+Na]⁺ calcd. for C₃₂H₃₂NaS₂O₂, 535.17359; found, 535.17560.

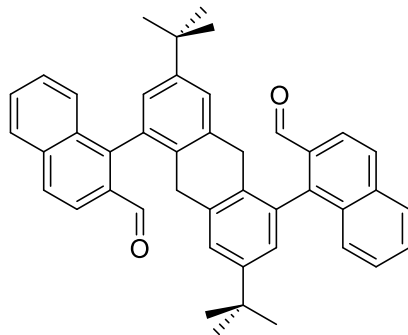
2,2'-(3,7-di-tert-butyl-9,10-dihydroanthracene-1,5-diyl)bis(1-naphthaldehyde) (5e)



According to **GP1**, boronic pinacol ester **3** (163 mg, 0.3 mmol), Pd₂(dba)₃ (14 mg, 0.015 mmol), ^tBu₃PHBF₄ (14 mg, 0.049 mmol), K₂CO₃ (83 mg, 0.6 mmol) and 2-bromo-1-naphthaldehyde **4e** (183 mg, 0.78 mmol) gave after workup and silica gel column chromatography (light petroleum/dichloromethane/ethyl acetate 50:10:1), **5e** as colorless solid (mixture of atropisomers) (166 mg, 92%).

mp: >350 °C (dec.). ^1H NMR (500 MHz, CDCl_3) δ (ppm) = 10.16 (s, 1H), 10.14 (s, 1H), 9.41 (d, J = 3.1 Hz, 1H), 9.40 (d, J = 3.2 Hz, 1H), 8.17 (t, J = 8.0 Hz, 2H), 8.01 (d, J = 3.8 Hz, 1H), 7.99 (d, J = 3.8 Hz, 1H), 7.77 (t, J = 7.7 Hz, 2H), 7.66 (t, J = 7.5 Hz, 2H), 7.51 (d, J = 8.3 Hz, 1H), 7.48 (d, J = 8.3 Hz, 1H), 7.18 (t, J = 2.2 Hz, 2H), 7.15 (t, J = 2.2 Hz, 2H), 3.81-3.71 (m, 4H), 1.26 (s, 18H). ^{13}C NMR (125 MHz, CDCl_3) δ (ppm) = 194.76, 194.72, 148.88, 148.85, 148.52, 148.37, 136.57, 136.56, 136.52, 136.46, 134.28, 134.20, 133.18, 132.06, 132.03, 130.45, 129.44, 129.05, 128.94, 128.67, 128.58, 128.41, 128.36, 126.90, 126.03, 125.97, 125.73, 125.72, 124.89, 34.45, 34.42, 31.33. FT-IR (ATR) $\tilde{\nu}$ (cm^{-1}) = 3052 (w), 2961 (m), 2865 (w), 2768 (w), 1682 (s), 1619 (w), 1591 (m), 1572 (w), 1505 (m), 1475 (m), 1457 (w), 1430 (m), 1406 (w), 1360 (m), 1265 (w), 1244 (w), 1214 (w), 1201 (w), 1175 (m), 1144 (w), 1060 (m), 1032 (w), 965 (w), 946 (w), 930 (w), 867 (m), 825 (s), 745 (s), 709 (m), 671 (w), 642 (m). Elemental anal. calcd. for $\text{C}_{44}\text{H}_{40}\text{O}_2$: C 87.96 H 6.71, found: C 87.67 H 6.74. HRMS-MALDI (DCTB) (m/z): [M+Na]⁺ calcd. for $\text{C}_{44}\text{H}_{40}\text{NaO}_2$, 623.29205; found, 623.29539.

1,1'-(3,7-di-tert-butyl-9,10-dihydroanthracene-1,5-diyl)bis(2-naphthaldehyde) (5f)

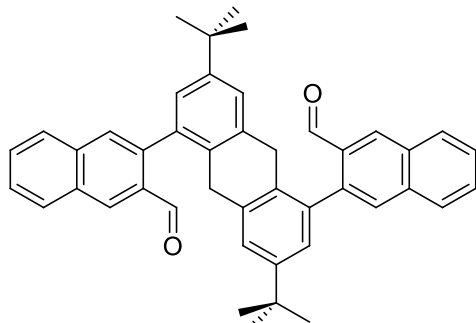


According to **GP1**, boronic pinacol ester **3** (163 mg, 0.3 mmol), $\text{Pd}_2(\text{dba})_3$ (14 mg, 0.015 mmol), $^3\text{Bu}_3\text{PHBF}_4$ (14 mg, 0.049 mmol), K_2CO_3 (83 mg, 0.6 mmol) and 1-bromo-2-naphthaldehyde **4f** (183 mg, 0.78 mmol) gave after workup and silica gel column chromatography (light petroleum/dichloromethane/ethyl acetate 50:10:1), **5f** as colorless solid (mixture of atropisomers) (160 mg, 89%).

mp: >350 °C (dec.). ^1H NMR (500 MHz, CDCl_3) δ (ppm) = 9.87 (s, 1H), 9.86 (s, 1H), 8.17 (dd, J = 8.6, 4.1 Hz, 2H), 8.04 (d, J = 9.1 Hz, 2H), 8.01 (d, J = 6.7 Hz, 2H), 7.68 (dd, J = 8.1, 6.9 Hz, 2H), 7.57 (d, J = 8.4 Hz, 2H), 7.50-7.46 (m, 2H), 7.16 (t, J = 1.6 Hz, 2H), 7.04 (dd, J = 5.58, 1.91 Hz, 2H), 3.62-3.53 (m, 4H), 1.22(s, 9H), 1.22 (s, 9H). ^{13}C NMR (125 MHz, CDCl_3) δ (ppm) = 193.06, 192.84, 148.86, 146.59, 146.38, 136.25, 136.22, 135.94, 135.88, 132.80, 132.79, 132.54, 132.49, 132.43, 132.41, 131.43, 131.32, 129.04, 128.90, 128.43, 128.37, 128.35, 127.76, 127.71, 127.19, 127.02, 126.33, 126.25, 125.08, 125.04, 122.30, 122.12, 34.41, 34.40, 33.78, 33.74, 31.31. FT-IR (ATR) $\tilde{\nu}$ (cm^{-1}) = 3061 (w), 2959 (m), 2902 (w), 2864 (w), 2840 (w), 1686 (s), 1619 (w), 1596 (m), 1571 (w), 1473 (m), 1460 (m), 1428 (m), 1380 (m), 1361 (w), 1330 (w), 1309 (w), 1262 (w), 1240 (m), 1227 (m), 1158 (w), 1141 (w), 1031 (w), 951 (m), 919 (w), 896 (w), 866 (w), 811 (s), 789 (w), 771 (m), 758 (m), 741 (s), 701 (w), 669 (w), 635 (w), 617 (m). Elemental anal. calcd. for $\text{C}_{44}\text{H}_{40}\text{O}_2 \cdot 0.2\text{H}_2\text{O}$: C 87.44 H 6.74, found: C

87.30 H 6.58. HRMS-MALDI (DCTB) (*m/z*): [M+H]⁺ calcd. for C₄₄H₄₁O₂, 601.31011; found, 601.31490.

3,3'-(3,7-di-tert-butyl-9,10-dihydroanthracene-1,5-diyl)bis(2-naphthaldehyde) (5g)



According to **GP1**, boronic pinacol ester **3** (163 mg, 0.3 mmol), Pd₂(dba)₃ (14 mg, 0.015 mmol), ^tBu₃PHBF₄ (14 mg, 0.049 mmol), K₂CO₃ (83 mg, 0.6 mmol) and 3-bromo-2-naphthaldehyde **4g** (183 mg, 0.78 mmol) gave after workup and silica gel column (light petroleum/dichloromethane/ethyl acetate 50:10:1), **5g** as colorless solid (mixture of atropisomers) (165 mg, 92%).

mp: >350 °C (dec.). ¹H NMR (500 MHz, CDCl₃) δ (ppm) = 9.95 (s, 1H), 9.93 (s, 1H), 8.68 (d, *J* = 3.2 Hz, 2H), 8.13 (d, *J* = 8.2 Hz, 2H), 7.95 (t, *J* = 8.0 Hz, 2H), 7.88 (s, 1H), 7.84 (s, 1H), 7.72-7.68 (m, 2H), 7.64 (t, *J* = 7.4 Hz, 2H), 7.22 (t, *J* = 1.7 Hz, 2H), 7.14 (t, *J* = 1.6 Hz, 2H), 3.80-3.71 (m, 4H), 1.27 (s, 18H). ¹³C NMR (125 MHz, CDCl₃) δ (ppm) = 192.60, 192.54, 148.95, 148.92, 140.27, 140.23, 136.58, 136.53, 135.84, 135.77, 135.74, 132.41, 132.34, 132.29, 132.22, 131.97, 131.95, 130.11, 130.00, 129.96, 129.21, 129.17, 129.14, 127.94, 127.89, 127.03, 127.01, 125.65, 124.72, 124.68, 34.45, 34.44, 31.36. FT-IR (ATR) ν (cm⁻¹) = 3052 (w), 2961 (m), 2903 (w), 2865 (w), 2744 (w), 1691 (s), 1625 (m), 1590 (m), 1572 (w), 1475 (m), 1457 (w), 1442 (m), 1400 (w), 1377 (w), 1361 (w), 1304 (w), 1273 (w), 1246 (w), 1195 (w), 1156 (m), 1074 (w), 1017 (w), 958 (w), 920 (w), 886 (m), 742 (s), 714 (w), 629 (w). Elemental anal. calcd. for C₄₄H₄₀O₂: C 87.96 H 6.71, found: C 87.93 H 6.89. HRMS-MALDI (DCTB) (*m/z*): [M+Na]⁺ calcd. for C₄₄H₄₀NaO₂, 623.29205; found, 623.29442.

General Procedure (GP2) for the condensation of aldehyde and methylene.

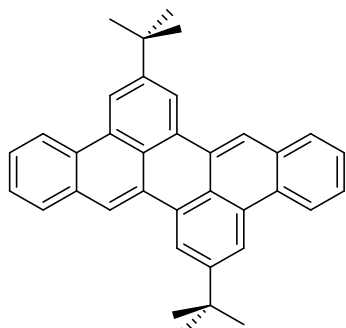
In a screw-capped vial ^tBuOK was added to a suspension of aldehyde atropisomer **5** in dry THF under argon. The reaction mixture was stirred at 60 °C for 16 hours. After cooling down to room temperature, the reaction mixture was poured into water (20 mL) and extracted with dichloromethane (3×50 mL) and the solvent was removed by rotary evaporation. The crude product was purified by silica gel column chromatography to give the product **6** as yellow or orange solid.

General Procedure (GP3) for the synthesis of **6 by combining GP1 and GP2.**

Step 1: In a screw-capped vial the mixture of boronic pinacol ester **3**, Pd₂(dba)₃, ^tBu₃PHBF₄, K₂CO₃ and bromo-aldehyde **4** were dissolved in degassed THF and degassed water and the

reaction mixture was heated at 80 °C overnight. After cooling down to room temperature, the solvents were removed by rotary evaporation. **Step 2:** ^tBuOK was added to the crude product **5** and dry THF was added to the solid mixture under argon. The screw-capped vial was stirred at 60 °C overnight. After cooling down to room temperature, the reaction mixture was poured into water, the yellow suspension extracted with dichloromethane (3×50 mL) and the solvent removed by rotary evaporation. The crude product was purified by silica gel column chromatography to give the product **6** as yellow to orange colored solid.

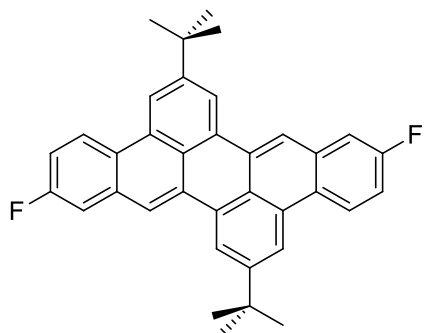
2,8-di-tert-butyldibenzo[*b,k*]perylene (6a)



According to **GP2**, the aldehyde **5a** (30 mg, 0.06 mmol), ^tBuOK (40 mg, 0.36 mmol) and dry THF (1 mL), after workup and silica gel column chromatography (light petroleum/dichloromethane 10:1) **6a** was obtained as yellow solid (22 mg, 79%).

According to **GP3, step 1**: boronic pinacol ester **3** (108 mg, 0.2 mmol), Pd₂(dba)₃ (9 mg, 0.01 mmol), ^tBu₃PHBF₄ (9 mg, 0.032 mmol), K₂CO₃ (55 mg, 0.4 mmol) and 2-bromo-benzaldehyde **4a** (89 mg, 0.48 mmol), degassed THF (1 mL), degassed water (0.25 mL). **Step 2:** ^tBuOK (135 mg, 1.20 mmol) and dry THF (4 mL) gave after workup and purification **6a** as yellow solid (72 mg, 77%). mp: 360 °C (dec.). ¹H NMR (500 MHz, CDCl₃) δ (ppm) = 8.68 (d, *J* = 1.2 Hz, 2H), 8.67-8.65 (m, 2H), 8.62 (d, *J* = 1.5 Hz, 2H), 8.47 (s, 2H), 7.99-7.97 (m, 2H), 7.64-7.59 (m, 4H), 1.63 (s, 18H). ¹³C NMR (125 MHz, CDCl₃) δ (ppm) = 149.3, 132.5, 131.0, 130.7, 130.2, 129.3, 129.0, 126.9, 126.5, 125.4, 122.7, 120.2, 119.5, 119.0, 35.4, 31.6. FT-IR (ATR) $\tilde{\nu}$ (cm⁻¹) = 3064(w), 3049 (w), 2951 (m), 2903 (w), 2864 (w), 1924 (w), 1909 (w), 1896 (w), 1869 (w), 1606 (m), 1571 (w), 1515 (w), 1459 (w), 1447 (w), 1413 (w), 1386 (w), 1362 (m), 1311 (w), 1284 (w), 1255 (m), 1222 (w), 1202 (w), 1152 (w), 1080 (w), 1036 (w), 1000 (w), 936 (w), 871 (m), 844 (m), 806 (w), 786 (m), 742 (s), 633 (m). Elemental anal. calcd. for C₃₆H₃₂: C 93.06 H 6.94, found: C 92.94 H 6.90. HRMS-MALDI (DCTB) (*m/z*): [M]⁺ calcd. for C₃₆H₃₂, 464.24985; found, 464.25055. UV/Vis (CHCl₃): λ_{max} (nm) (log ε) = 294(4.39), 306(4.49), 409(4.41), 434 (4.47). Fluorescence (CHCl₃): λ_{em} (λ_{ex}) (nm) = 448, 475, 508 (434).

2,8-di-tert-butyl-di-(4-fluorobenzo)-[b,k]perylene (6b)

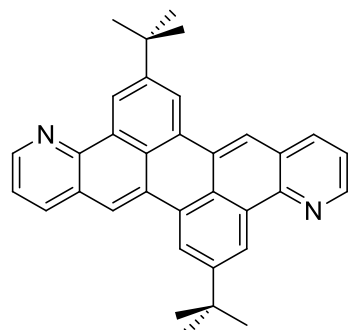


According to **GP2**, aldehyde **5b** (81 mg, 0.15 mmol), ¹BuOK (101 mg, 0.90 mmol) and dry THF (3 mL) gave after workup and silica gel column chromatography (light petroleum/dichloromethane 10:1) **6b** as yellow solid (39 mg, 51%).

According to **GP3, step 1**: boronic pinacol ester **3** (163 mg, 0.3 mmol), Pd₂(dba)₃ (14 mg, 0.015 mmol), ¹Bu₃PHBF₄ (14 mg, 0.049 mmol), K₂CO₃ (83 mg, 0.6 mmol) and 2-bromo-5-fluorobenzaldehyde **4b** (146 mg, 0.72 mmol), degassed THF (2 mL), degassed water (0.5 mL).

Step 2: ¹BuOK (202 mg, 1.80 mmol) and dry THF (5 mL), gave after workup and purification **6b** as yellow solid (78 mg, 52%). mp: > 400 °C (dec.). ¹H NMR (300 MHz, C₂D₂Cl₄, 373 K) δ (ppm) = 8.64-8.59 (m, 6H), 8.38 (s, 2H), 7.64 (dd, *J* = 9.8, 2.2 Hz, 2H), 7.38 (td, *J* = 8.8, 2.2 Hz, 2H), 1.65 (s, 18H). ¹³C NMR (75 MHz, C₂D₂Cl₄, 373 K) δ (ppm) = 161.6 (d, *J*_{C,F} = 246.7 Hz), 150.1, 133.9 (d, *J*_{C,F} = 8.8 Hz), 130.9, 130.4, 130.3, 126.8 (d, *J*_{C,F} = 1.5 Hz), 124.9 (d, *J*_{C,F} = 8.8 Hz), 124.8, 119.4, 119.4, 119.0, 115.3 (d, *J*_{C,F} = 23.9 Hz), 112.6 (d, *J*_{C,F} = 20.6 Hz), 35.2, 31.4. FT-IR (ATR) $\tilde{\nu}$ (cm⁻¹) = 3093(w), 3066 (w), 2961 (m), 2905 (w), 2867 (w), 1620 (m), 1607 (m), 1573 (w), 1520 (m), 1492 (m), 1462 (w), 1440 (m), 1411 (w), 1376 (w), 1360 (m), 1284 (m), 1259 (m), 1221 (m), 1168 (s), 1136 (m), 1111 (w), 1083 (w), 1002 (w), 974 (s), 931 (w), 886 (s), 865 (m), 855 (m), 839 (w), 812 (s), 783 (m), 769 (m), 756 (w), 723(w), 632 (m), 619 (m). Elemental anal. calcd. for C₃₆H₃₀F₂: C 86.37 H 6.04, found: C 86.26 H 6.03. HRMS-MALDI (DCTB) (*m/z*): [M]⁺ calcd. for C₃₆H₃₀F₂, 500.23101; found, 500.23405. UV/Vis (CHCl₃): λ_{max} (nm) (log ε) = 298 (4.36), 307(4.43), 389(4.17), 408 (4.44), 433 (4.48). Fluorescence (CHCl₃): λ_{em} (λ_{ex}) (nm) = 447, 474, 507 (433).

2,10-di-tert-butylanthra[9,1-*gh*:10,5-*g'h'*]diquinoline (6c)

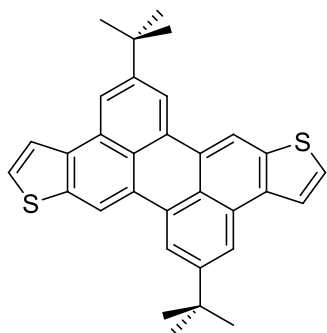


According to **GP2**, the aldehyde **5c** (103 mg, 0.21 mmol), ^tBuOK (135 mg, 1.21 mmol) and dry THF (4 mL) gave after workup and silica gel column chromatography (light petroleum/dichloromethane/ethyl acetate 10:1:1), **6c** as yellow-brown solid (53 mg, 55%).

According to **GP3, step 1**: boronic pinacol ester **3** (55 mg, 0.1 mmol), Pd₂(dba)₃ (4 mg, 0.004 mmol), ^tBu₃PHBF₄ (4 mg, 0.014 mmol), K₂CO₃ (28 mg, 0.2 mmol) and 2-bromonicotinaldehyde **4c** (45 mg, 0.24 mmol), degassed THF (0.5 mL), degassed water (0.1 mL). **Step 2**: ^tBuOK (68 mg, 0.6 mmol) and dry THF (2 mL), gave after workup and purification **6c** as yellow-brown solid (25 mg, 54%).

mp: > 400 °C (dec.). ¹H NMR (500 MHz, C₂D₂Cl₄) δ (ppm) = 9.36 (d, *J* = 1.6 Hz, 2H), 8.93 (dd, *J* = 4.3, 1.5 Hz, 2H), 8.66 (d, *J* = 1.6 Hz, 2H), 8.38 (s, 2H), 8.26 (d, *J* = 6.7 Hz, 2H), 7.52 (dd, *J* = 8.0, 4.3 Hz, 2H), 1.62 (s, 18H). ¹³C NMR (125 MHz, C₂D₂Cl₄) δ (ppm) = 150.2, 148.7, 146.1, 136.0, 132.0, 129.7, 129.5, 126.8, 126.6, 122.3, 121.2, 121.1, 118.5, 35.4, 31.5. FT-IR (ATR) $\tilde{\nu}$ (cm⁻¹) = 3053(w), 2950 (m), 2903 (m), 2864 (m), 1607 (m), 1589 (m), 1566 (m), 1509 (m), 1471 (m), 1406 (m), 1392 (m), 1361 (m), 1318 (w), 1301 (w), 1254 (m), 1214 (w), 1143 (m), 1106 (w), 1088 (w), 1048 (w), 1006 (w), 979 (w), 949 (w), 910 (m), 890 (m), 876 (s), 864 (s), 810 (m), 786 (s), 755 (w), 744 (w), 634 (m), 611 (m). Elemental anal. calcd. for C₃₄H₃₀N₂: C 87.52 H 6.48 N 6.00, found: C 87.20 H 6.57 N 5.77. HRMS-MALDI (DCTB) (*m/z*): [M+H]⁺ calcd. for C₃₄H₃₁N₂, 467.24818; found, 467.25114. UV/Vis (CHCl₃): λ_{max} (nm) (log ε) = 301(4.37), 314(4.36), 386(4.26), 408(4.48), 432(4.52). Fluorescence (CHCl₃): λ_{em} (λ_{ex}) (nm) = 446, 473, 506 (432).

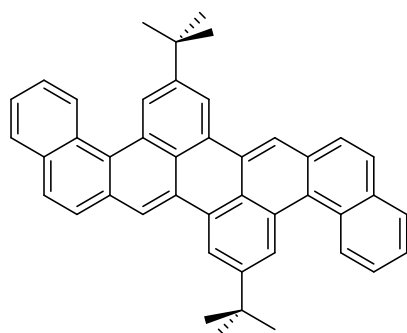
2,9-di-tert-butylperylene[2,3-*b*:8,9-*b'*]dithiophene (6d)



According to **GP2**, the aldehyde **5d** (64 mg, 0.12 mmol), $^t\text{BuOK}$ (84 mg, 0.75 mmol) and dry THF (3 mL) gave after workup and silica gel column chromatography (light petroleum/dichloromethane 10:1), **6d** as yellow solid (33 mg, 55%).

According to **GP3, step 1**: boronic pinacol ester **3** (55 mg, 0.1 mmol), $\text{Pd}_2(\text{dba})_3$ (4 mg, 0.004 mmol), $^t\text{Bu}_3\text{PHBF}_4$ (4 mg, 0.014 mmol), K_2CO_3 (28 mg, 0.2 mmol) and 3-bromothiophene-2-carbaldehyde **4d** (44 mg, 0.24 mmol), degassed THF (0.5 mL), degassed water (0.1 mL). **Step 2**: $^t\text{BuOK}$ (68 mg, 0.6 mmol) and dry THF (2 mL) gave after workup and purification **6d** as yellow solid (26 mg, 54%). mp: $> 400^\circ\text{C}$ (dec.). $^1\text{H NMR}$ (500 MHz, $\text{C}_2\text{D}_2\text{Cl}_4$) δ (ppm) = 8.60 (s, 2H), 8.39 (s, 2H), 8.17 (s, 2H), 7.95 (d, $J = 5.4$ Hz, 2H), 7.59 (d, $J = 5.4$ Hz, 2H), 1.54 (s, 18H). $^{13}\text{C NMR}$ (125 MHz, $\text{C}_2\text{D}_2\text{Cl}_4$) δ (ppm) = 149.7, 138.4, 135.6, 131.1, 130.0, 128.1, 126.4, 124.2, 122.3, 119.3, 118.2, 114.1, 35.0, 31.4. FT-IR (ATR) $\tilde{\nu}$ (cm^{-1}) = 2952 (m), 2901 (m), 2865 (m), 1607 (m), 1591 (m), 1519 (w), 1477 (m), 1460 (m), 1416 (w), 1389 (m), 1365 (m), 1294 (m), 1255 (m), 1203 (m), 1085 (m), 958 (m), 879 (w), 857 (m), 834 (m), 784 (m), 759 (m), 712 (m), 674 (m), 651 (s). Elemental anal. calcd. for $\text{C}_{32}\text{H}_{28}\text{S}_2$: C 80.63 H 5.92, found: C 80.45 H 6.26. HRMS-MALDI (DCTB) (m/z): [M] $^+$ calcd. for $\text{C}_{32}\text{H}_{28}\text{S}_2$, 476.16269; found, 476.16764. UV/Vis (CHCl_3): λ_{max} (nm) ($\log \varepsilon$) = 279(4.38), 289(4.50), 433(4.41), 461(4.49). Fluorescence (CHCl_3): λ_{em} (λ_{ex}) (nm) = 477, 510, 546 (461).

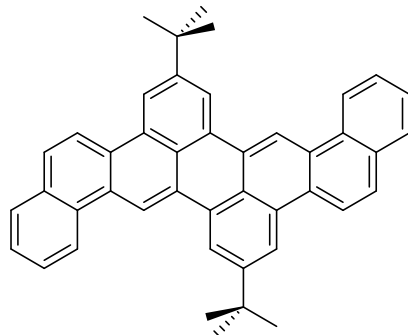
2,8-di-tert-butylidinaphtho[2,1-*b*:2',1'-*k*]perylene (6e)



According to **GP2**, the aldehyde **5e** (61 mg, 0.10 mmol) and $^t\text{BuOK}$ (68 mg, 0.60 mmol) were reacted in dry THF (2 mL). After cooling down to room temperature, the reaction mixture was poured into water (20 mL) and the yellow suspension was filtered off, washed with water (2×20 mL), methanol (10 mL), acetone (10 mL) and dichloromethane (10 mL) to give the product **6e**

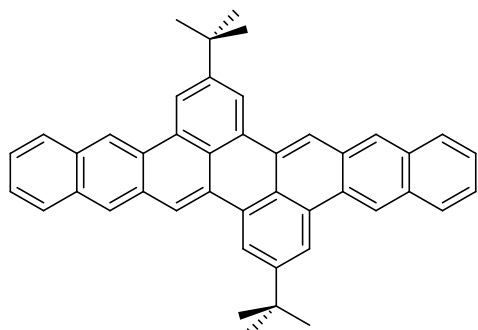
as yellow powder (45 mg, 79%). mp: > 400 °C (dec.). ^1H NMR (300 MHz, $\text{C}_2\text{D}_2\text{Cl}_4$, 403K) δ (ppm) = 9.12 (s, 2H), 9.09 (s, 2H), 8.65 (s, 2H), 8.54 (s, 2H), 8.05-7.91 (m, 6H), 7.72 (t, J = 7.6 Hz, 2H), 7.64 (t, J = 7.3 Hz, 2H), 1.68 (s, 18H). ^{13}C NMR (75 MHz, $\text{C}_2\text{D}_2\text{Cl}_4$, 403K) δ (ppm) = 149.1, 133.7, 131.7, 131.4, 130.5, 130.5, 130.4, 130.2, 128.5, 127.6, 127.4, 126.9, 126.8, 126.0, 125.7, 124.6, 120.5, 119.4, 35.2, 31.4. FT-IR (ATR) $\tilde{\nu}$ (cm $^{-1}$) = 3050(w), 2961 (m), 2903 (w), 2866 (w), 1604 (m), 1496 (w), 1474 (w), 1462 (w), 1396 (w), 1364 (w), 1255 (m), 1202 (w), 1164 (w), 1135(w), 1065 (w), 1051 (w), 1024 (w), 946 (w), 911 (w), 883 (s), 818 (s), 797 (m), 771 (w), 749 (s), 706 (w), 682 (m), 634 (m). Elemental anal. calcd. for $\text{C}_{44}\text{H}_{36} \cdot 0.6\text{THF}$: C 91.66 H 6.76, found: C 91.76 H 6.46. HRMS-MALDI (DCTB) (m/z): [M] $^+$ calcd. for $\text{C}_{44}\text{H}_{36}$, 564.28115; found, 564.28779. UV/Vis (CHCl_3): λ_{max} (nm) (log ε) = 266(4.52), 300(4.49), 310(4.47), 325(4.58), 340(4.25), 443(4.42), 471(4.52). Fluorescence (CHCl_3): λ_{em} (λ_{ex}) (nm) = 490, 524 567 (471).

2,8-di-tert-butylidinaphtho[1,2-*b*:1',2'-*k*]perylene (6f)



According to **GP2**, the aldehyde **5f** (60 mg, 0.10 mmol) and $^t\text{BuOK}$ (67 mg, 0.60 mmol) were reacted in dry THF (2 mL). After cooling down to room temperature, the reaction mixture was poured into water (20 mL) and the yellow suspension was filtered off, washed with water (2×20 mL), methanol (10 mL), acetone (10 mL) and refluxed in chloroform (5 mL) for 3 minutes. After cooling down to room temperature, the chloroform suspension was filtered off to give the product **6f** as orange powder (48 mg, 86%). mp: > 400 °C (dec.). ^1H NMR (300 MHz, $\text{C}_2\text{D}_2\text{Cl}_4$, 403K) δ (ppm) = 9.51 (s, 2H), 8.94 (d, J = 8.38 Hz, 2H), 8.82 (s, 2H), 8.80 (s, 2H), 8.70 (d, J = 9.10 Hz, 2H), 7.99-8.04 (m, 4H), 7.81 (t, J = 7.6 Hz, 2H), 7.69 (t, J = 7.4 Hz, 2H), 1.74 (s, 18H). ^{13}C NMR (125 MHz, $\text{C}_2\text{D}_2\text{Cl}_4$, 403K) δ (ppm) = 149.9, 132.6, 131.6, 131.2, 130.8, 129.8, 128.8, 128.5, 128.2, 127.2, 126.6, 126.3, 125.8, 122.7, 121.1, 119.3, 119.3, 114.7, 35.3, 31.5. FT-IR (ATR) $\tilde{\nu}$ (cm $^{-1}$) = 3086(w), 3066 (w), 2951 (m), 2904 (w), 2863 (w), 1606 (m), 1511 (w), 1478(w), 1461 (w), 1435 (w), 1425 (w), 1404 (w), 1360 (w), 1303 (w), 1262 (m), 1233 (w), 1203 (w), 1173 (w), 1153 (w), 1031 (w), 974 (w), 955 (w), 929 (w), 865 (s), 817 (s), 764 (s), 741 (s), 676 (m), 643 (w), 617 (m). Elemental anal. calcd. for $\text{C}_{44}\text{H}_{36} \cdot 0.3\text{THF}$: C 92.58 H 6.60, found: C 92.52 H 6.50. HRMS-MALDI (DCTB) (m/z): [M] $^+$ calcd. for $\text{C}_{44}\text{H}_{36}$, 564.28115; found, 564.28395. UV/Vis (CHCl_3): λ_{max} (nm) (log ε) = 269(4.81), 293(4.55), 306(4.69), 415(4.15), 439(4.47), 467(4.56). Fluorescence (CHCl_3): λ_{em} (λ_{ex}) (nm) = 484, 518, 558 (467).

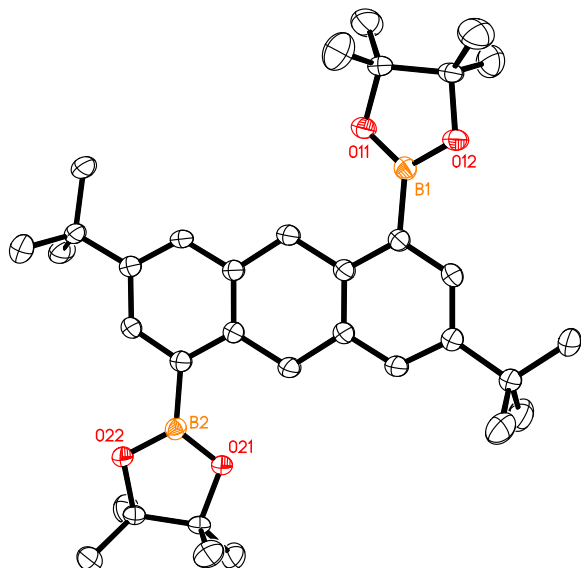
2,8-di-tert-butylidinapho[2,3-*b*:2',3'-*k*]perylene (6g)



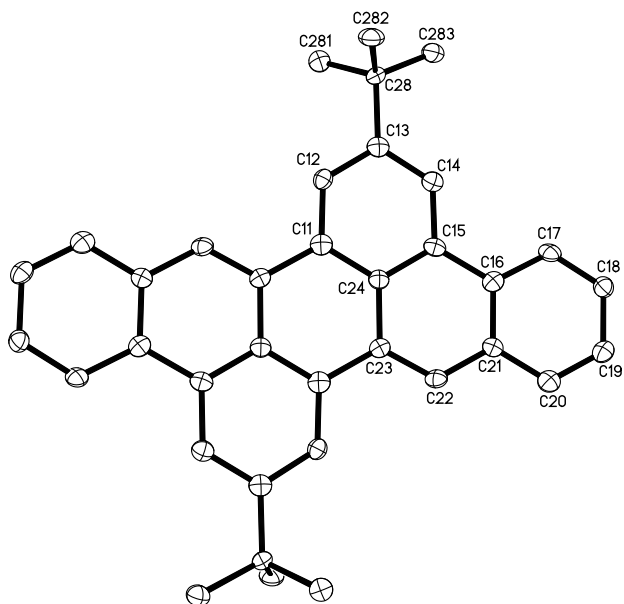
According to **GP2**, the aldehyde **5g** (90 mg, 0.15 mmol) and ^tBuOK (102 mg, 0.90 mmol) were reacted in dry THF (3 mL). After cooling down to room temperature, the reaction mixture was poured into water (20 mL) and the yellow suspension was filtered off, washed with water (2×20 mL), methanol (10 mL), acetone (10 mL) and refluxed in chloroform (5 mL) for 3 minutes. After cooling down to room temperature, the chloroform suspension was filtered off to give the product as yellow powder (69 mg, 84%). mp: > 400 °C (dec.). ¹H NMR (300 MHz, C₂D₂Cl₄, 403K) δ (ppm) = 9.12 (s, 2H), 8.92 (s, 2H), 8.72 (s, 2H), 8.57 (s, 2H), 8.49 (s, 2H), 8.17 (dd, *J* = 5.8, 2.8 Hz, 2H), 8.07 (dd, *J* = 5.8, 3.2 Hz, 2H), 7.56 (dd, *J* = 6.3, 3.1 Hz, 4H), 1.73 (s, 18H). ¹³C NMR (75 MHz, C₂D₂Cl₄, 403K) δ (ppm) = 150.0, 132.6, 132.3, 131.2, 131.1, 130.6, 129.3, 129.0, 128.3, 127.4, 127.0, 125.8, 125.5, 125.1, 121.3, 120.5, 119.7, 119.6, 35.2, 31.5. FT-IR (ATR) $\tilde{\nu}$ (cm⁻¹) = 3086(w), 3055 (w), 2952 (m), 2903 (w), 2862 (w), 1605 (m), 1511 (w), 1478 (w), 1461 (w), 1434 (w), 1425 (w), 1404 (w), 1390 (w), 1356 (m), 1302 (w), 1259 (m), 1203 (w), 1174 (w), 1153 (w), 1082 (w), 1001 (w), 955 (w), 943 (w), 892 (s), 865 (s), 833 (w), 818 (s), 765 (s), 753 (w), 737 (s), 677 (w), 644 (w), 626 (m), 618 (m). Elemental anal. calcd. for C₄₄H₃₆·0.1THF: C 93.24 H 6.49, found: C 93.11 H 6.46. HRMS-MALDI (DCTB) (*m/z*): [M]⁺ calcd. for C₄₄H₃₆, 564.28115; found, 564.28658. UV/Vis (CHCl₃): λ_{max} (nm) (log ε) = 269(5.14), 292(4.71), 346(4.40), 355(4.38), 373(4.29), 397(4.46), 419 (4.76), 445(4.81). Fluorescence (CHCl₃): λ_{em} (λ_{ex}) (nm) = 491, 527, 569 (445).

3. X-ray crystallographic structure determination

Table S1. Crystal data and structure refinement for **3** (CCDC 1482798).

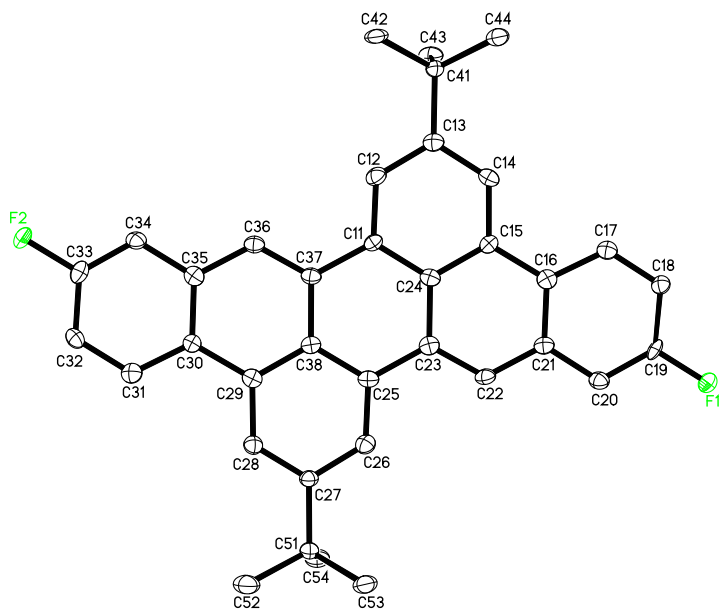


Empirical formula	$C_{34}H_{50}B_2O_4$		
Formula weight	544.36		
Temperature	200(2) K		
Wavelength	0.71073 Å		
Crystal system	monoclinic		
Space group	$P2_1/n$		
Z	4		
Unit cell dimensions	$a = 12.4137(5)$ Å	$\alpha = 90$ deg.	$b = 19.2998(9)$ Å
	$c = 13.6359(6)$ Å	$\beta = 92.0918(12)$ deg.	$\gamma = 90$ deg.
Volume	$3264.7(2)$ Å ³		
Density (calculated)	1.11 g/cm ³		
Absorption coefficient	0.07 mm ⁻¹		
Crystal shape	polyhedron		
Crystal size	$0.210 \times 0.170 \times 0.150$ mm ³		
Crystal colour	colourless		
Theta range for data collection	1.8 to 25.1 deg.		
Index ranges	$-14 \leq h \leq 14, -22 \leq k \leq 22, -12 \leq l \leq 16$		
Reflections collected	20729		
Independent reflections	5772 ($R(\text{int}) = 0.0339$)		
Observed reflections	4187 ($I > 2\sigma(I)$)		
Absorption correction	Semi-empirical from equivalents		
Max. and min. transmission	0.96 and 0.87		
Refinement method	Full-matrix least-squares on F^2		
Data/restraints/parameters	5772 / 0 / 375		
Goodness-of-fit on F^2	1.03		
Final R indices ($I > 2\sigma(I)$)	$R_1 = 0.054, wR_2 = 0.134$		
Largest diff. peak and hole	0.29 and -0.20 eÅ ⁻³		

Table S2. Crystal data and structure refinement for **6a**. (CCDC 1482799)

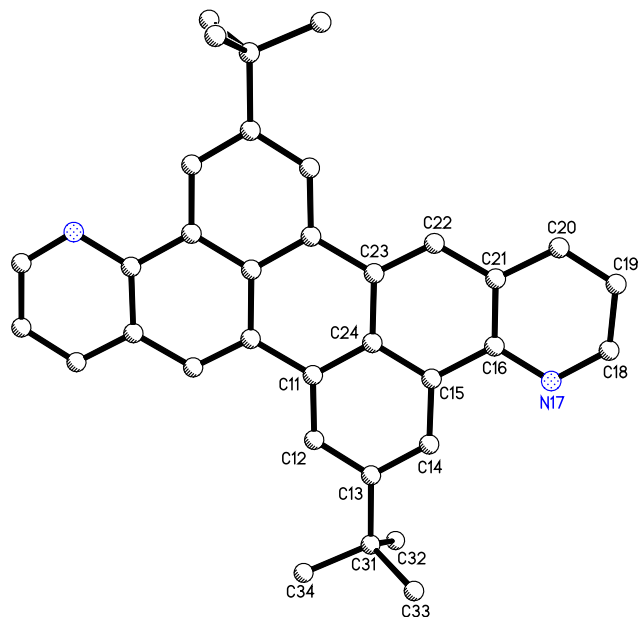
Empirical formula	$C_{30}H_{42}$		
Formula weight	474.69		
Temperature	100(2) K		
Wavelength	0.71073 Å		
Crystal system	monoclinic		
Space group	P2 ₁ /c		
Z	2		
Unit cell dimensions	$a = 12.654(4)$ Å	$\alpha = 90$ deg.	
	$b = 5.9003(19)$ Å	$\beta = 92.546(10)$ deg.	
	$c = 16.299(5)$ Å	$\gamma = 90$ deg.	
Volume	$1215.7(7)$ Å ³		
Density (calculated)	1.30 g/cm ³		
Absorption coefficient	0.07 mm ⁻¹		
Crystal shape	needle		
Crystal size	$0.950 \times 0.050 \times 0.040$ mm ³		
Crystal colour	orange		
Theta range for data collection	2.5 to 22.0 deg.		
Index ranges	$-13 \leq h \leq 13, -6 \leq k \leq 6, -17 \leq l \leq 14$		
Reflections collected	4969		
Independent reflections	1479 ($R(\text{int}) = 0.0661$)		
Observed reflections	1055 ($I > 2\sigma(I)$)		
Absorption correction	Semi-empirical from equivalents		
Max. and min. transmission	0.96 and 0.78		
Refinement method	Full-matrix least-squares on F^2		
Data/restraints/parameters	1479 / 150 / 166		
Goodness-of-fit on F^2	1.05		
Final R indices ($I > 2\sigma(I)$)	$R_1 = 0.069, wR_2 = 0.161$		
Largest diff. peak and hole	0.20 and -0.26 eÅ ⁻³		

Table S3. Crystal data and structure refinement for **6b**. (CCDC 1482802)



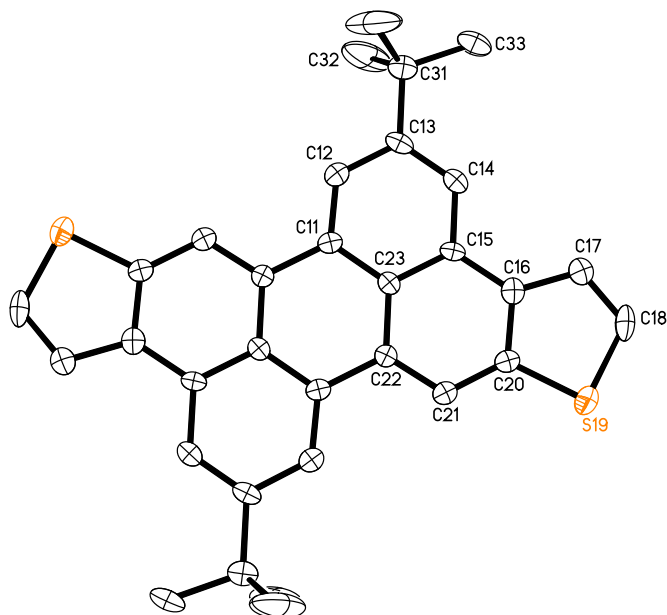
Empirical formula	$C_{36}H_{30}F_2$	
Formula weight	500.60	
Temperature	100(2) K	
Wavelength	0.71073 Å	
Crystal system	monoclinic	
Space group	P2 ₁ /c	
Z	4	
Unit cell dimensions	$a = 25.340(5)$ Å	$\alpha = 90$ deg.
	$b = 5.8908(12)$ Å	$\beta = 93.285(4)$ deg.
	$c = 16.810(3)$ Å	$\gamma = 90$ deg.
Volume	$2505.1(9)$ Å ³	
Density (calculated)	1.33 g/cm ³	
Absorption coefficient	0.09 mm ⁻¹	
Crystal shape	octahedron	
Crystal size	$0.310 \times 0.130 \times 0.100$ mm ³	
Crystal colour	yellow	
Theta range for data collection	0.8 to 24.6 deg.	
Index ranges	$-29 \leq h \leq 29, -4 \leq k \leq 6, -19 \leq l \leq 19$	
Reflections collected	9373	
Independent reflections	3904 ($R(\text{int}) = 0.0430$)	
Observed reflections	2617 ($I > 2\sigma(I)$)	
Absorption correction	Semi-empirical from equivalents	
Max. and min. transmission	0.96 and 0.87	
Refinement method	Full-matrix least-squares on F^2	
Data/restraints/parameters	3904 / 0 / 343	
Goodness-of-fit on F^2	1.07	
Final R indices ($I > 2\sigma(I)$)	$R_1 = 0.068, wR_2 = 0.136$	
Largest diff. peak and hole	0.21 and -0.33 eÅ ⁻³	

Table S4. Crystal data and structure refinement for **6c**. (CCDC 1482800)



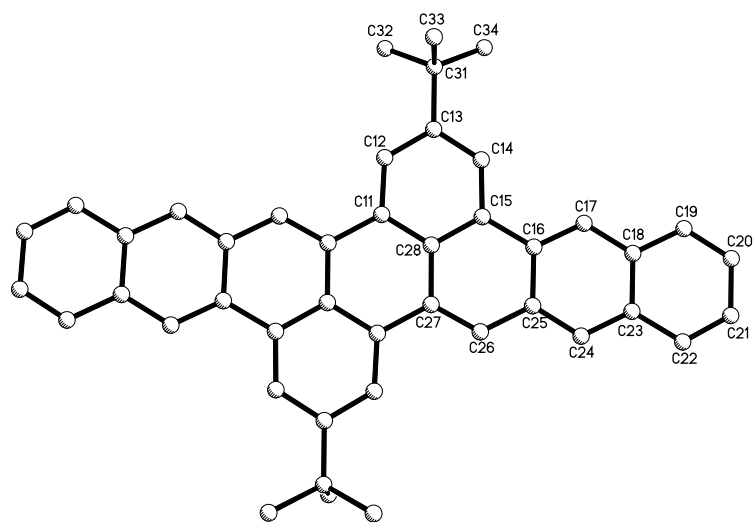
Empirical formula	$C_{36}H_{32}Cl_6N_2$		
Formula weight	705.33		
Temperature	100(2) K		
Wavelength	0.71073 Å		
Crystal system	triclinic		
Space group	$P\bar{1}$		
Z	1		
Unit cell dimensions	$a = 6.1980(13)$ Å	$\alpha = 82.109(5)$ deg.	
	$b = 9.0318(19)$ Å	$\beta = 80.926(5)$ deg.	
	$c = 14.731(3)$ Å	$\gamma = 80.752(5)$ deg.	
Volume	$798.4(3)$ Å ³		
Density (calculated)	1.47 g/cm ³		
Absorption coefficient	0.57 mm ⁻¹		
Crystal shape	needle		
Crystal size	$0.350 \times 0.060 \times 0.050$ mm ³		
Crystal colour	yellow		
Theta range for data collection	2.3 to 22.1 deg.		
Index ranges	$-6 \leq h \leq 6, -9 \leq k \leq 9, -15 \leq l \leq 15$		
Reflections collected	4549		
Independent reflections	1960 ($R(\text{int}) = 0.0404$)		
Observed reflections	1512 ($I > 2\sigma(I)$)		
Absorption correction	Semi-empirical from equivalents		
Max. and min. transmission	0.96 and 0.84		
Refinement method	Full-matrix least-squares on F^2		
Data/restraints/parameters	1960 / 0 / 199		
Goodness-of-fit on F^2	1.08		
Final R indices ($I > 2\sigma(I)$)	$R1 = 0.054, wR2 = 0.104$		
Largest diff. peak and hole	0.25 and -0.42 eÅ ⁻³		

Table S5. Crystal data and structure refinement for **6d**. (CCDC 1482803)



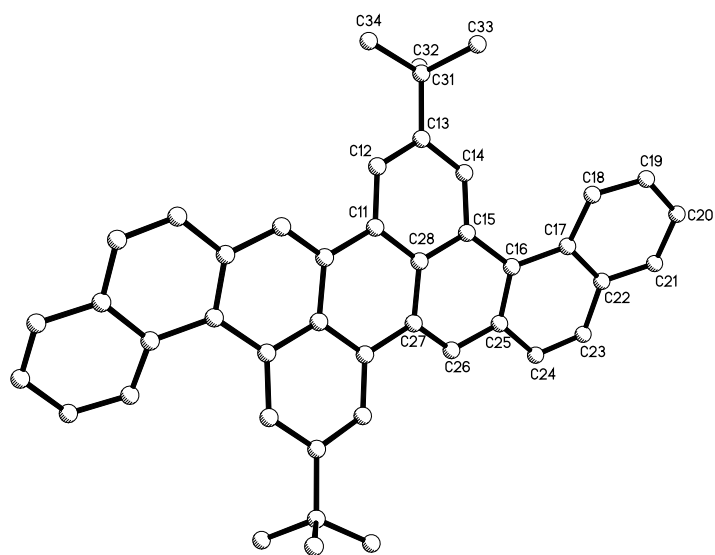
Empirical formula	$C_{32}H_{28}S_2$		
Formula weight	476.66		
Temperature	200(2) K		
Wavelength	0.71073 Å		
Crystal system	monoclinic		
Space group	P2/m		
Z	4		
Unit cell dimensions	$a = 14.1153(14)$ Å	$\alpha = 90$ deg.	
	$b = 6.9565(7)$ Å	$\beta = 91.144(3)$ deg.	
	$c = 24.324(3)$ Å	$\gamma = 90$ deg.	
Volume	$2388.0(4)$ Å ³		
Density (calculated)	1.33 g/cm ³		
Absorption coefficient	0.24 mm ⁻¹		
Crystal shape	needle		
Crystal size	$0.350 \times 0.060 \times 0.040$ mm ³		
Crystal colour	yellow		
Theta range for data collection	0.8 to 24.2 deg.		
Index ranges	$-16 \leq h \leq 13, -8 \leq k \leq 8, -27 \leq l \leq 27$		
Reflections collected	14215		
Independent reflections	4151 ($R(\text{int}) = 0.0476$)		
Observed reflections	3172 ($I > 2\sigma(I)$)		
Absorption correction	Semi-empirical from equivalents		
Max. and min. transmission	0.96 and 0.84		
Refinement method	Full-matrix least-squares on F^2		
Data/restraints/parameters	4151 / 0 / 405		
Goodness-of-fit on F^2	1.12		
Final R indices ($I > 2\sigma(I)$)	$R_1 = 0.069, wR_2 = 0.162$		
Largest diff. peak and hole	0.59 and -0.43 eÅ ⁻³		

Table S6. Crystal data and structure refinement for **6g**. (CCDC 1482801)



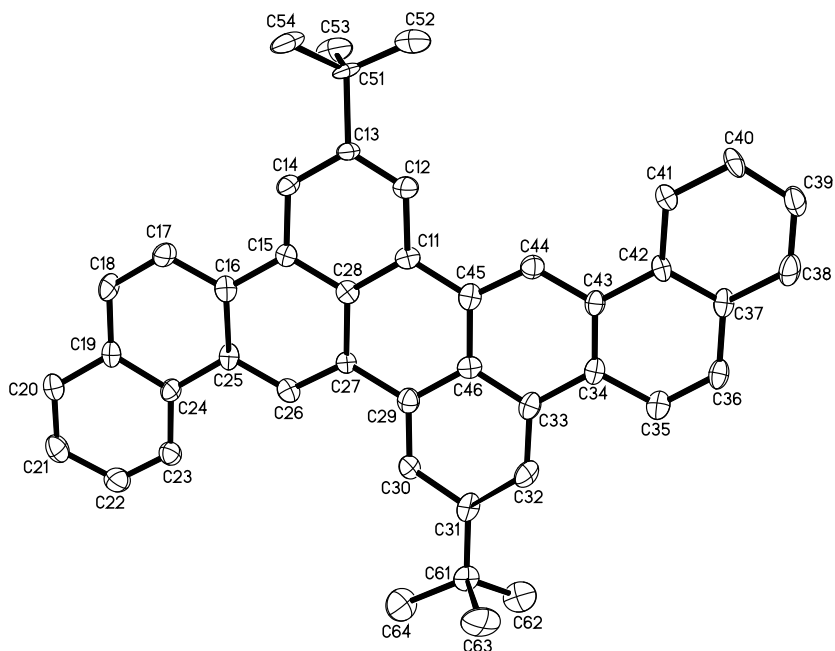
Empirical formula	C ₄₄ H ₃₆
Formula weight	564.73
Temperature	200(2) K
Wavelength	0.71073 Å
Crystal system	triclinic
Space group	P $\bar{1}$
Z	1
Unit cell dimensions	$a = 6.0472(16)$ Å $\alpha = 82.367(7)$ deg. $b = 9.675(3)$ Å $\beta = 79.563(8)$ deg. $c = 13.478(4)$ Å $\gamma = 71.879(7)$ deg.
Volume	734.6(3) Å ³
Density (calculated)	1.28 g/cm ³
Absorption coefficient	0.07 mm ⁻¹
Crystal shape	needle
Crystal size	0.330 x 0.060 x 0.030 mm ³
Crystal colour	yellow
Theta range for data collection	1.5 to 22.2 deg.
Index ranges	-6 ≤ h ≤ 6, -10 ≤ k ≤ 10, -14 ≤ l ≤ 14
Reflections collected	5965
Independent reflections	1857 (R(int) = 0.0527)
Observed reflections	1081 ($I > 2\sigma(I)$)
Absorption correction	Semi-empirical from equivalents
Max. and min. transmission	0.96 and 0.86
Refinement method	Full-matrix least-squares on F ²
Data/restraints/parameters	1857 / 0 / 202
Goodness-of-fit on F ²	1.08
Final R indices (I>2sigma(I))	R1 = 0.066, wR2 = 0.168
Largest diff. peak and hole	0.19 and -0.27 eÅ ⁻³

Table S7. Crystal data and structure refinement for **6e**. (CCDC 1482805)



Empirical formula	$C_{44}H_{36}$		
Formula weight	564.73		
Temperature	200(2) K		
Wavelength	0.71073 Å		
Crystal system	monoclinic		
Space group	C2/c		
Z	4		
Unit cell dimensions	$a = 28.725(3)$ Å	$\alpha = 90$ deg.	
	$b = 6.0124(6)$ Å	$\beta = 119.579(2)$ deg.	
	$c = 19.5850(19)$ Å	$\gamma = 90$ deg.	
Volume	$2941.6(5)$ Å ³		
Density (calculated)	1.27 g/cm ³		
Absorption coefficient	0.07 mm ⁻¹		
Crystal shape	needle		
Crystal size	$0.820 \times 0.050 \times 0.030$ mm ³		
Crystal colour	yellow		
Theta range for data collection	1.6 to 23.8 deg.		
Index ranges	$-32 \leq h \leq 32, -6 \leq k \leq 6, -22 \leq l \leq 22$		
Reflections collected	12133		
Independent reflections	2258 (R(int) = 0.0470)		
Observed reflections	1714 ($I > 2\sigma(I)$)		
Absorption correction	Semi-empirical from equivalents		
Max. and min. transmission	0.96 and 0.89		
Refinement method	Full-matrix least-squares on F ²		
Data/restraints/parameters	2258 / 0 / 210		
Goodness-of-fit on F ²	1.06		
Final R indices (I>2sigma(I))	R1 = 0.043, wR2 = 0.099		
Largest diff. peak and hole	0.14 and -0.25 eÅ ⁻³		

Table S8. Crystal data and structure refinement for **6f**. (CCDC 1482804)



Empirical formula	C ₄₄ H ₃₆
Formula weight	564.73
Temperature	200(2) K
Wavelength	0.71073 Å
Crystal system	orthorhombic
Space group	Pca2 ₁
Z	4
Unit cell dimensions	$a = 22.119(6)$ Å $\alpha = 90$ deg. $b = 6.2411(16)$ Å $\beta = 90$ deg. $c = 21.509(6)$ Å $\gamma = 90$ deg. 2969.2(14) Å ³
Volume	1.26 g/cm ³
Density (calculated)	0.07 mm ⁻¹
Absorption coefficient	needle
Crystal shape	0.180 × 0.070 × 0.070 mm ³
Crystal size	orange
Crystal colour	1.8 to 25.1 deg.
Theta range for data collection	$-26 \leq h \leq 26$, $-7 \leq k \leq 7$, $-25 \leq l \leq 25$
Index ranges	17056
Reflections collected	5239 (R(int) = 0.1124)
Independent reflections	3016 ($I > 2\sigma(I)$)
Observed reflections	Semi-empirical from equivalents
Absorption correction	0.96 and 0.73
Max. and min. transmission	Full-matrix least-squares on F ²
Refinement method	5239 / 673 / 398
Data/restraints/parameters	1.04
Goodness-of-fit on F ²	R1 = 0.092, wR2 = 0.239
Final R indices (I>2sigma(I))	10.0(10)
Absolute structure parameter	0.51 and -0.35 eÅ ⁻³
Largest diff. peak and hole	

4. NMR and FT-IR spectra

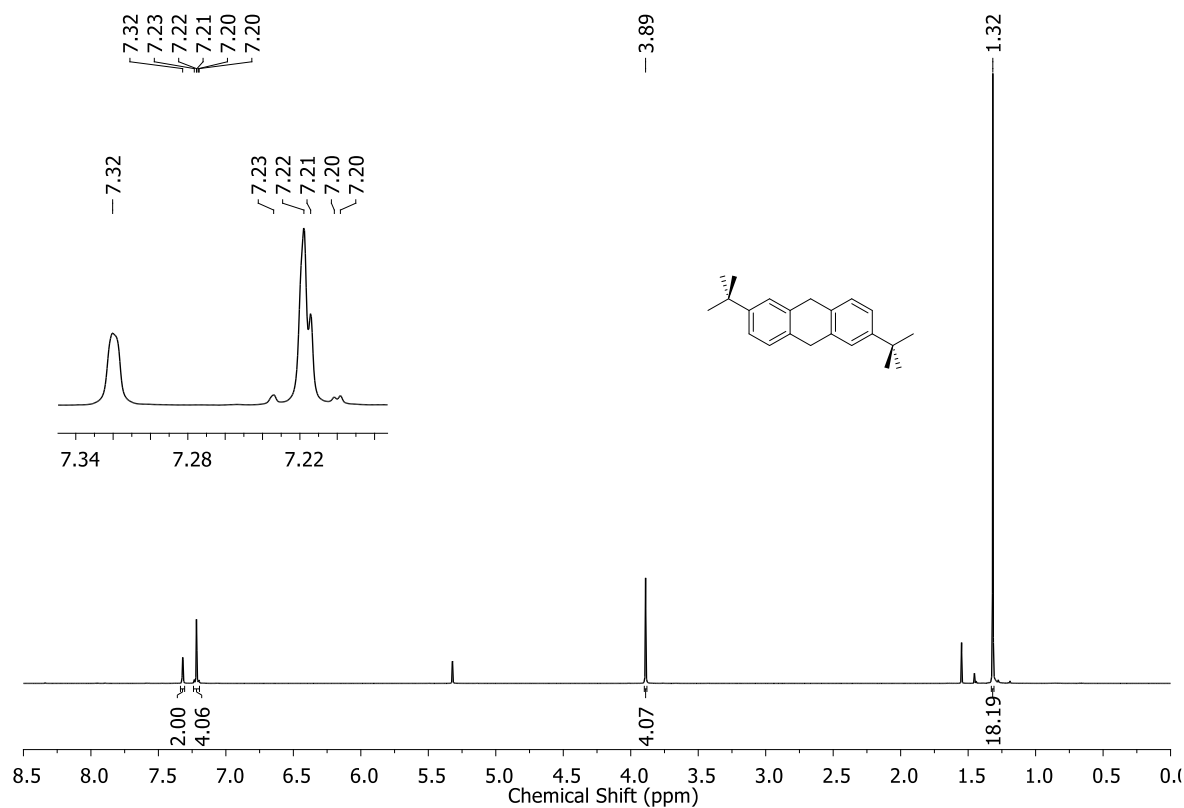


Figure S1. ^1H NMR spectrum (CD_2Cl_2 , 500MHz) of **2**.

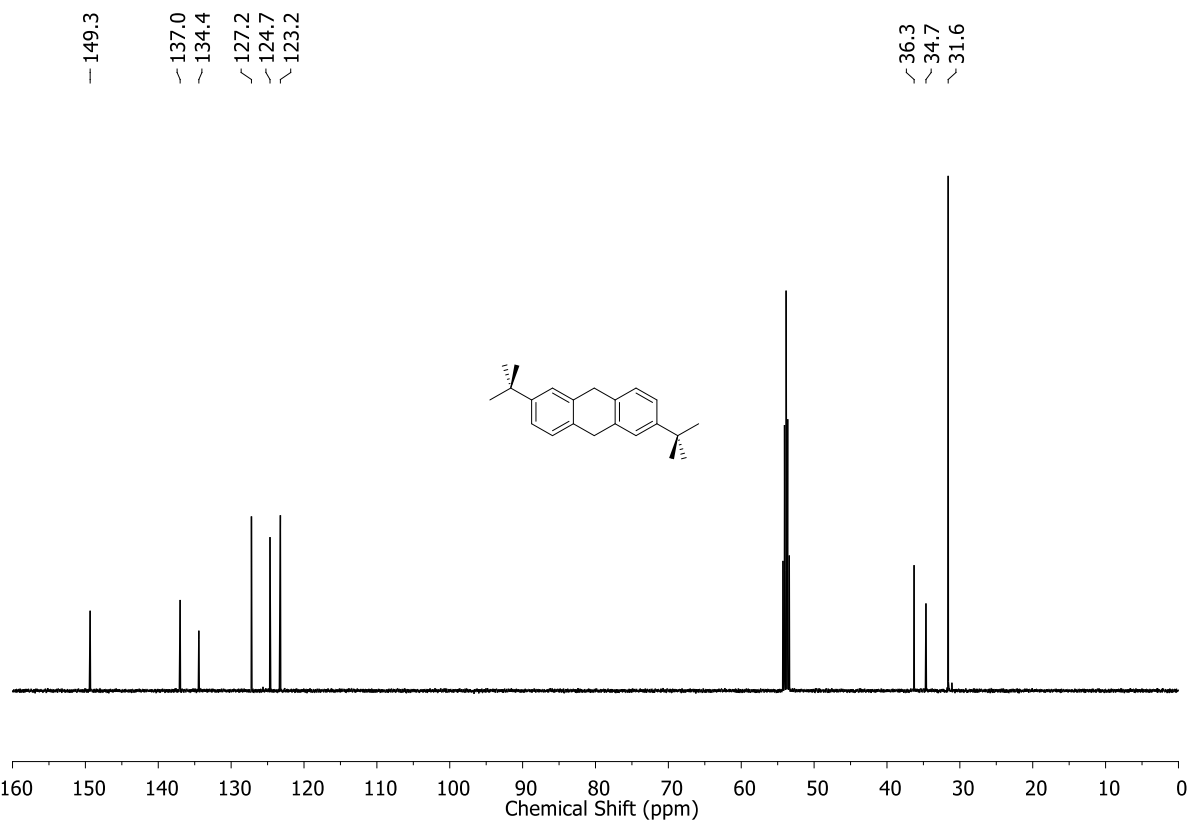


Figure S2. ^{13}C NMR spectrum (CD_2Cl_2 , 125MHz) of **2**.

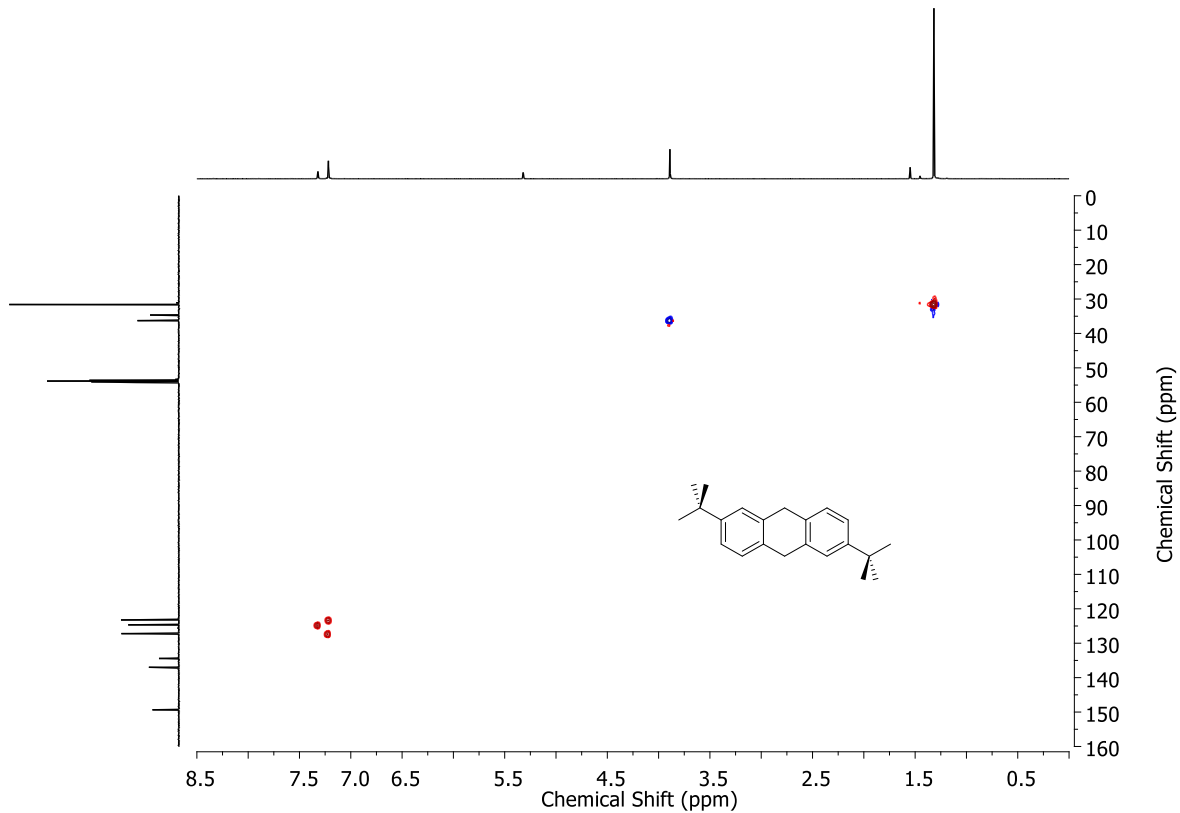


Figure S3. HSQC NMR spectrum of **2**.

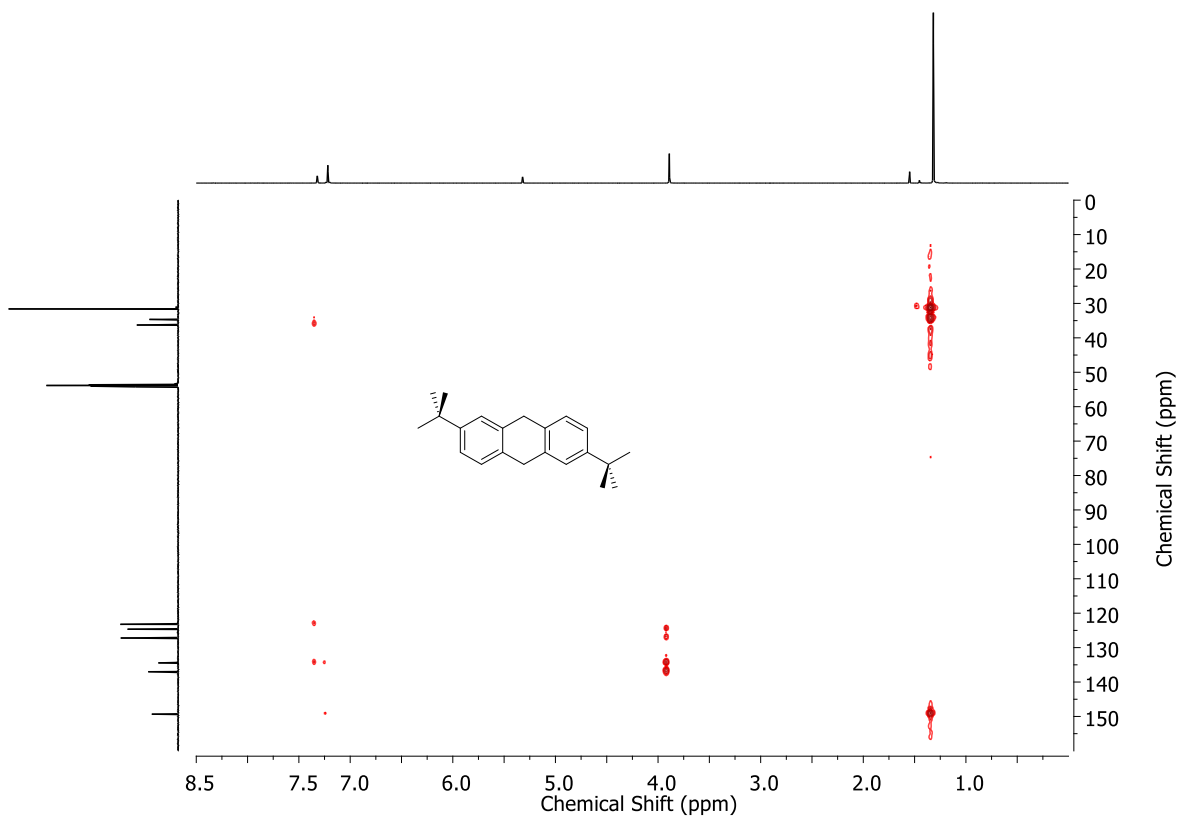


Figure S4. HMBC NMR spectrum of **2**.

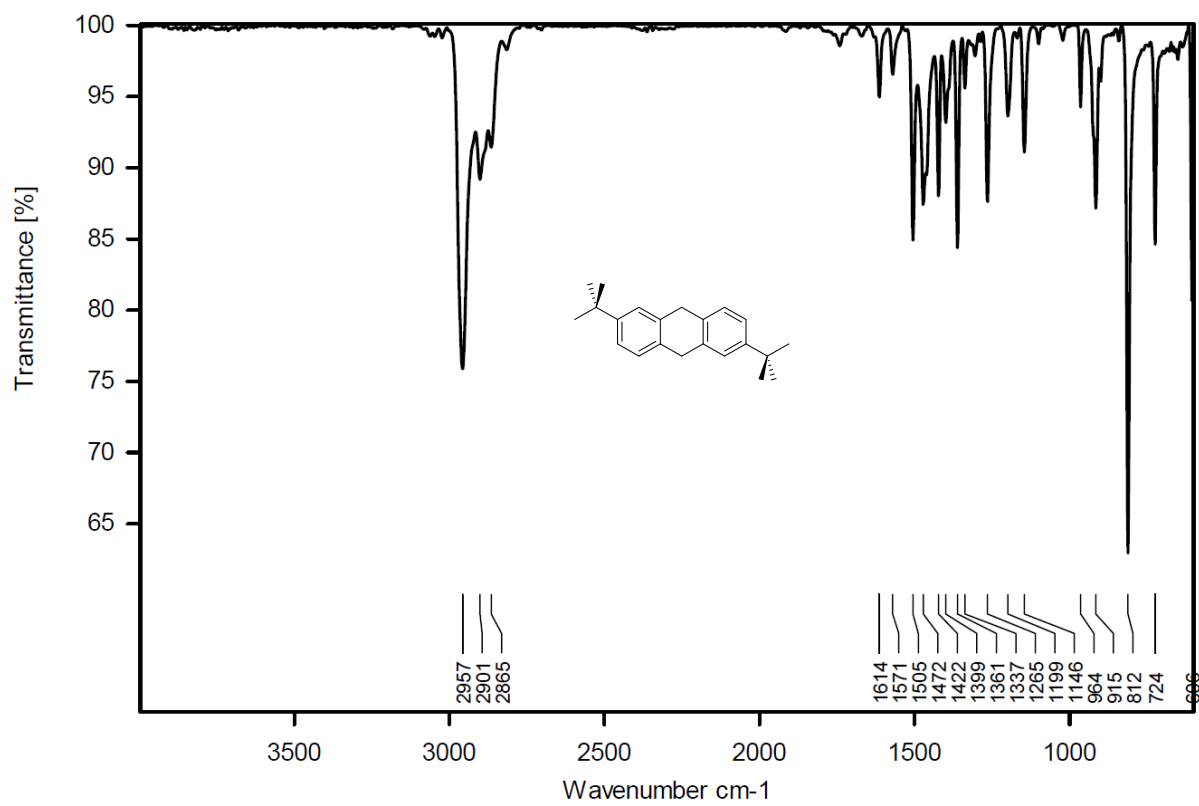


Figure S5. FT-IR spectrum (ATR) of **2**.

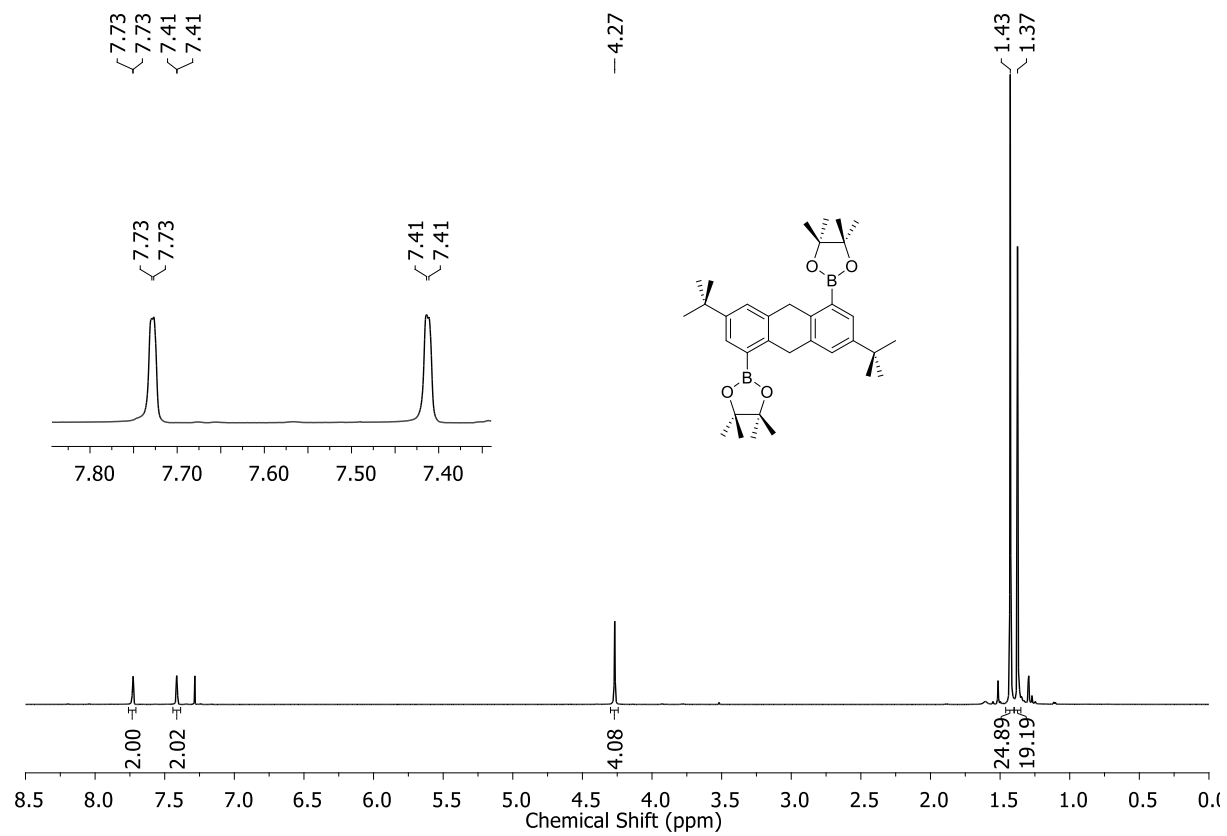


Figure S6. ^1H NMR spectrum (CDCl_3 , 500MHz) of **3**.

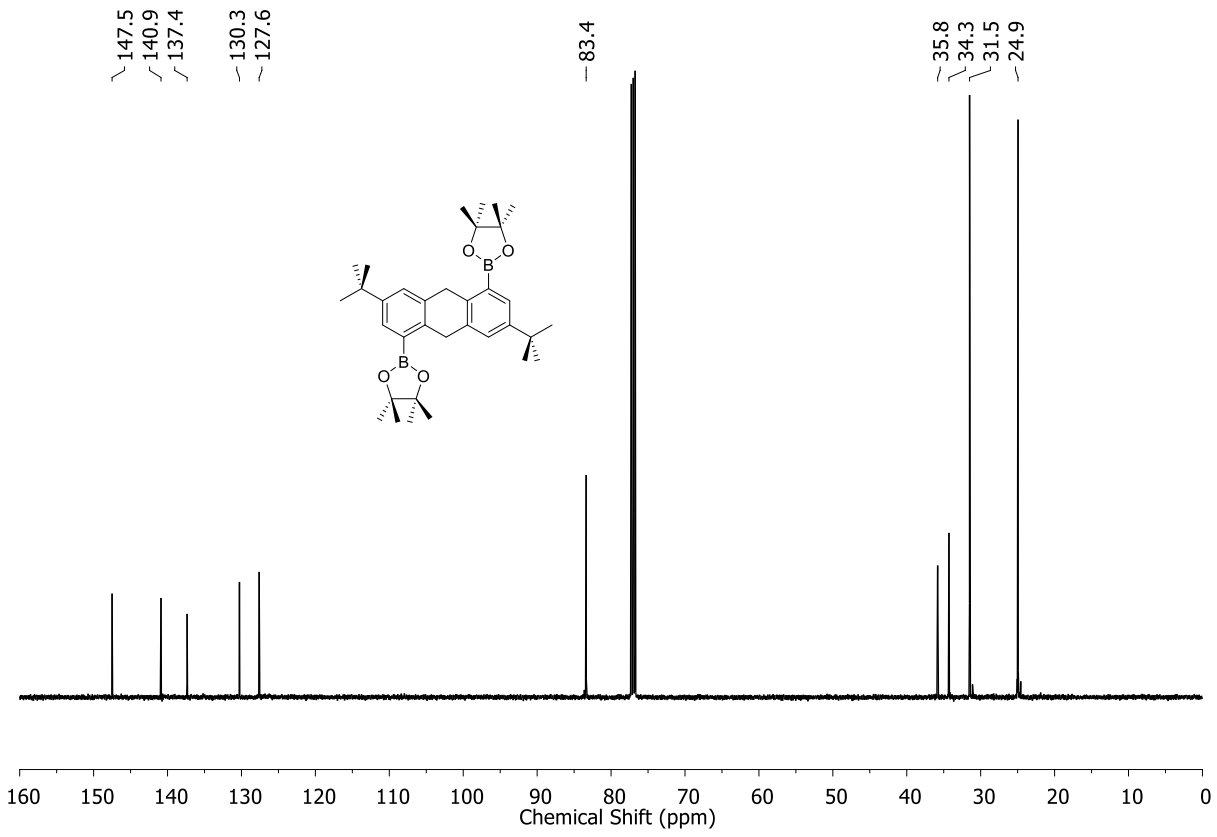


Figure S7. ^{13}C NMR spectrum (CDCl_3 , 125MHz) of **3**.

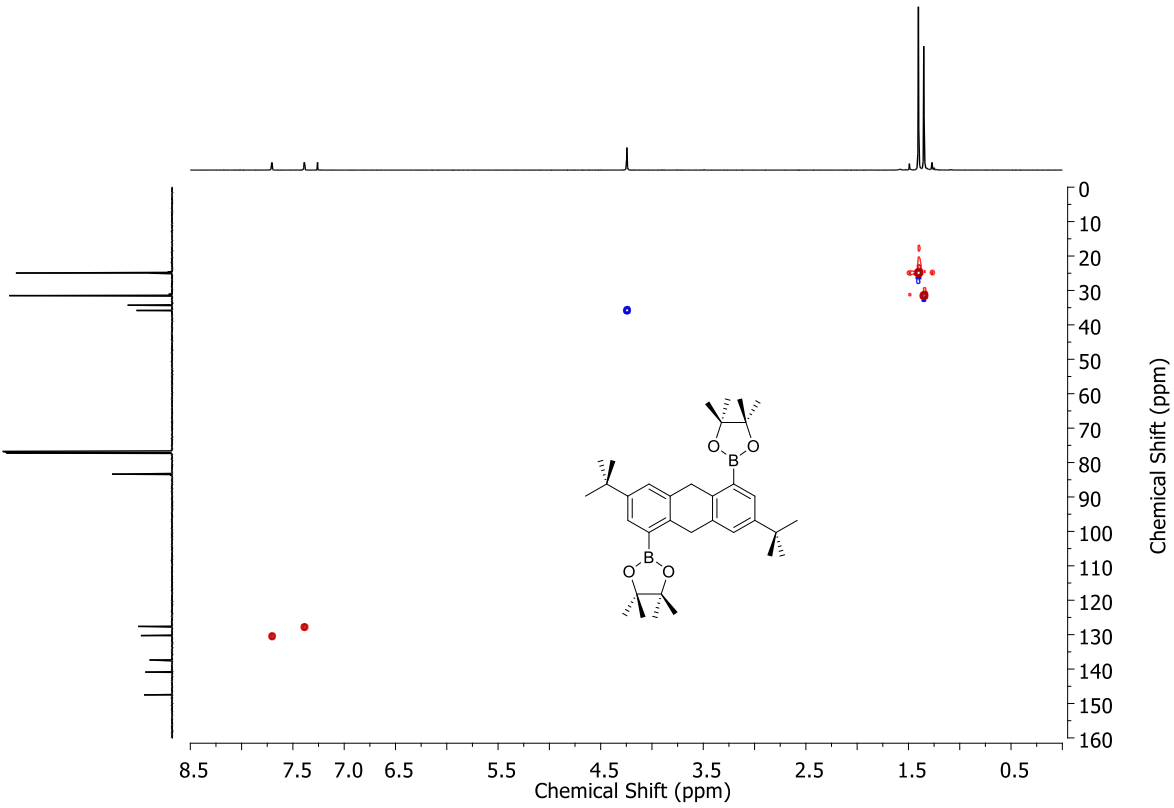


Figure S8. HSQC NMR spectrum of **3**.

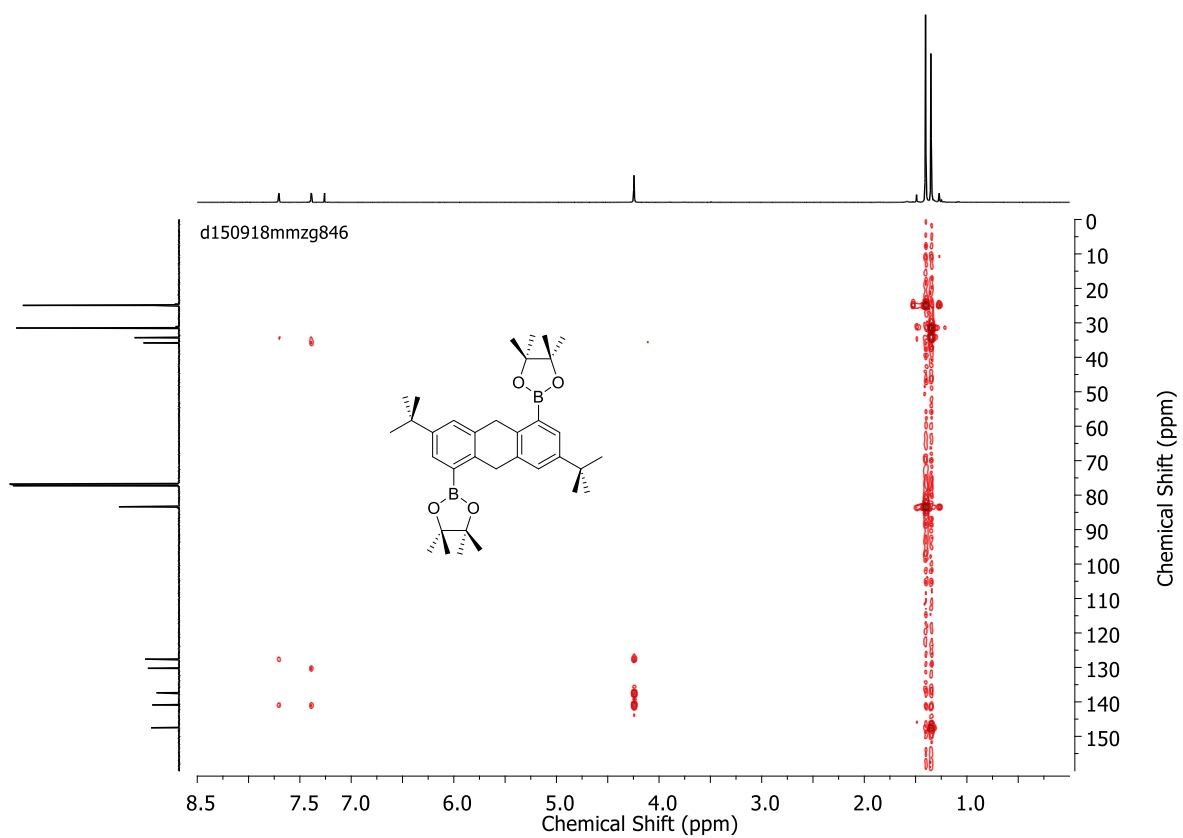


Figure S9. HMBC NMR spectrum of **3**.

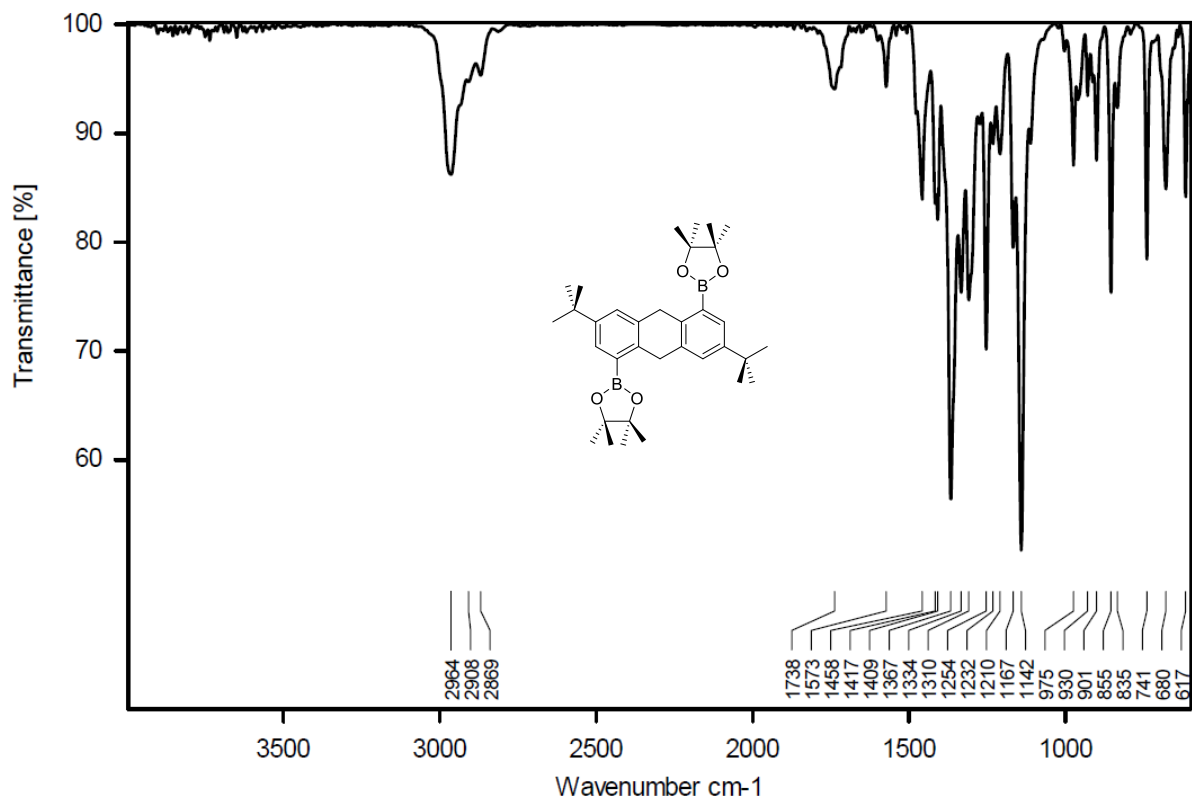


Figure S10. FT-IR spectrum (ATR) of **3**.

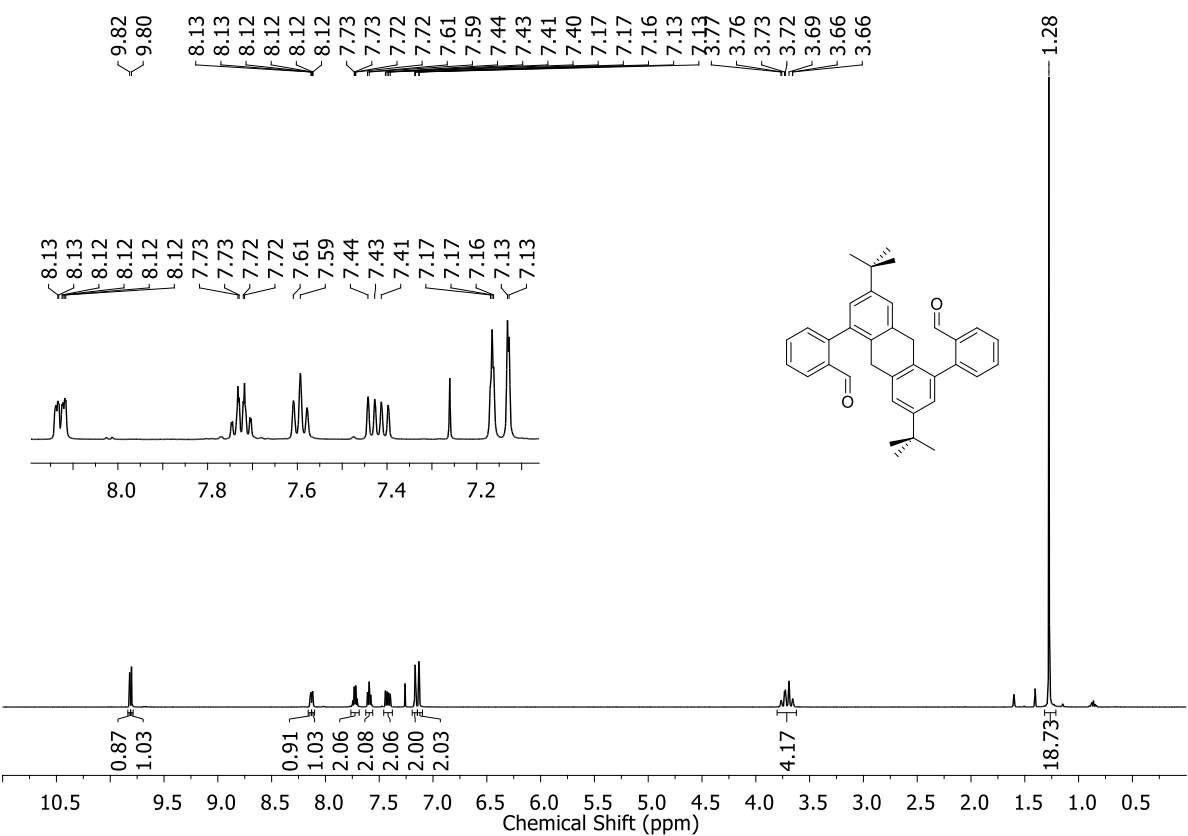


Figure S11. ^1H NMR spectrum (CDCl_3 , 500MHz) of the atropisomeric mixture of **5a**.

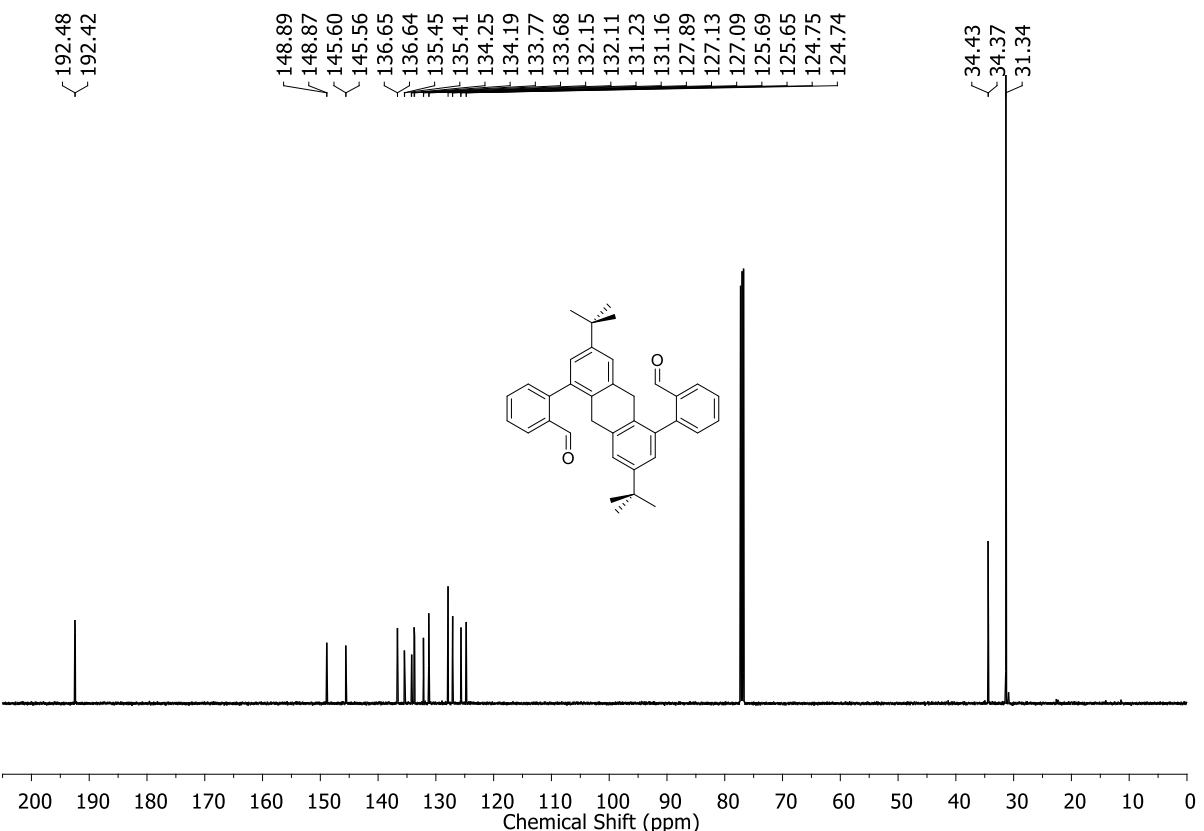


Figure S12. ^{13}C NMR spectrum (CDCl_3 , 125MHz) of the atropisomeric mixture of **5a**.

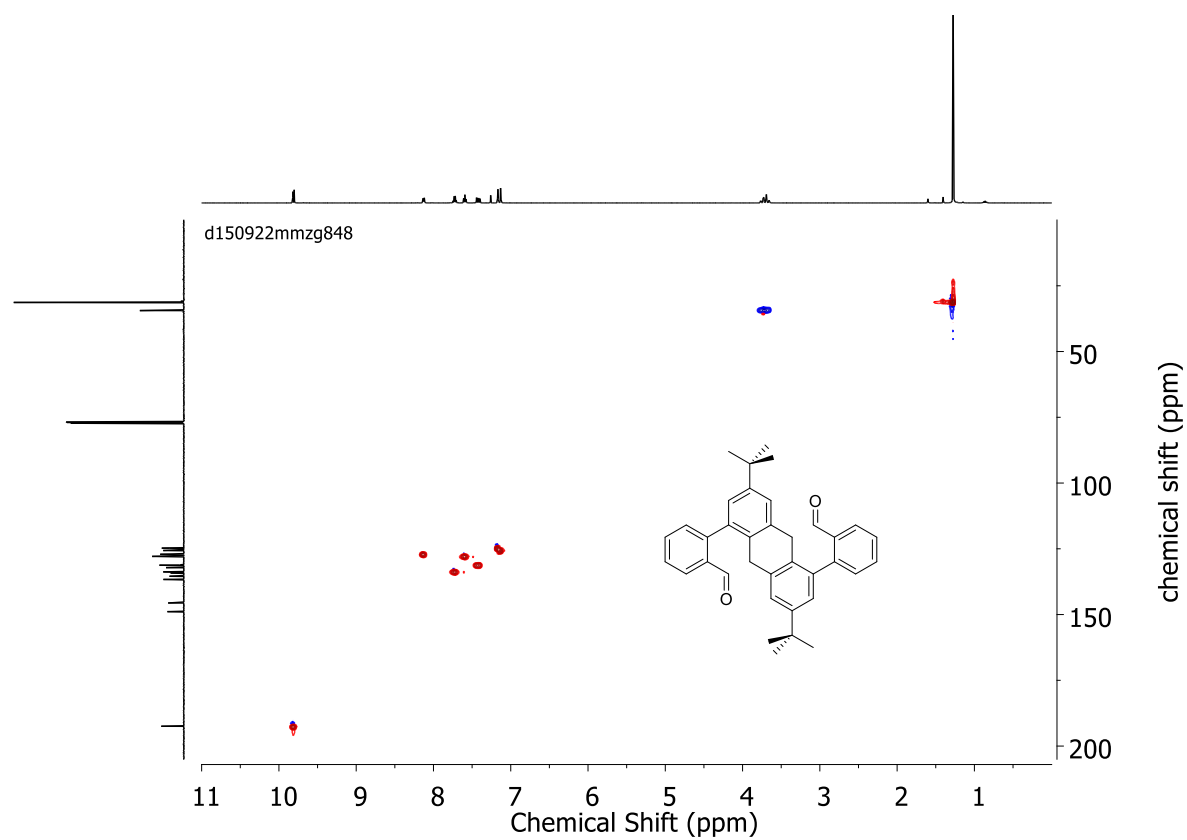


Figure S13. HSQC NMR spectrum of the atropisomeric mixture of **5a**.

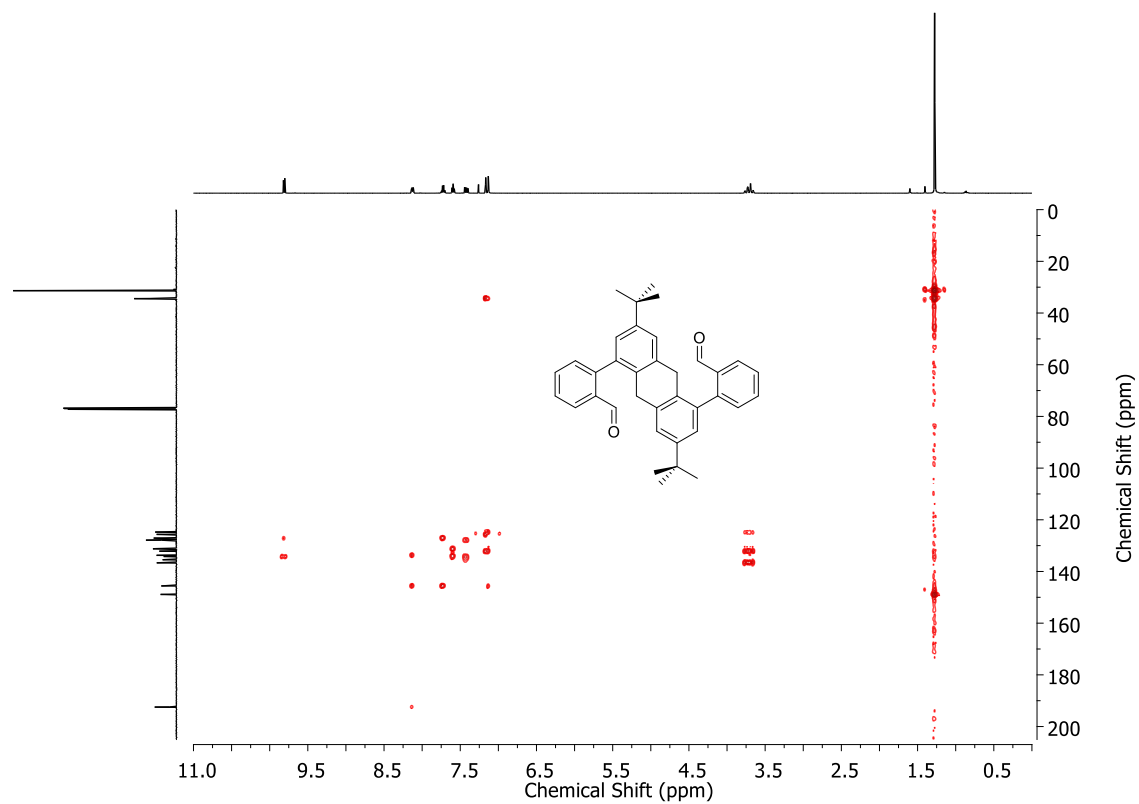


Figure S14. HMBC NMR spectrum of the atropisomeric mixture of **5a**.

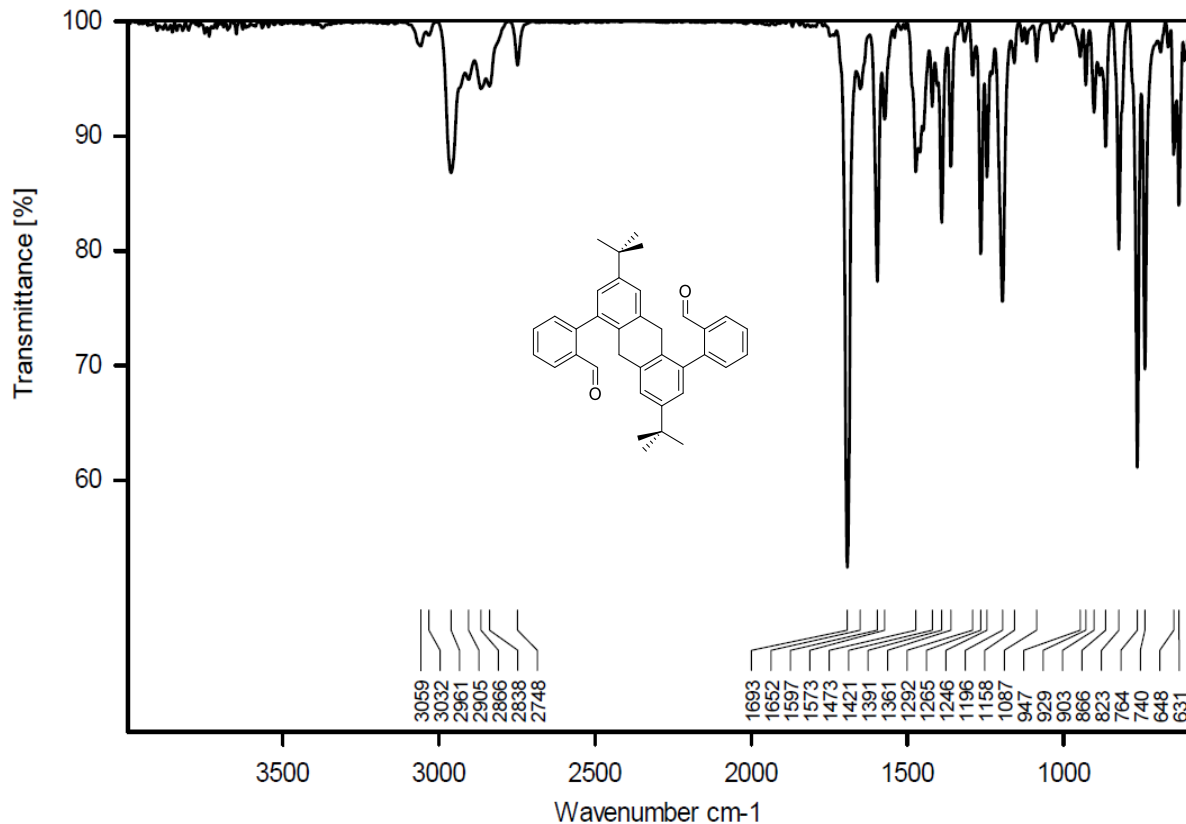


Figure S15. FT-IR spectrum (ATR) of the atropisomeric mixture of **5a**.

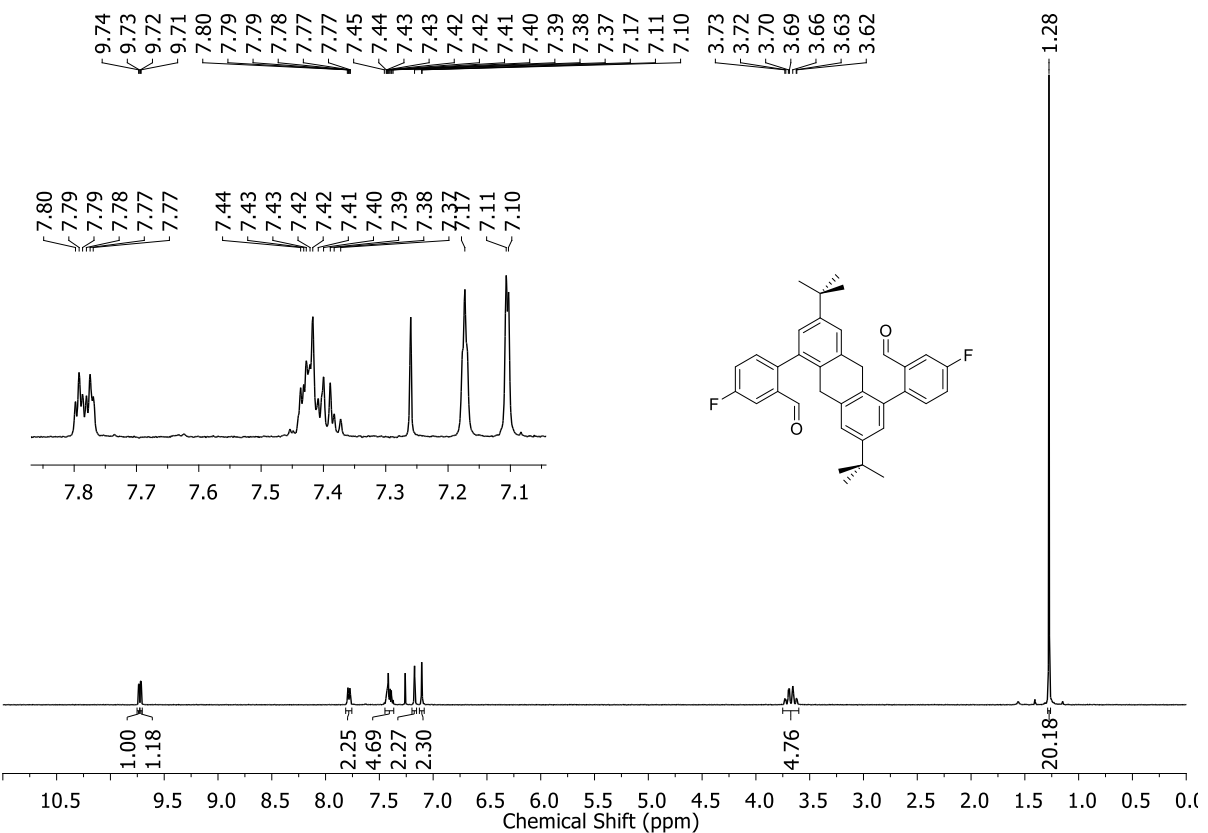


Figure S16. ^1H NMR spectrum (CDCl_3 , 500MHz) of the atropisomeric mixture of **5b**.

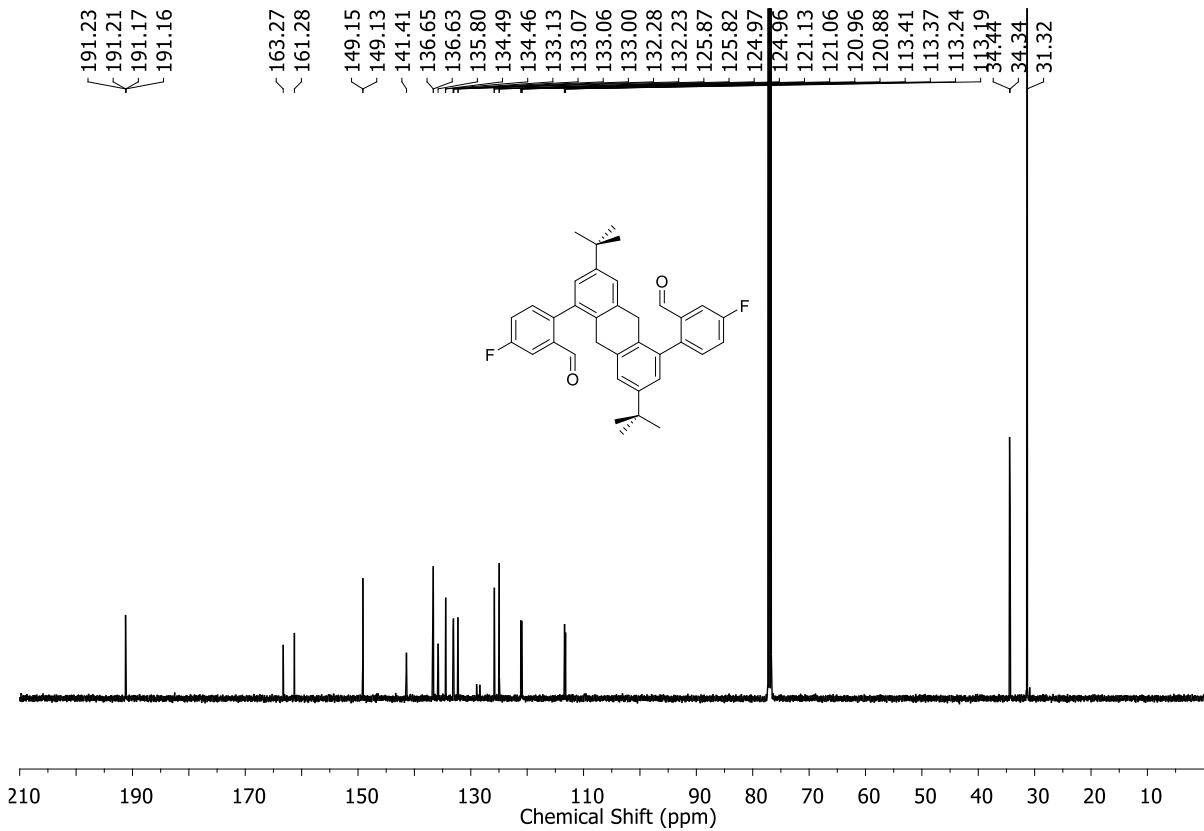


Figure S17. ^{13}C NMR spectrum (CDCl_3 , 125 MHz) of the atropisomeric mixture of **5b**.

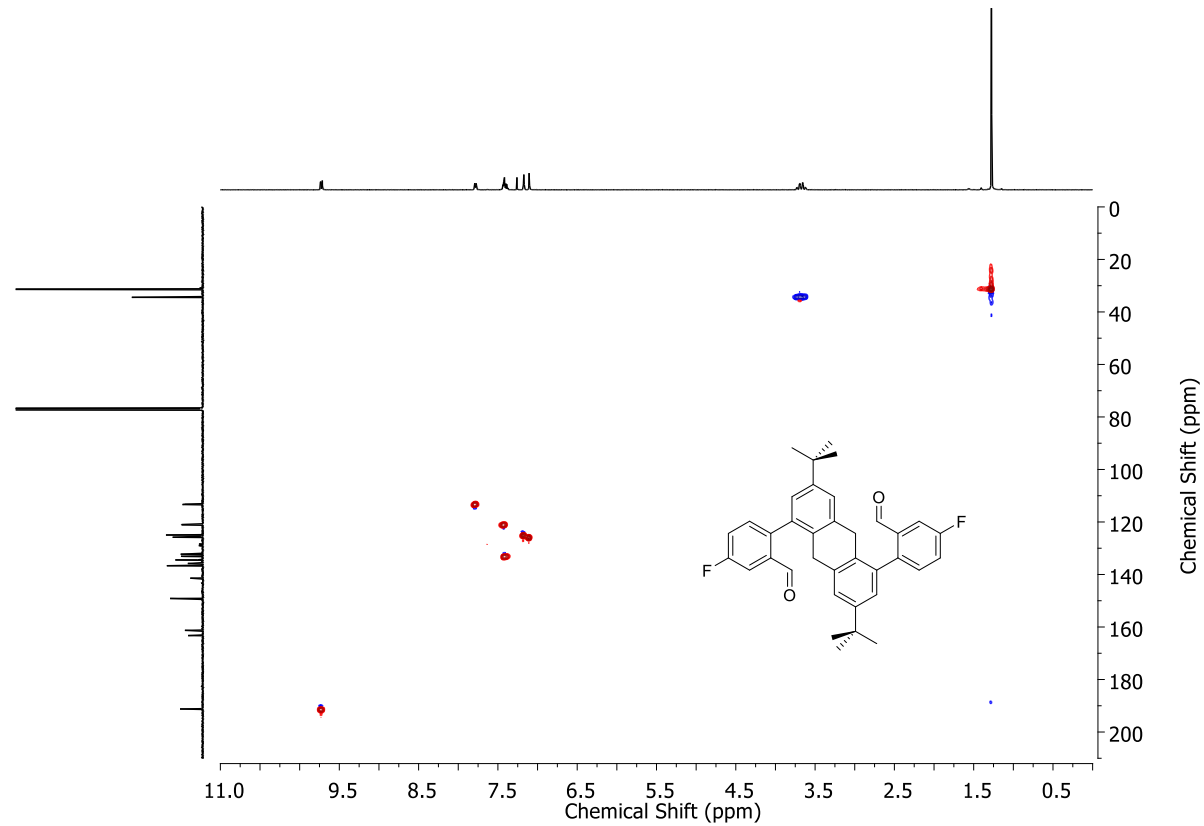


Figure S18. HSQC NMR spectrum of the atropisomeric mixture of **5b**.

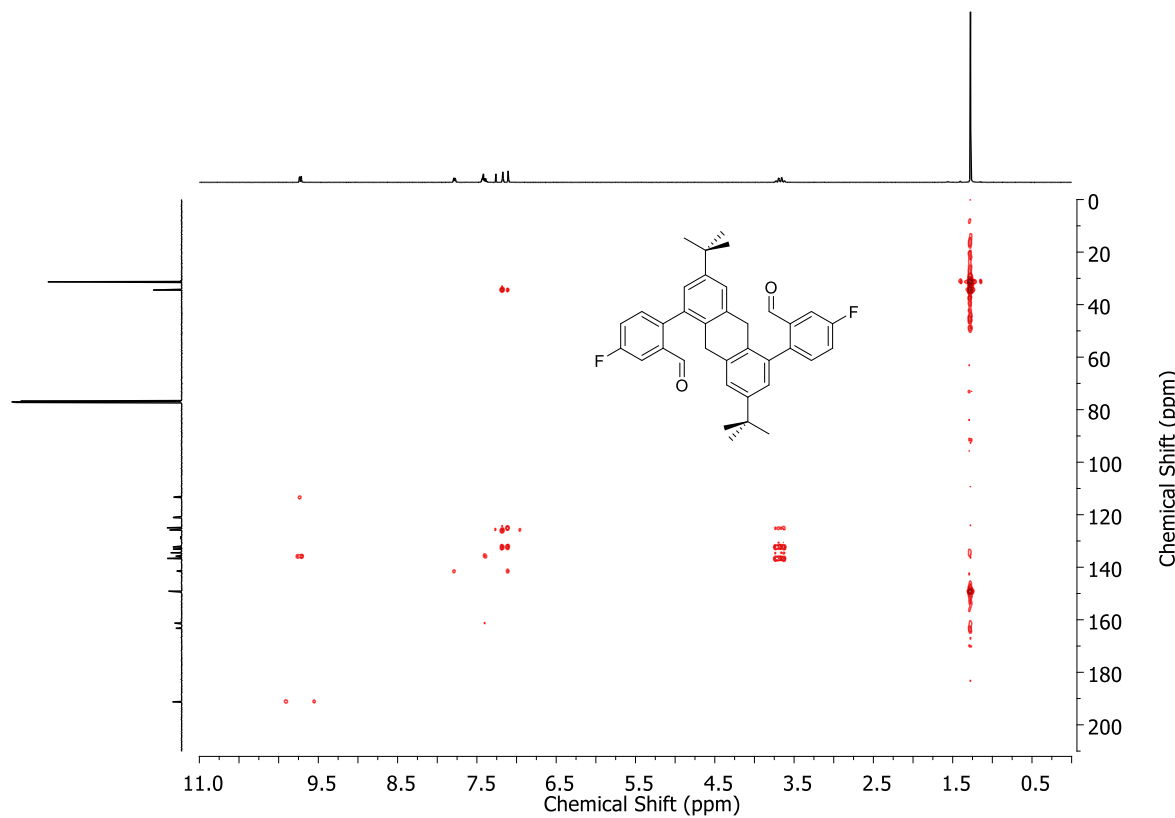


Figure S19. HMBC NMR spectrum of the atropisomeric mixture of **5b**.

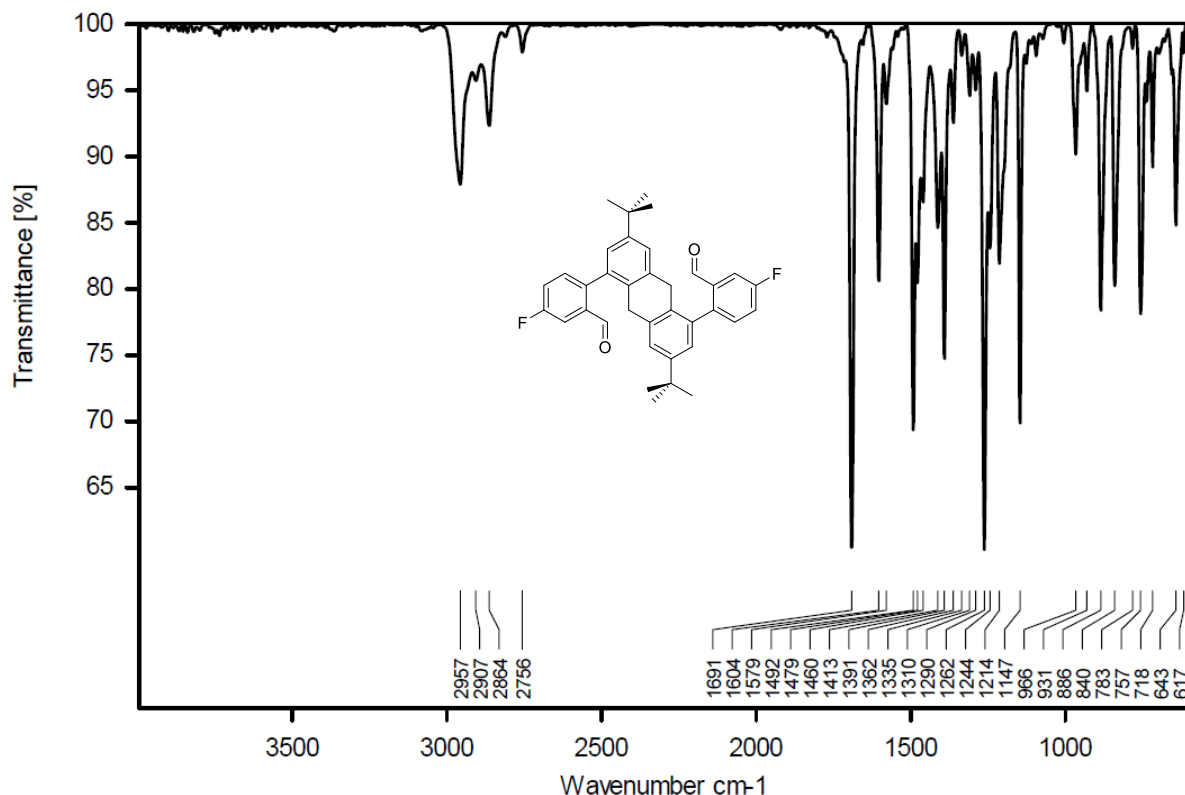


Figure S20. FT-IR spectrum (ATR) of the atropisomeric mixture of **5b**.

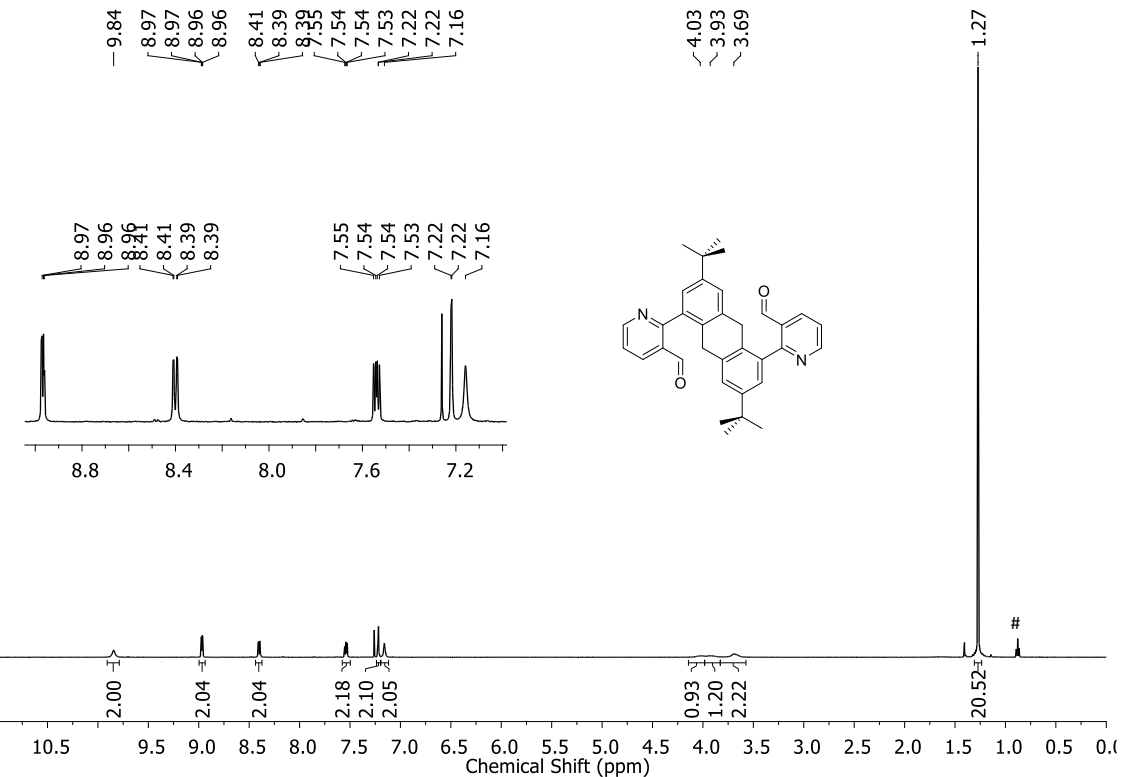


Figure S21. ¹H NMR spectrum (CDCl₃, 500MHz) of the atropisomeric mixture of **5c**. # residual pentane.

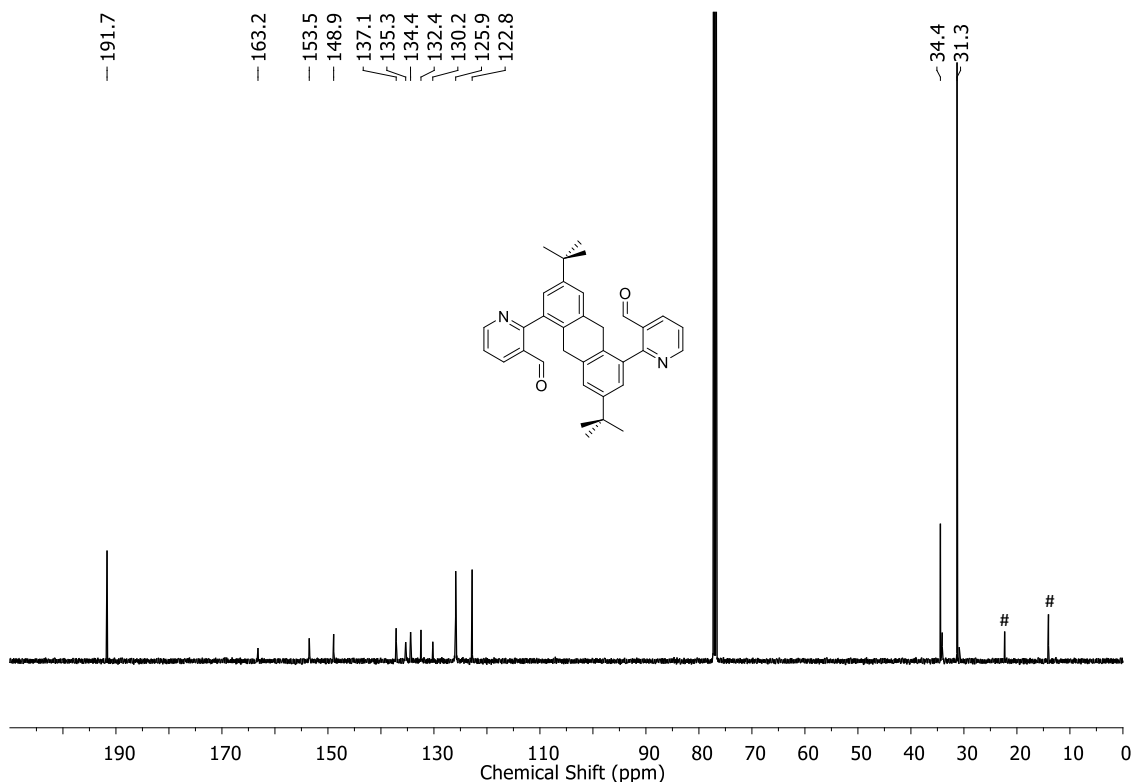


Figure S22. ¹³C NMR spectrum (CDCl₃, 125MHz) of the atropisomeric mixture of **5c**. #, residual pentane.

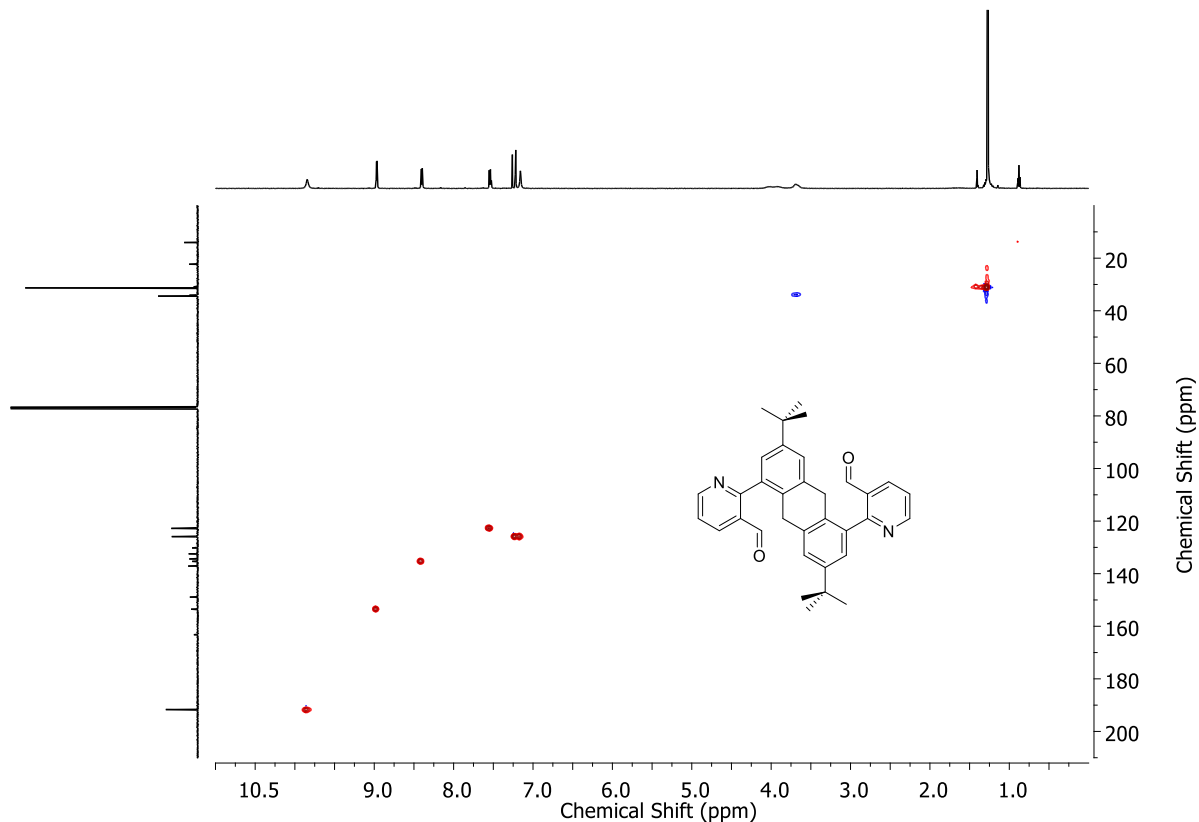


Figure S23. HSQC NMR spectrum of the atropisomeric mixture of **5c**.

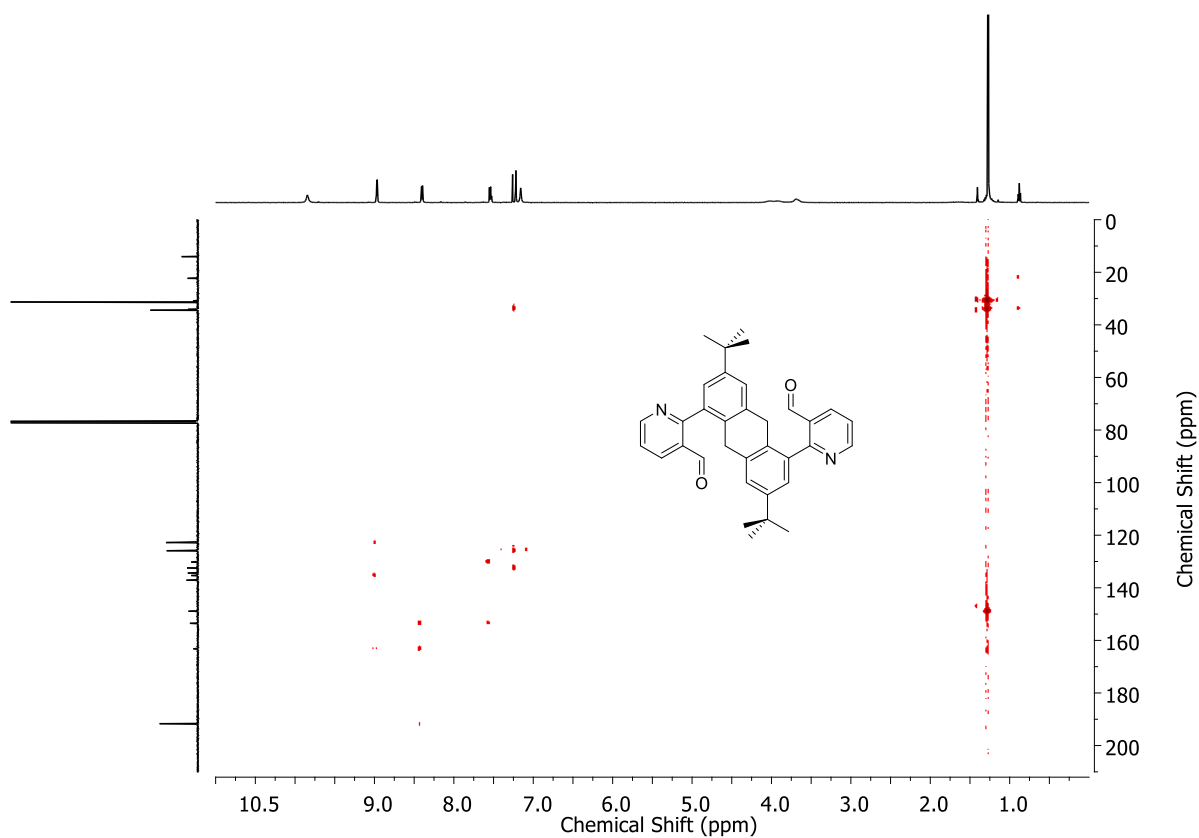


Figure S24. HMBC NMR spectrum of the atropisomeric mixture of **5c**.

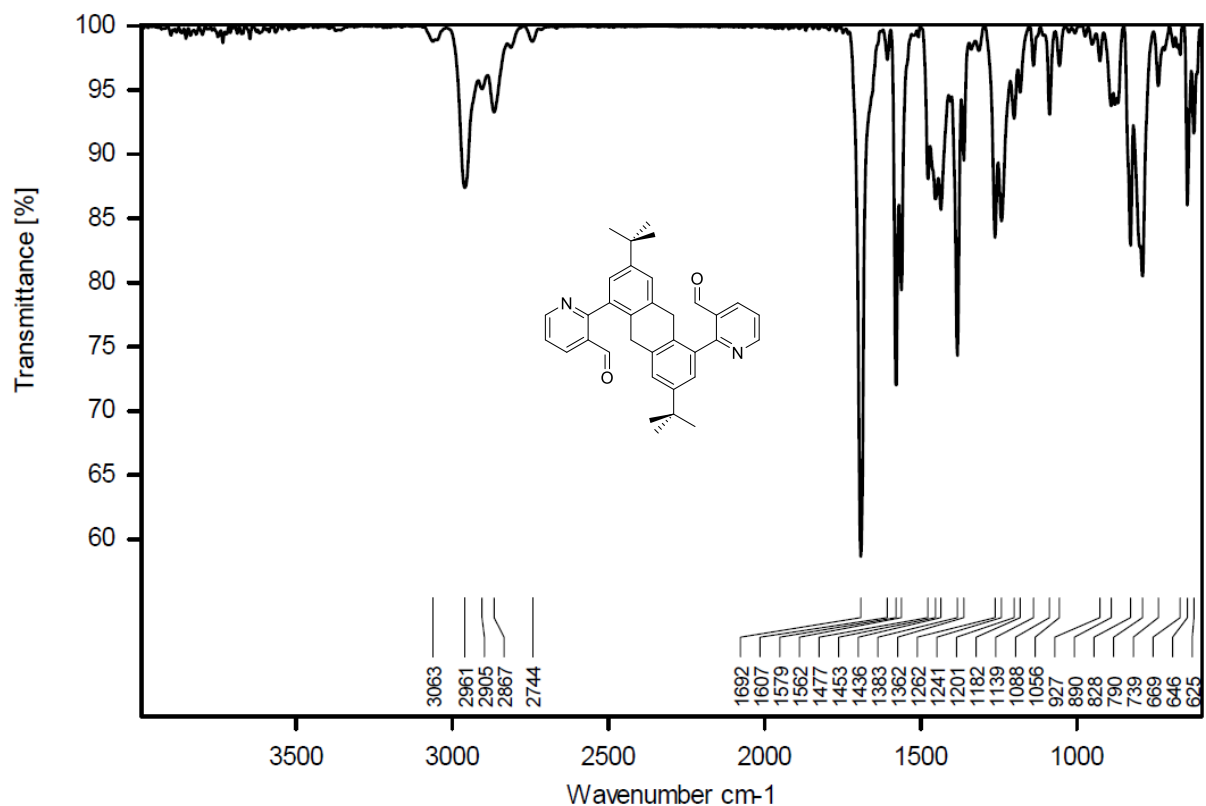


Figure S25. FT-IR spectrum (ATR) of the atropisomeric mixture of **5c**.

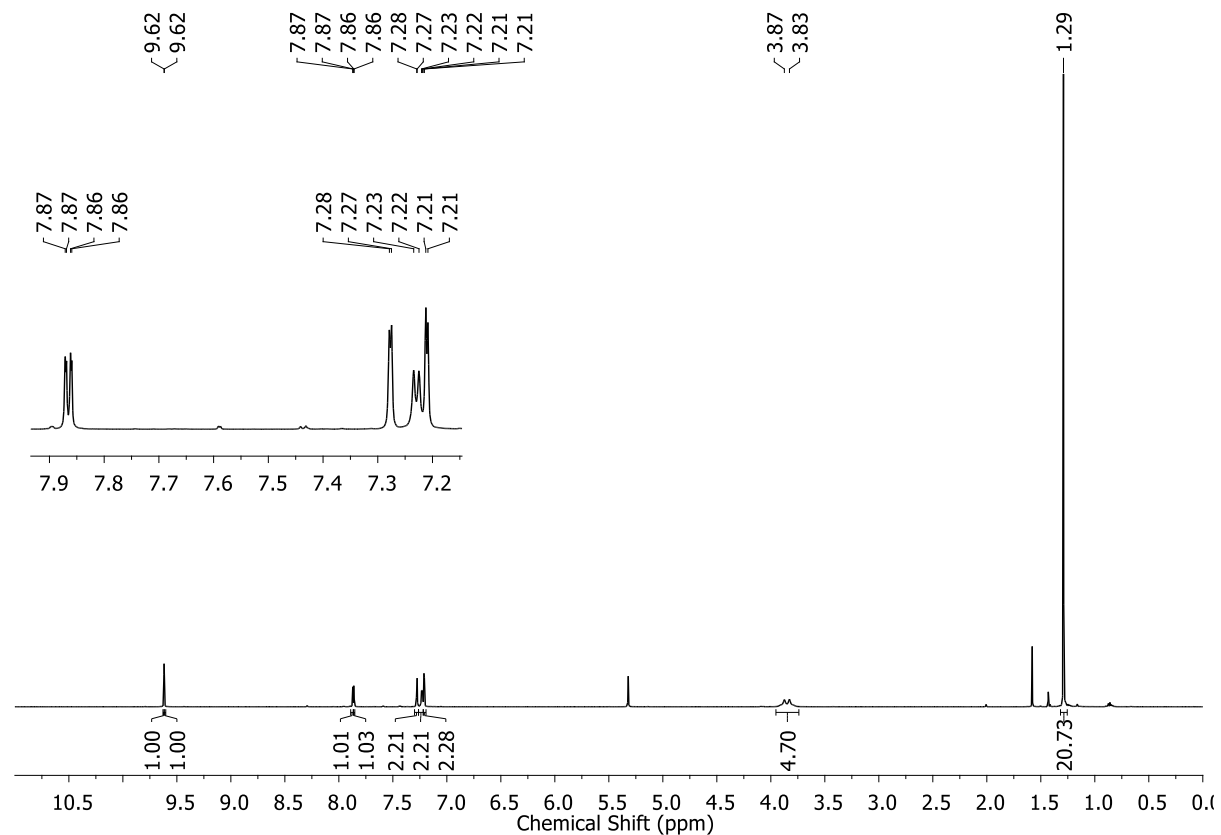


Figure S26. ^1H NMR spectrum (CD_2Cl_2 , 500MHz) of the atropisomeric mixture of **5d**.

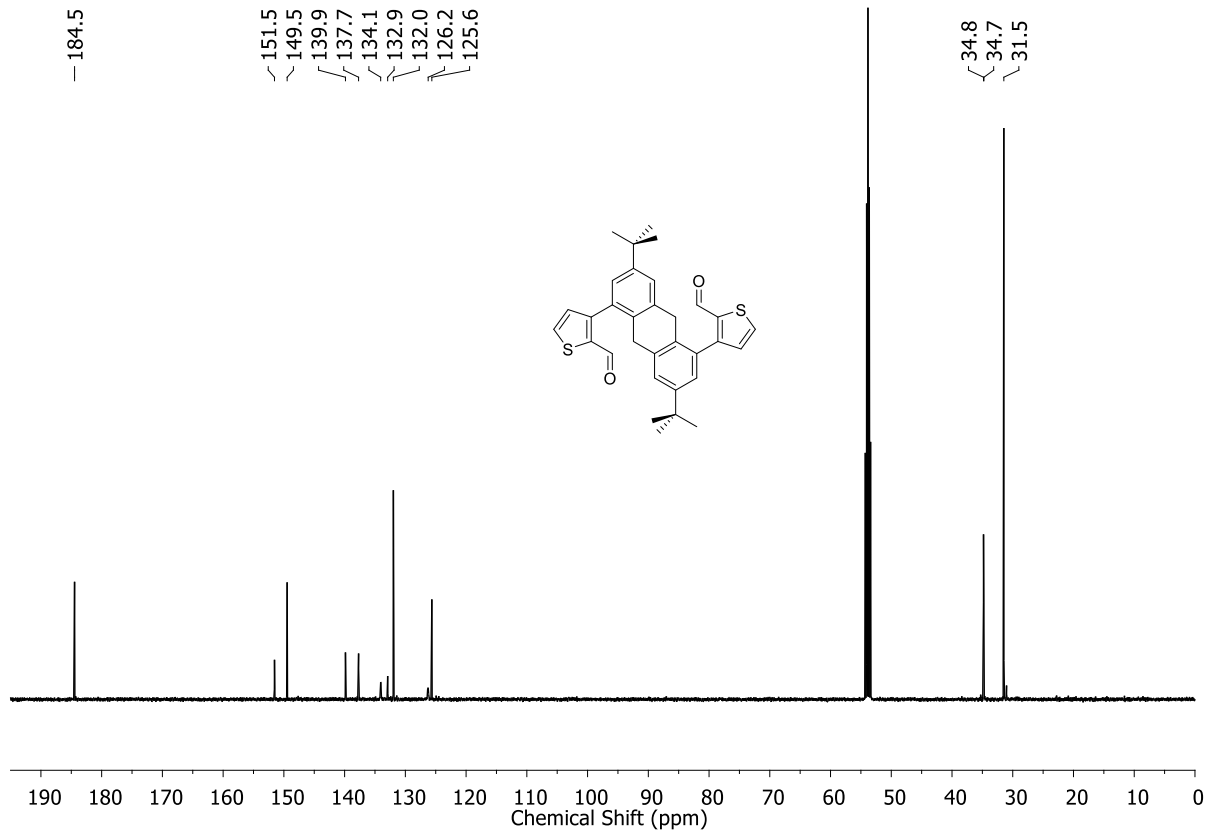


Figure S27. ^{13}C NMR spectrum (CD_2Cl_2 , 125MHz) of the atropisomeric mixture of **5d**.

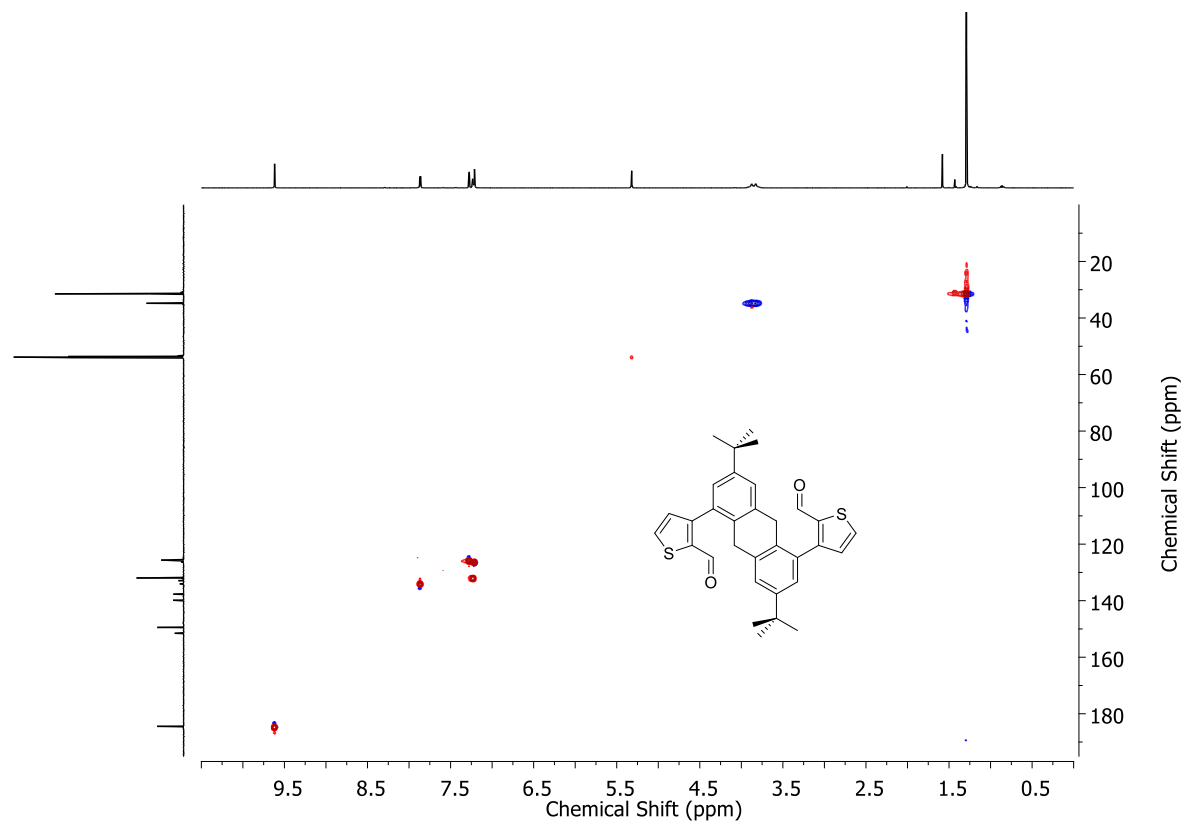


Figure S28. HSQC NMR spectrum of the atropisomeric mixture of **5d**.

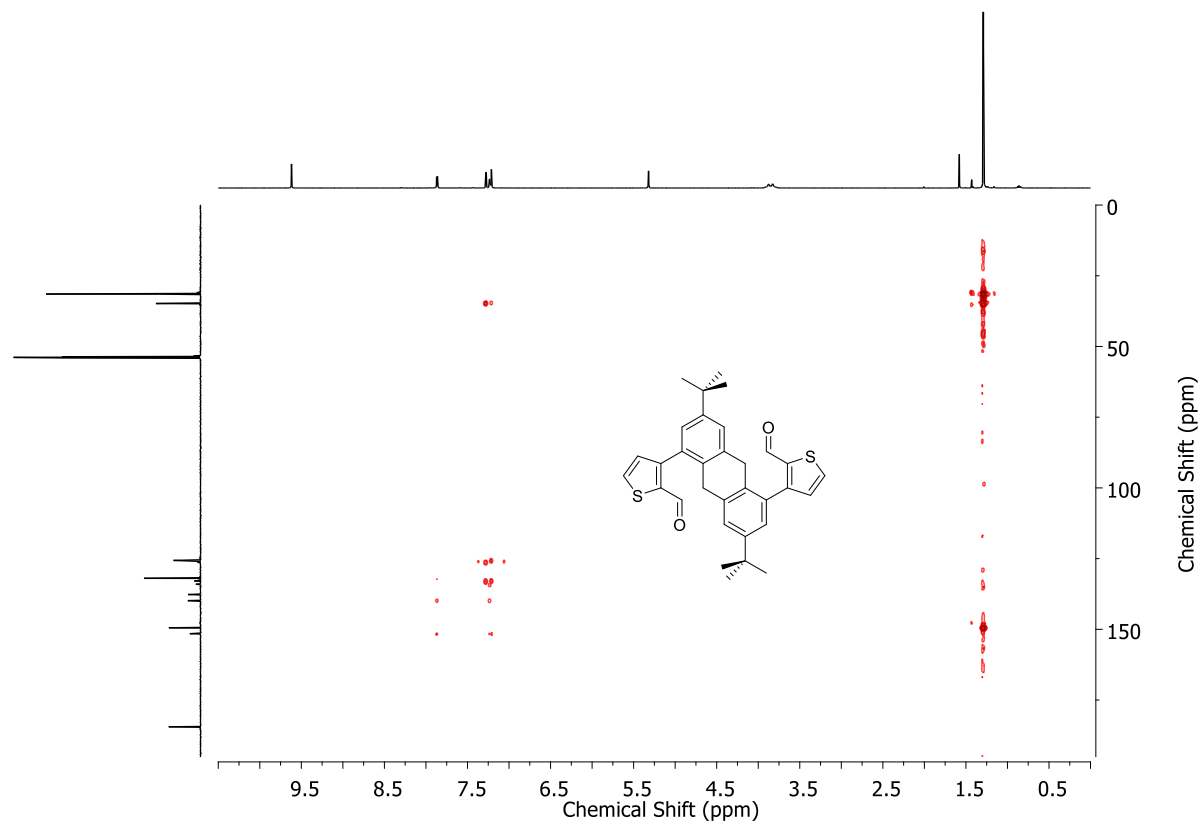


Figure S29. HMBC NMR spectrum of the atropisomeric mixture of **5d**.

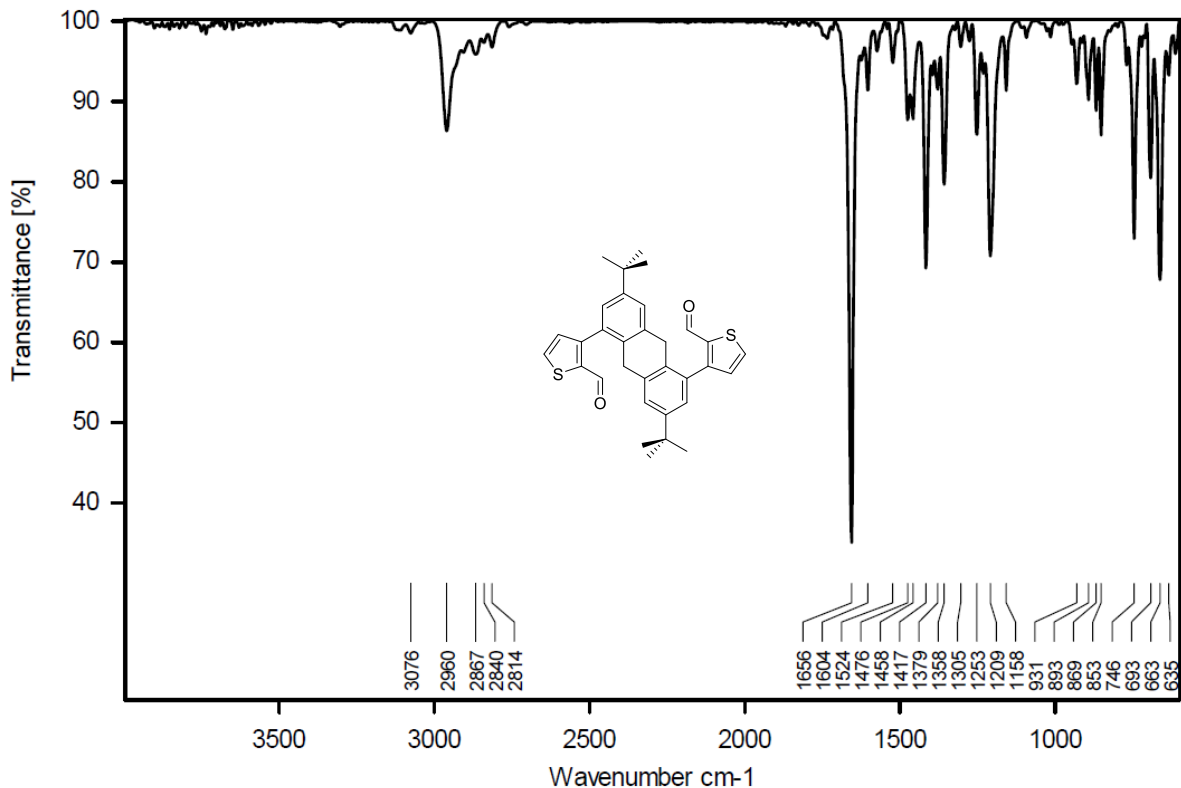
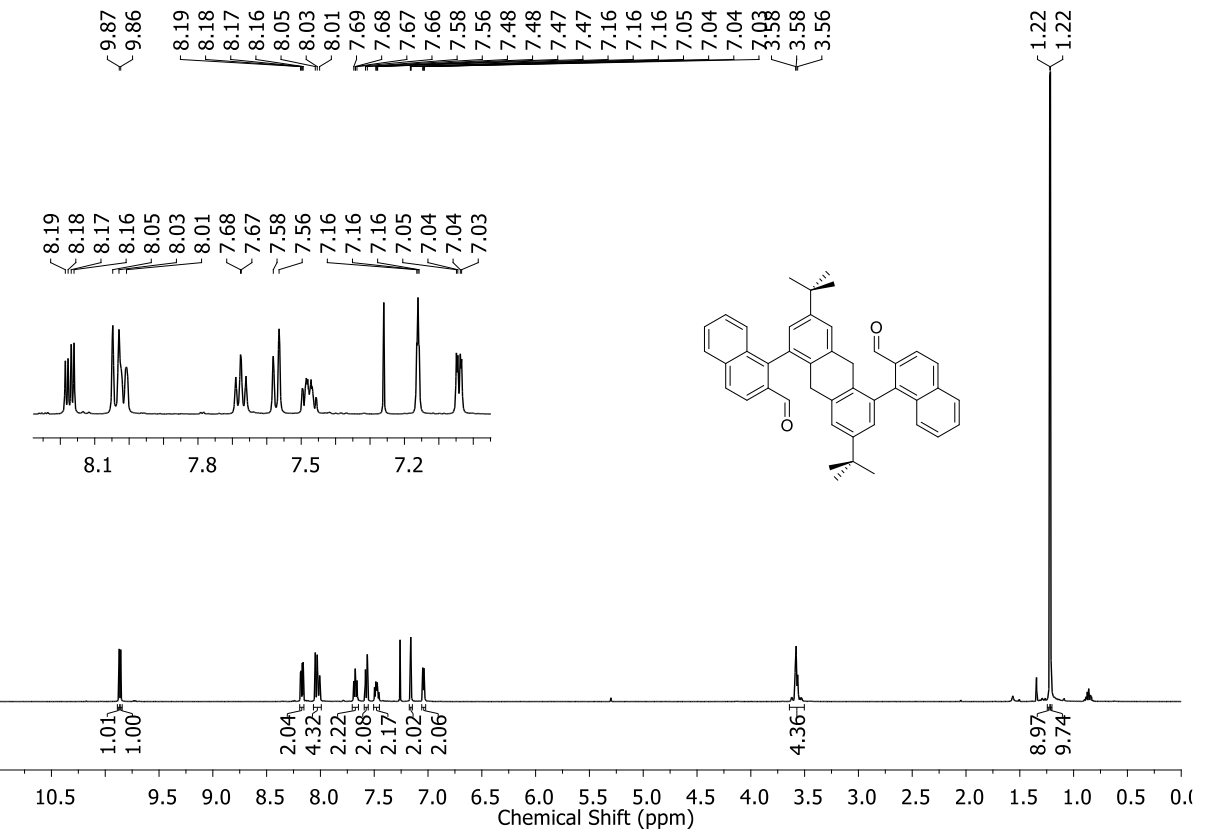


Figure S30. FT-IR spectrum (ATR) of the atropisomeric mixture of **5d**.



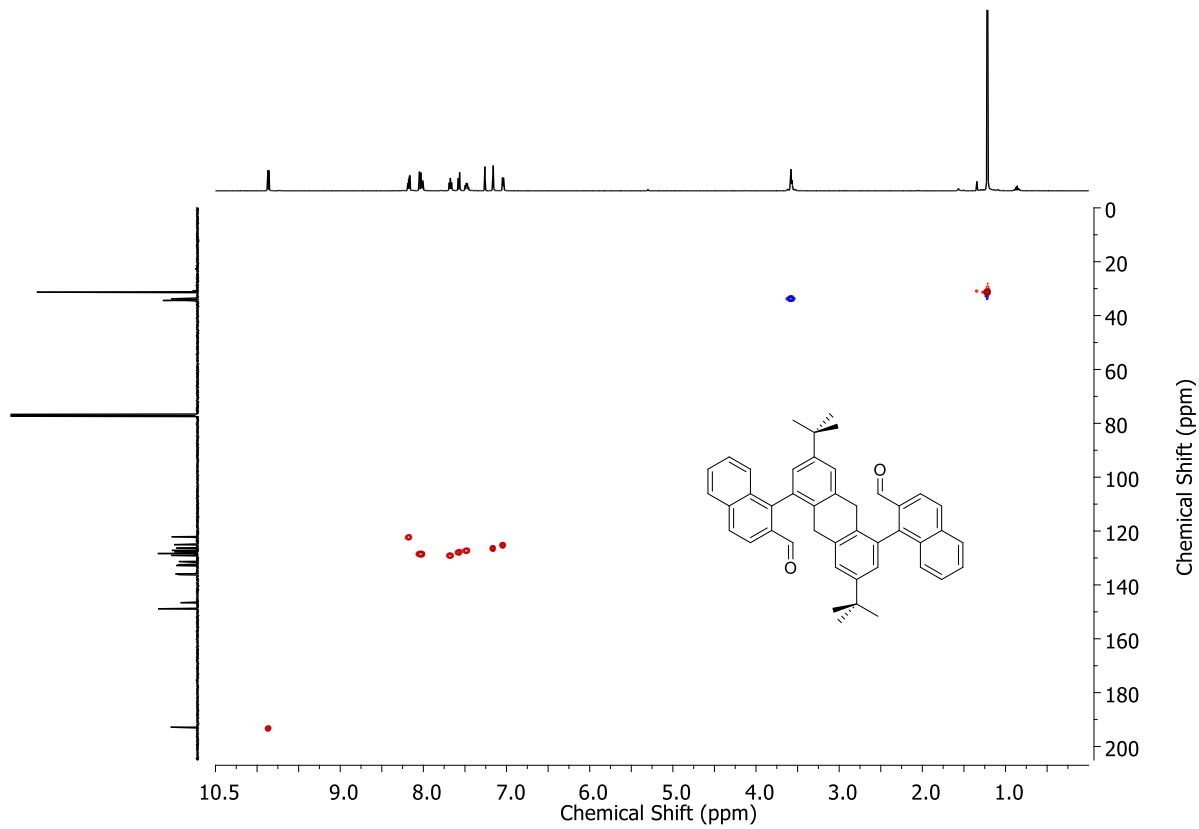


Figure S33. HSQC NMR spectrum of the atropisomeric mixture of **5e**.

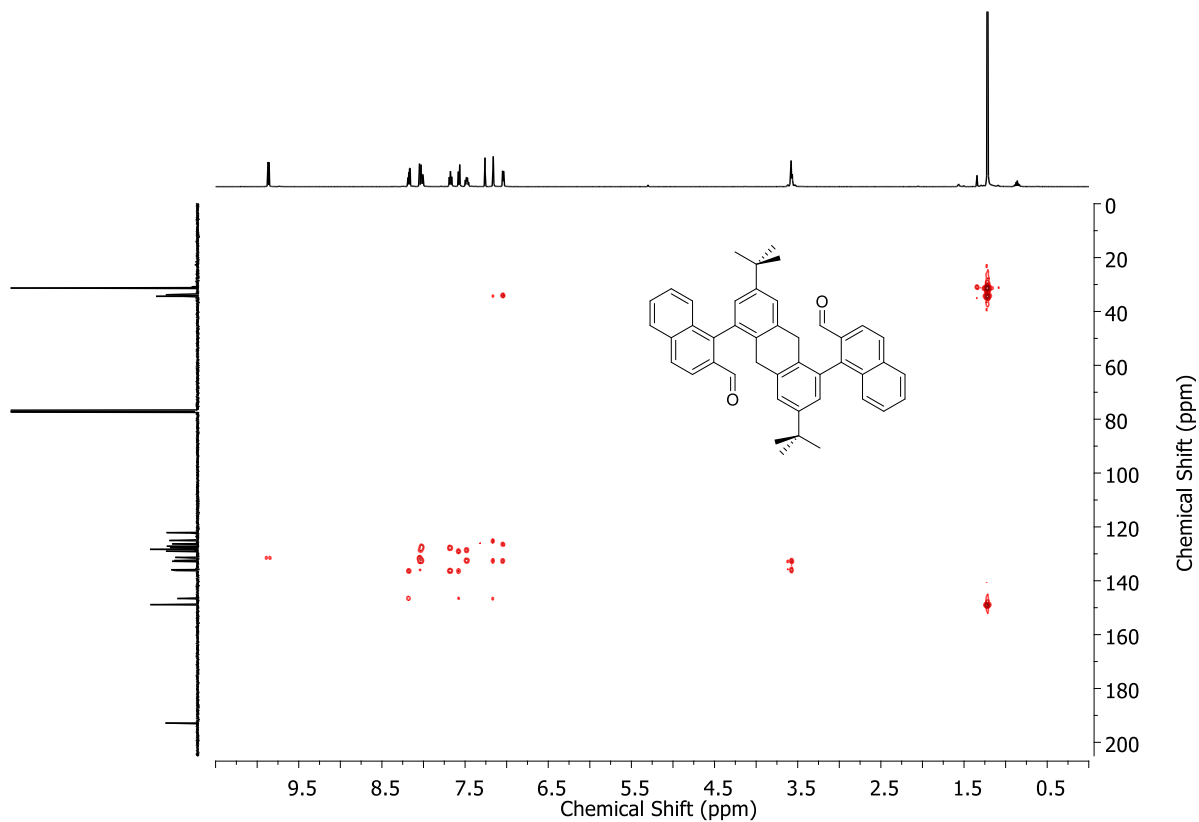


Figure S34. HMBC NMR spectrum of the atropisomeric mixture of **5e**.

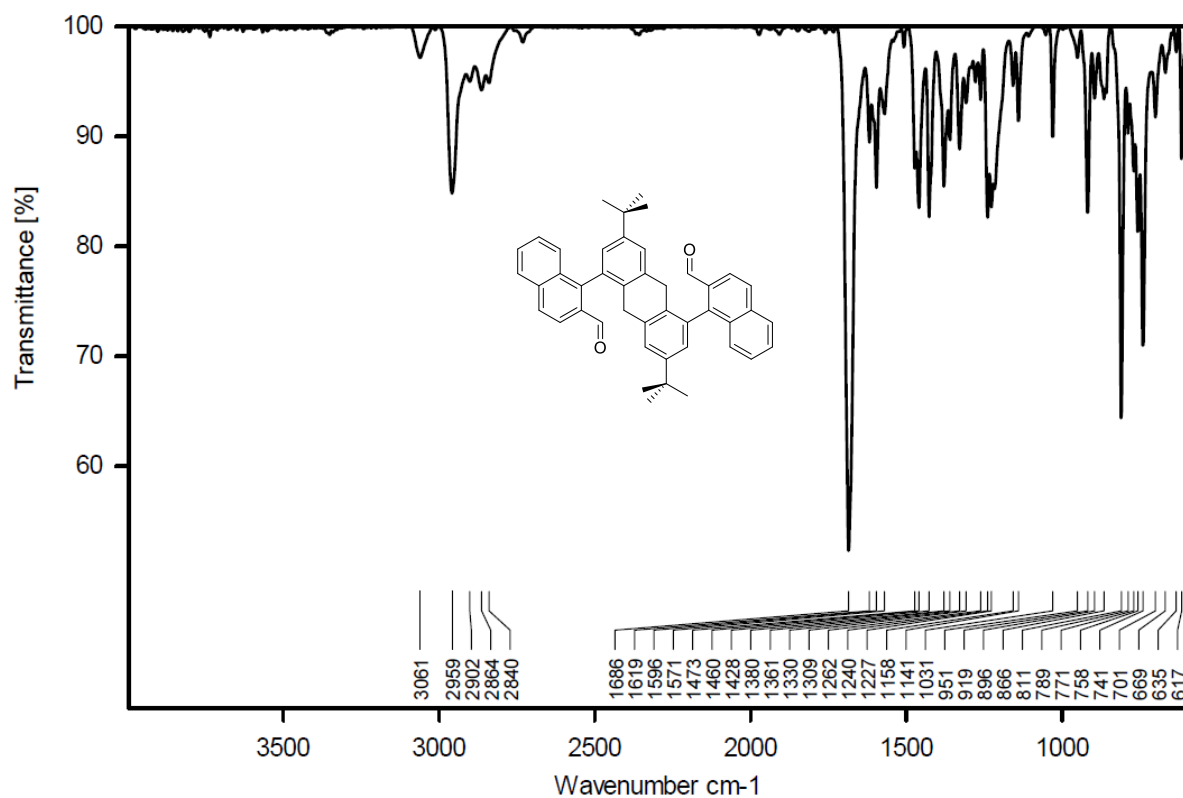


Figure S35. FT-IR spectrum (ATR) of the atropisomeric mixture of **5e**.

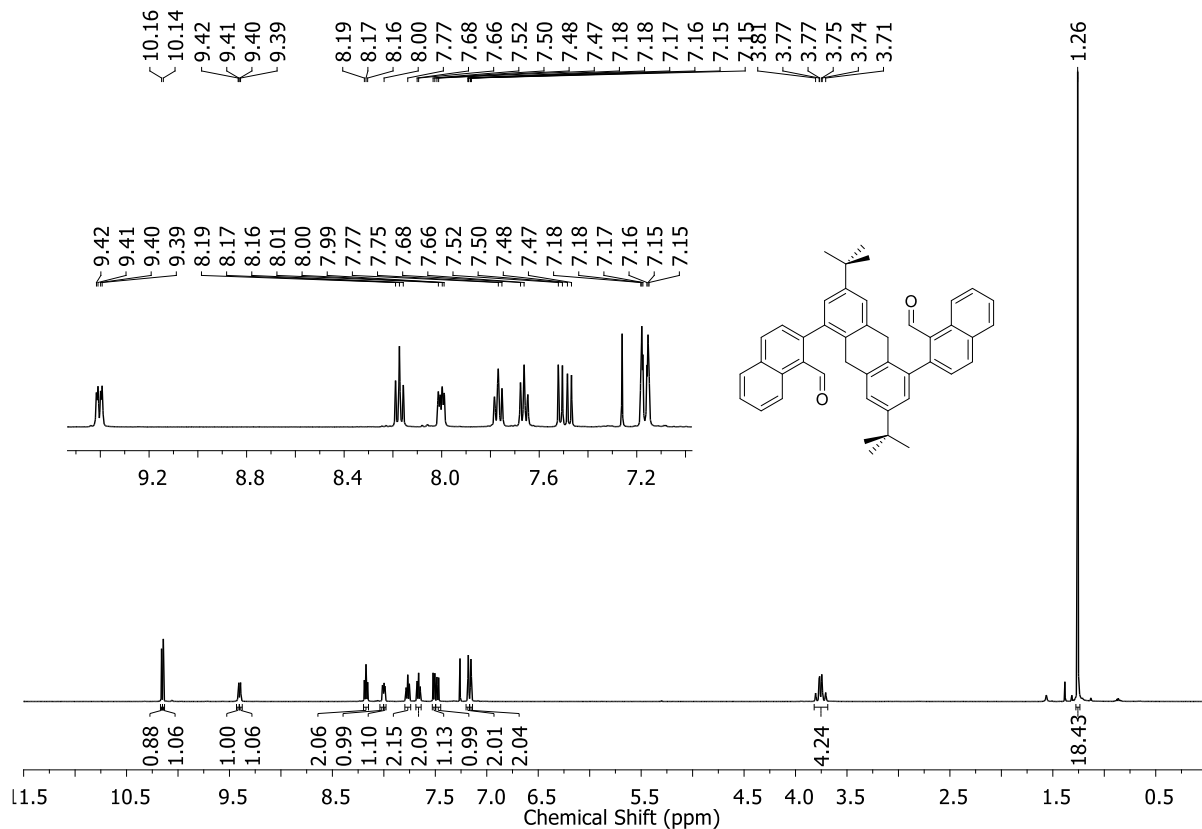


Figure S36. ^1H NMR spectrum (CDCl_3 , 500MHz) of the atropisomeric mixture of **5f**.

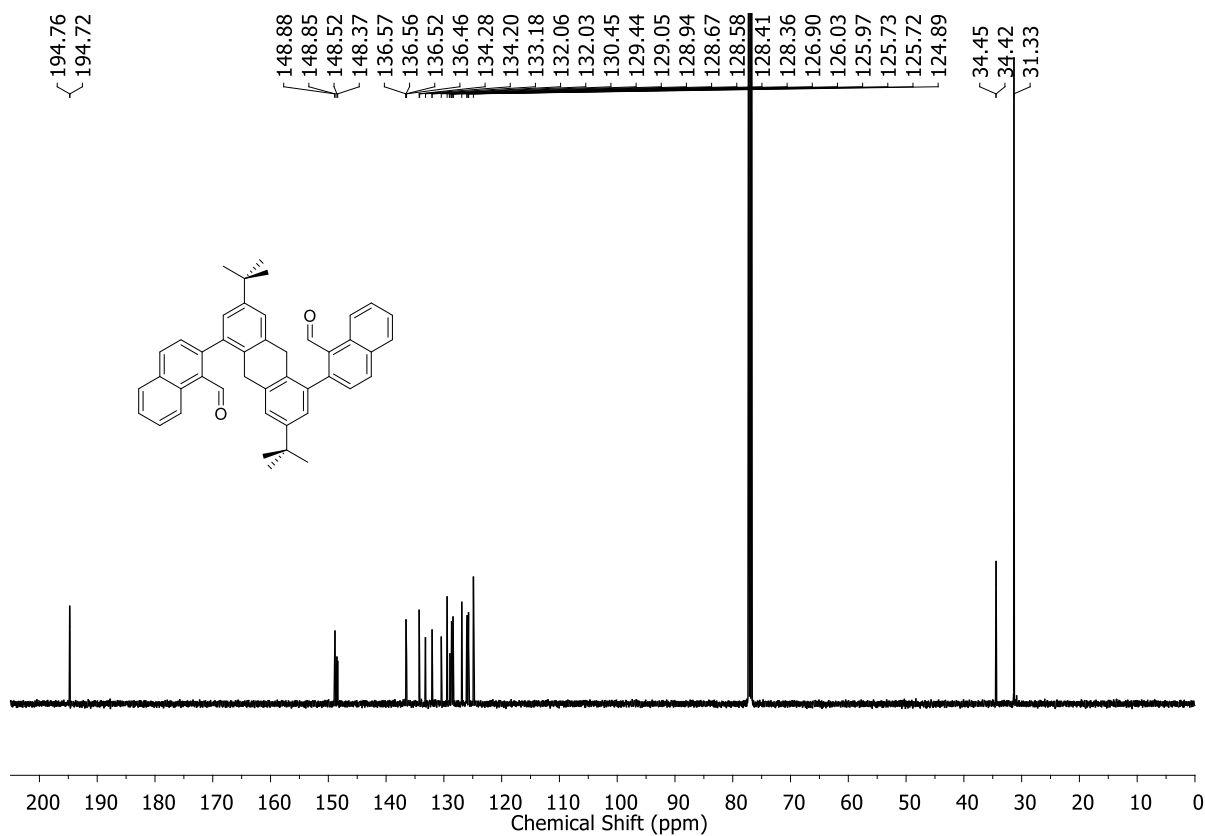


Figure S37. ^{13}C NMR spectrum (CDCl_3 , 125MHz) of the atropisomeric mixture of **5f**.

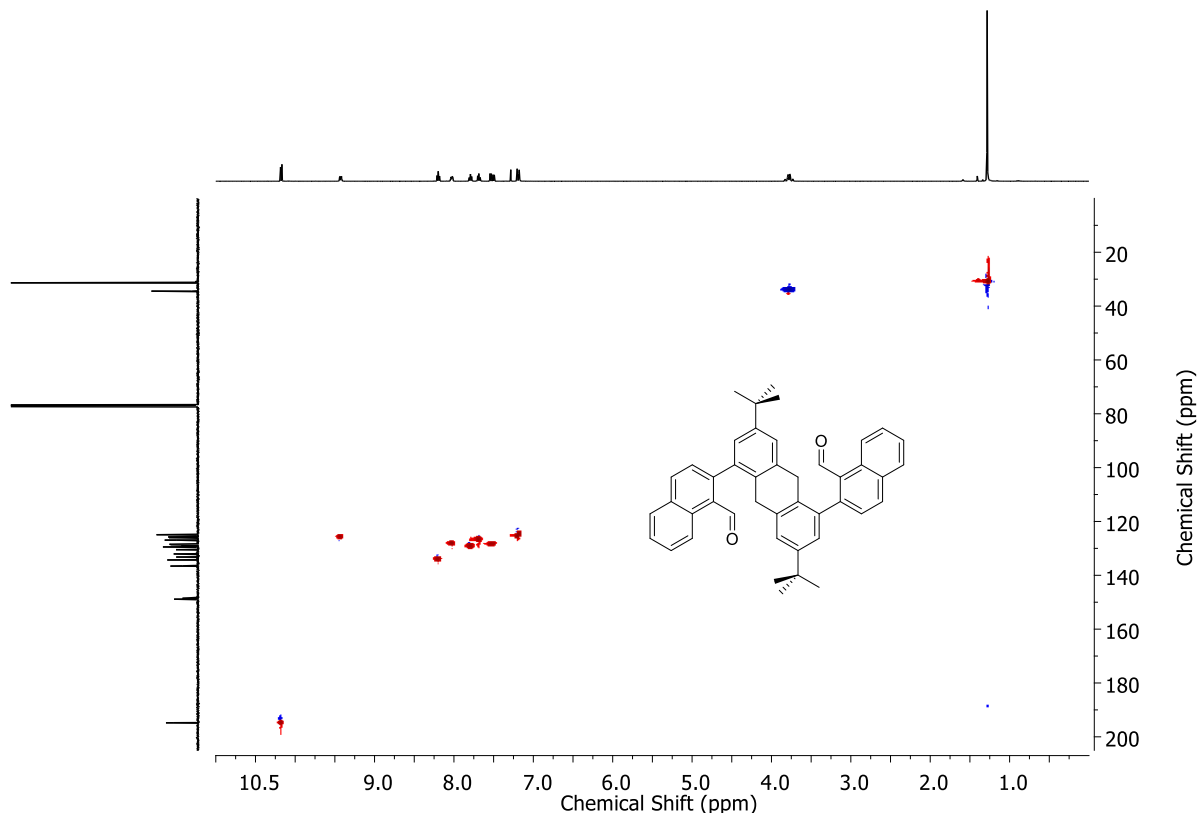


Figure S38. HSQC NMR spectrum of the atropisomeric mixture of **5f**.

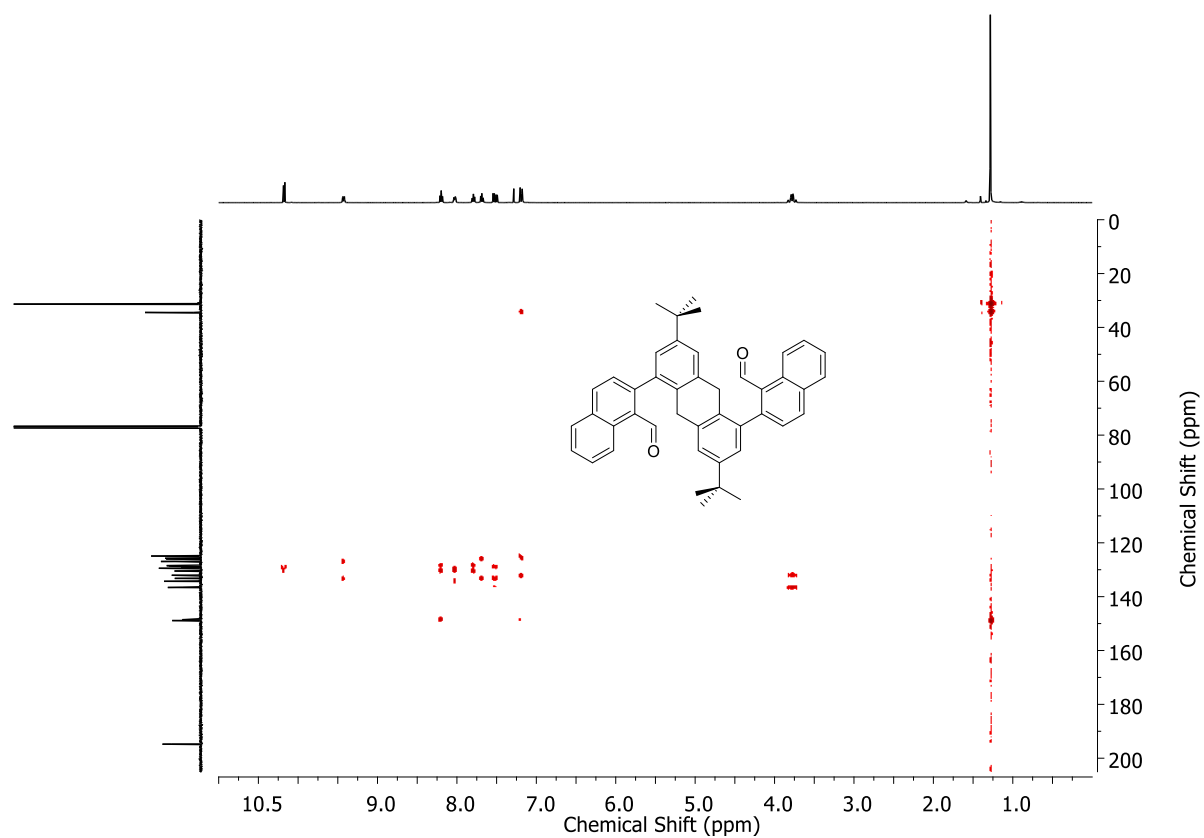


Figure S39. HMBC NMR spectrum of the atropisomeric mixture of **5f**.

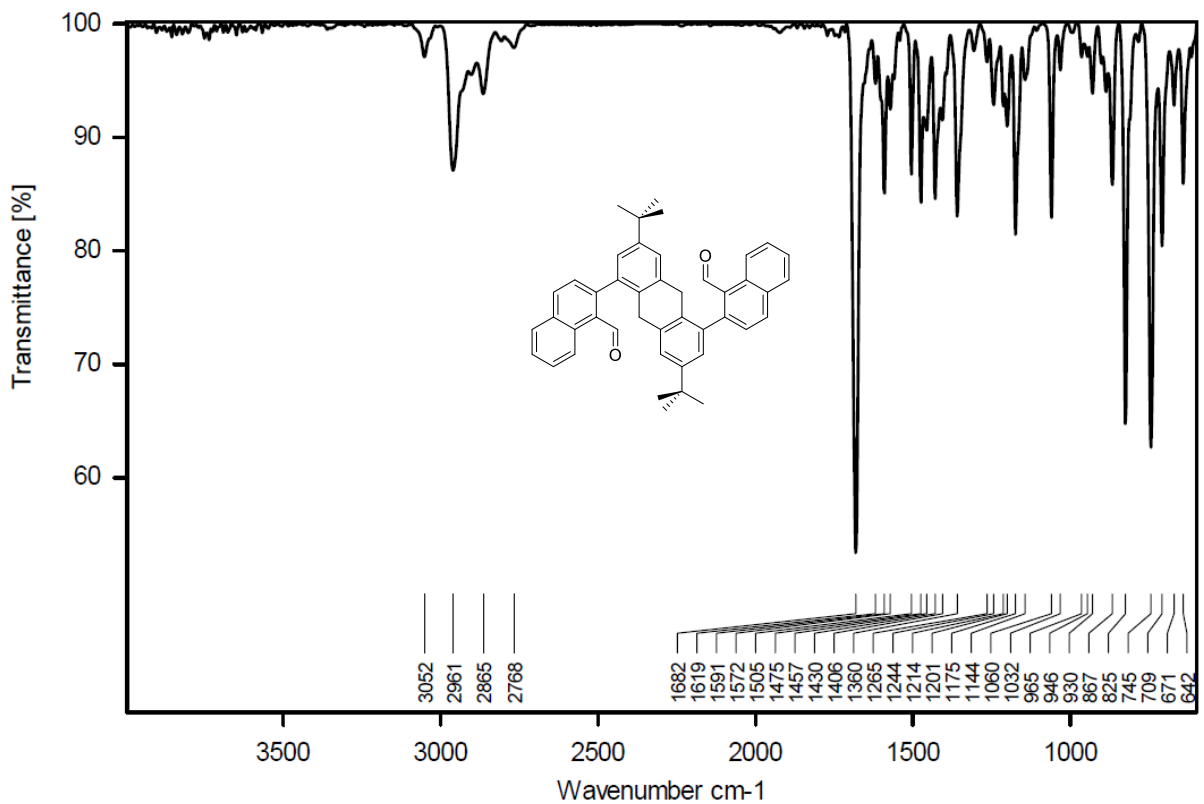


Figure S40. FT-IR spectrum (ATR) of the atropisomeric mixture of **5f**.

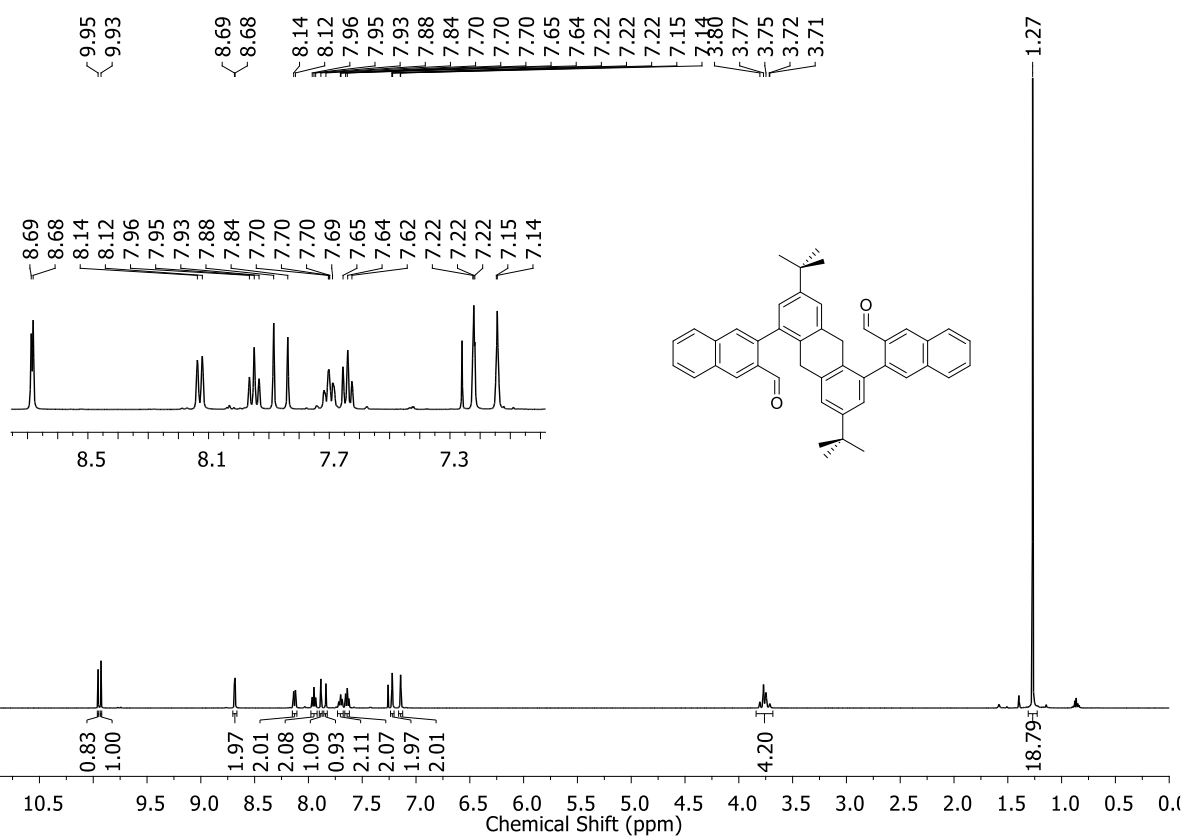


Figure S41. ¹H NMR spectrum (CDCl₃, 500MHz) of the atropisomeric mixture of **5g**.

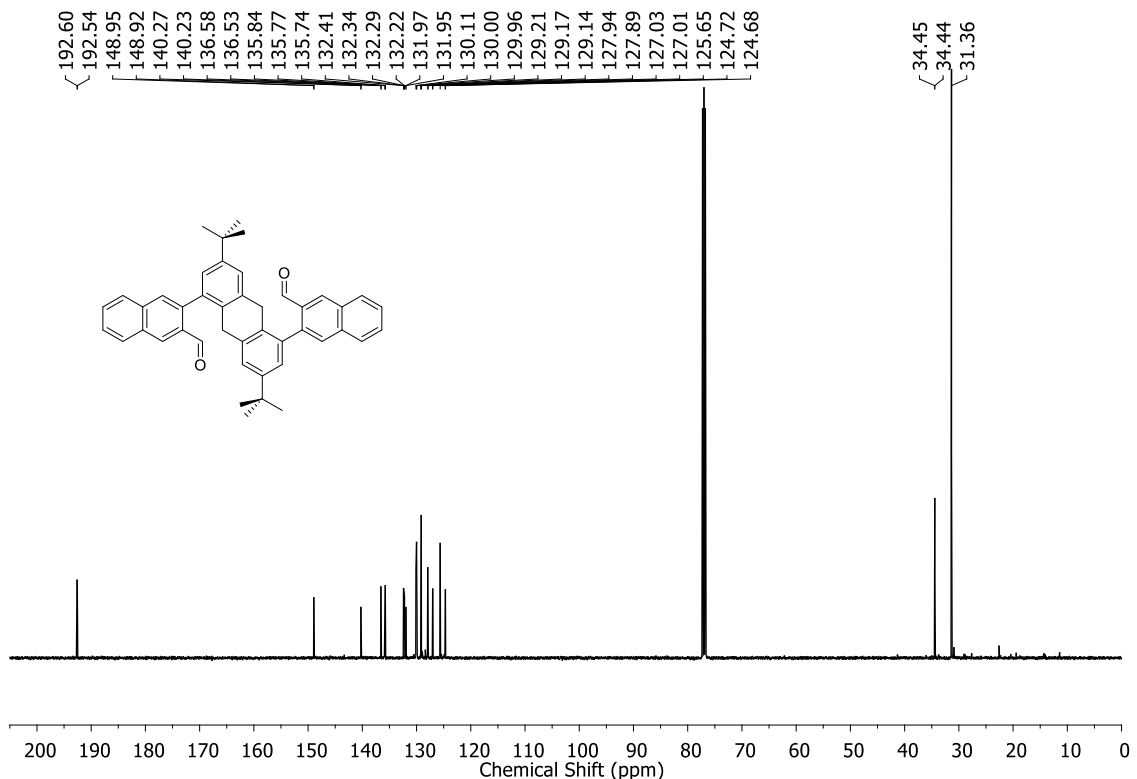


Figure S42. ¹³C NMR spectrum (CDCl₃, 125MHz) of the atropisomeric mixture of **5g**.

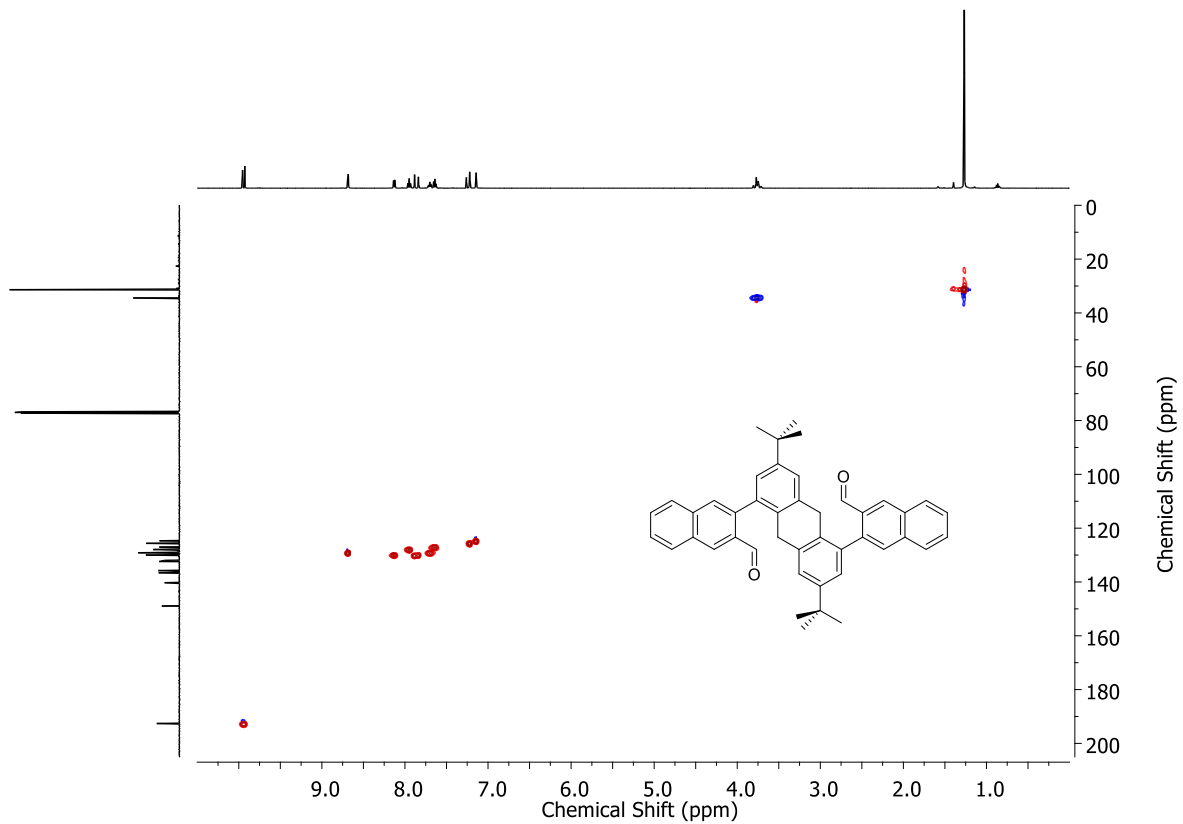


Figure S43. HSQC NMR spectrum of the atropisomeric mixture of **5g**.

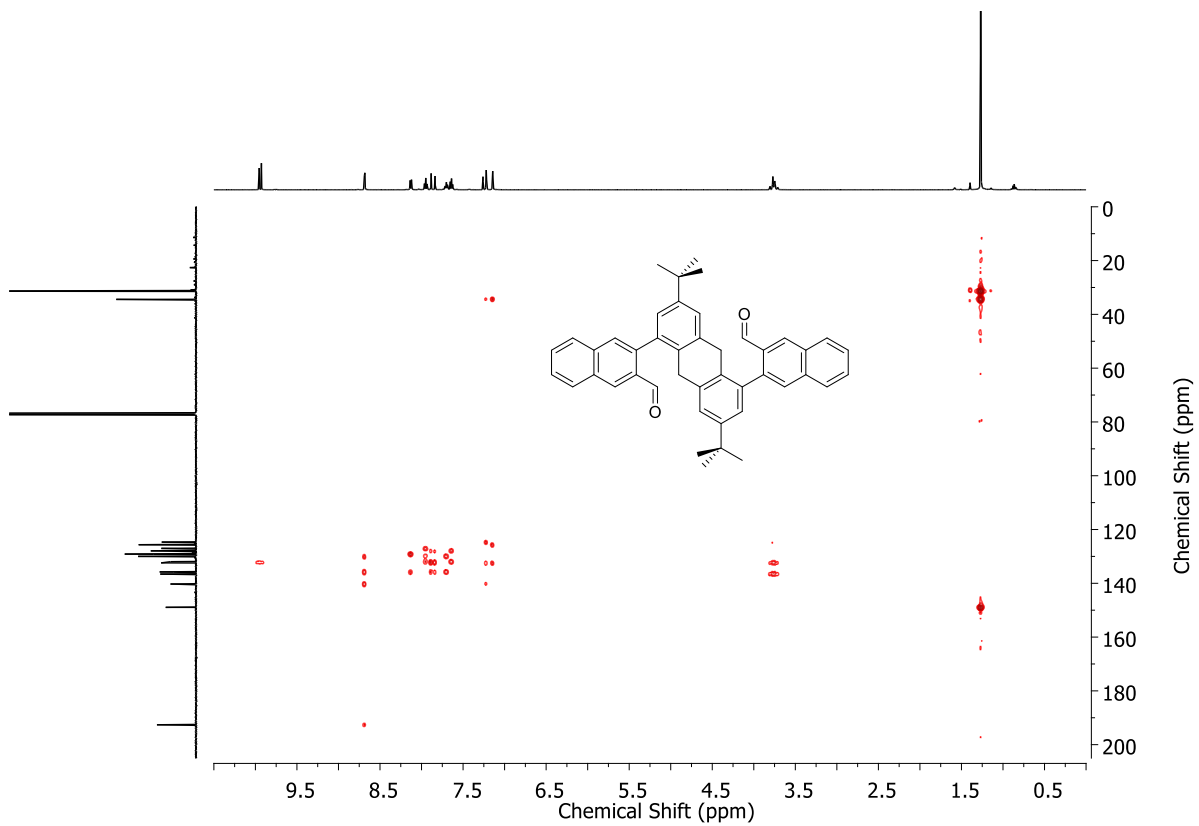


Figure S44. HMBC NMR spectrum of the atropisomeric mixture of **5g**.

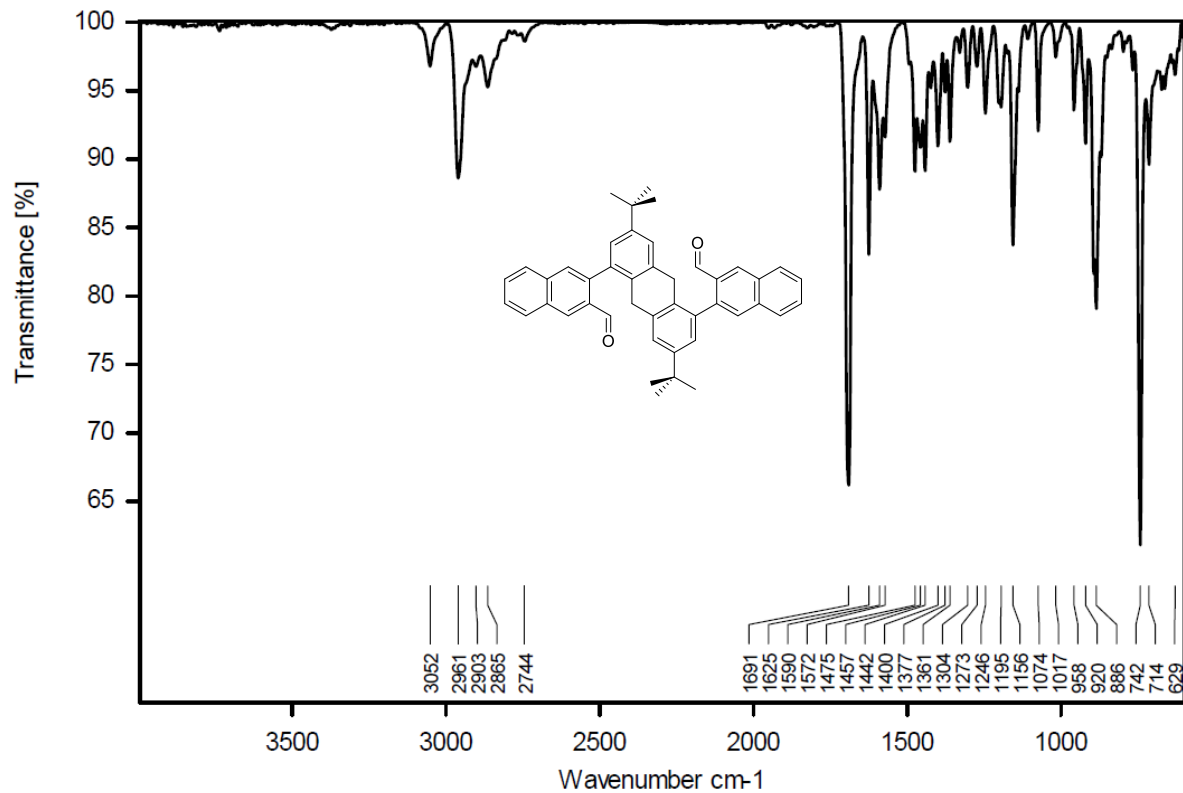


Figure S45. FT-IR spectrum (ATR) of the atropisomeric mixture of **5g**.

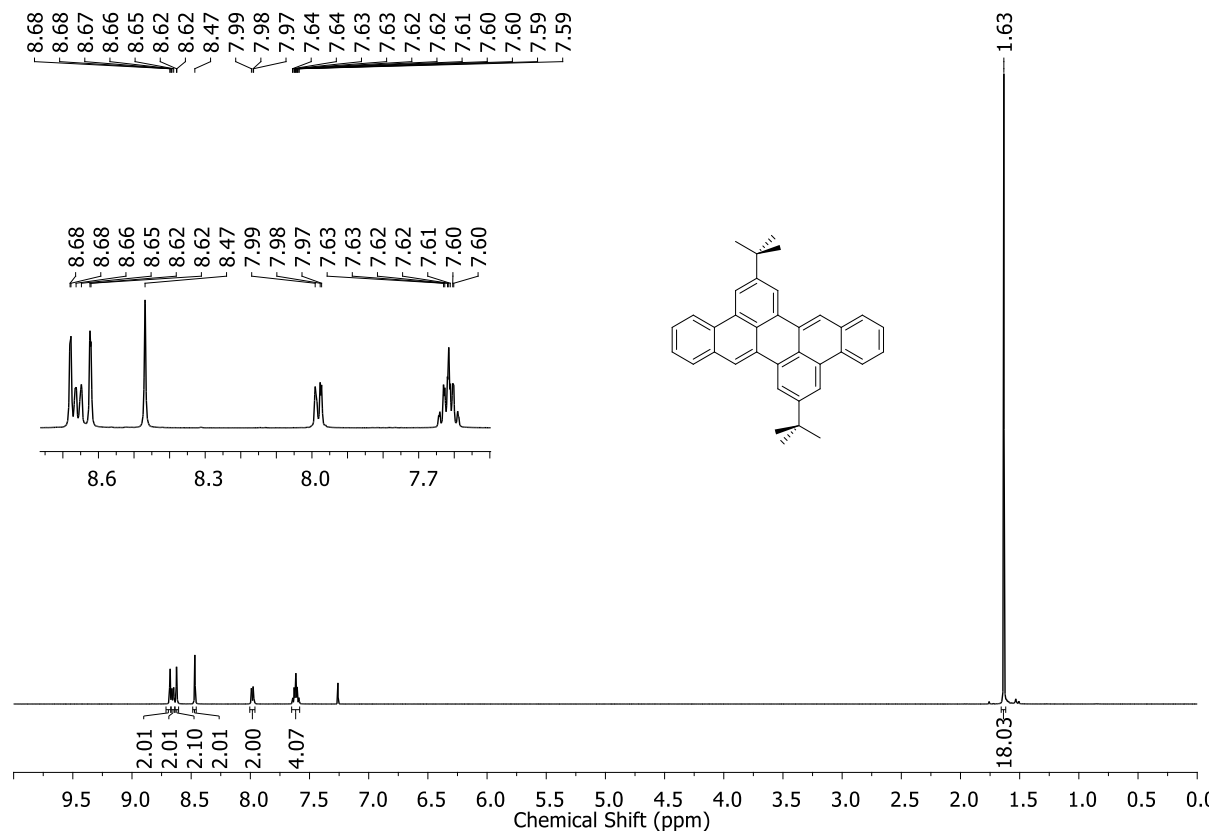


Figure S46. ^1H NMR spectrum (CDCl_3 , 500MHz) of **6a**.

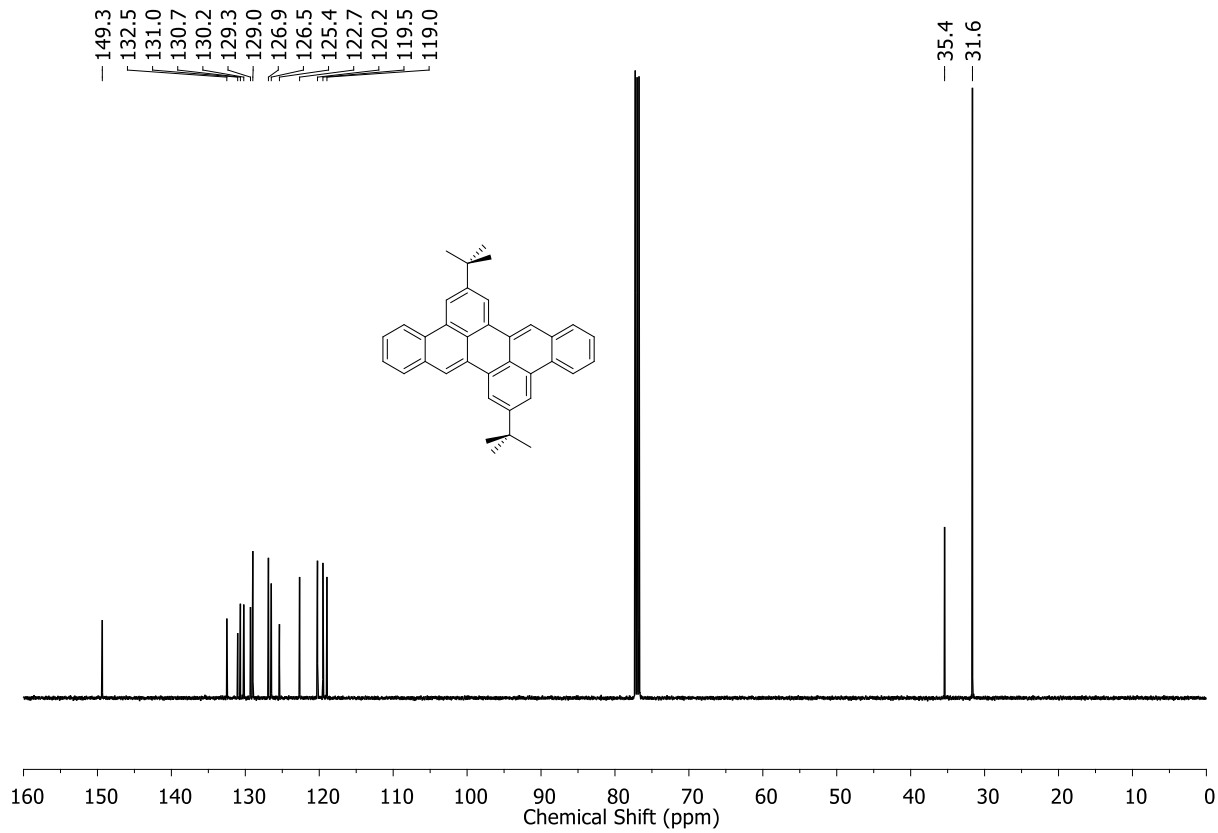


Figure S47. ^{13}C NMR spectrum (CDCl_3 , 125MHz) of **6a**.

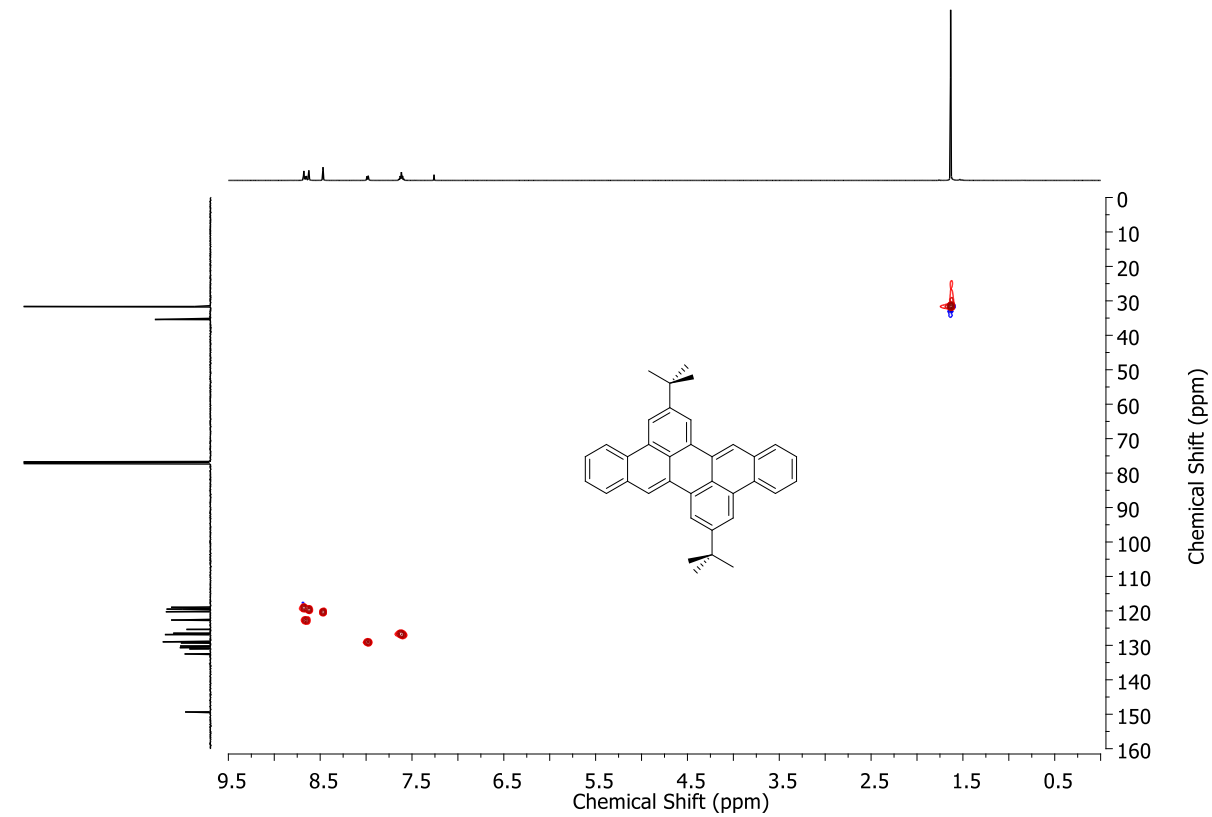


Figure S48. HSQC NMR spectrum of **6a**.

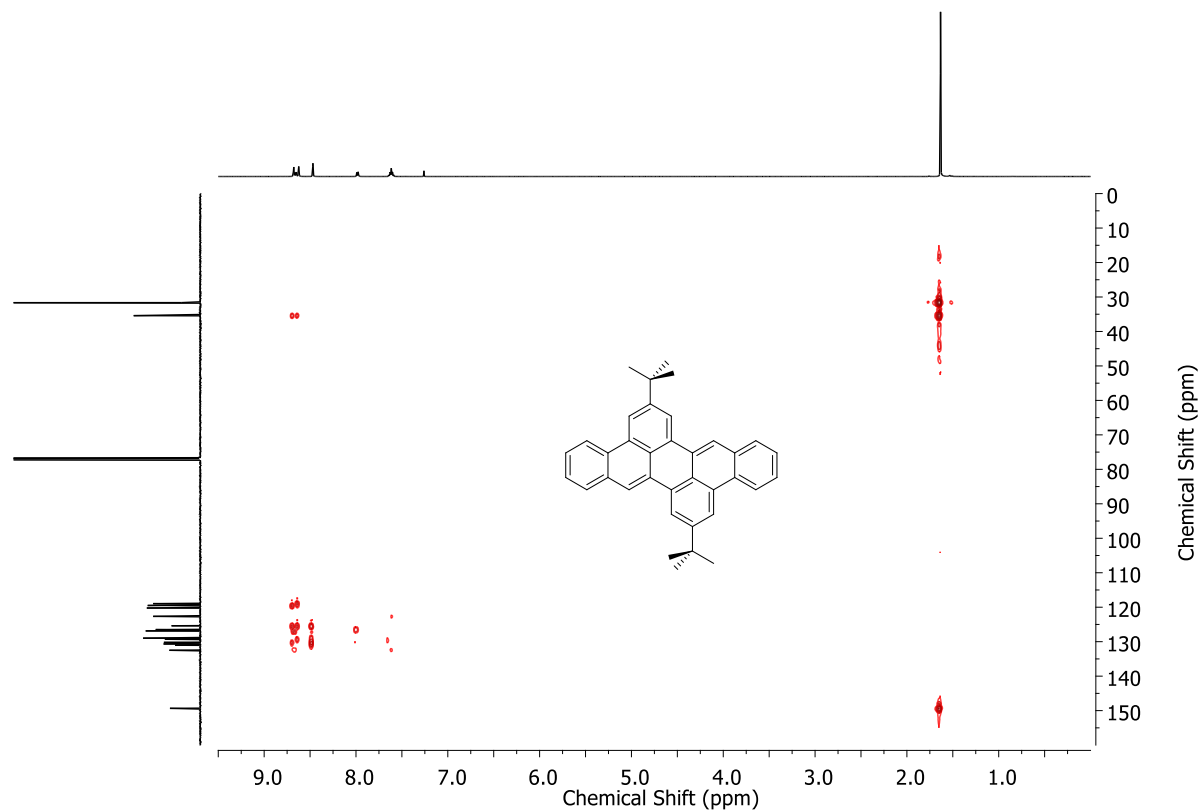


Figure S49. HMBC NMR spectrum of **6a**.

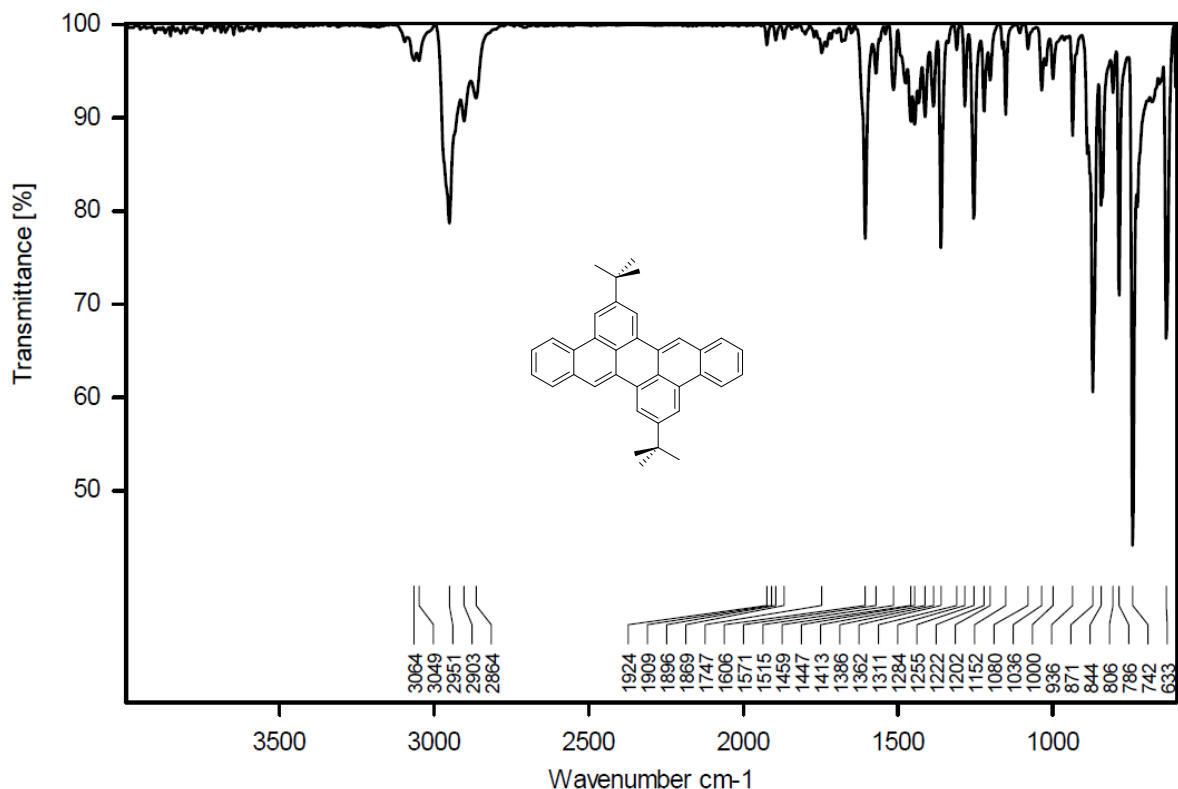


Figure S50. FT-IR spectrum (ATR) of **6a**.

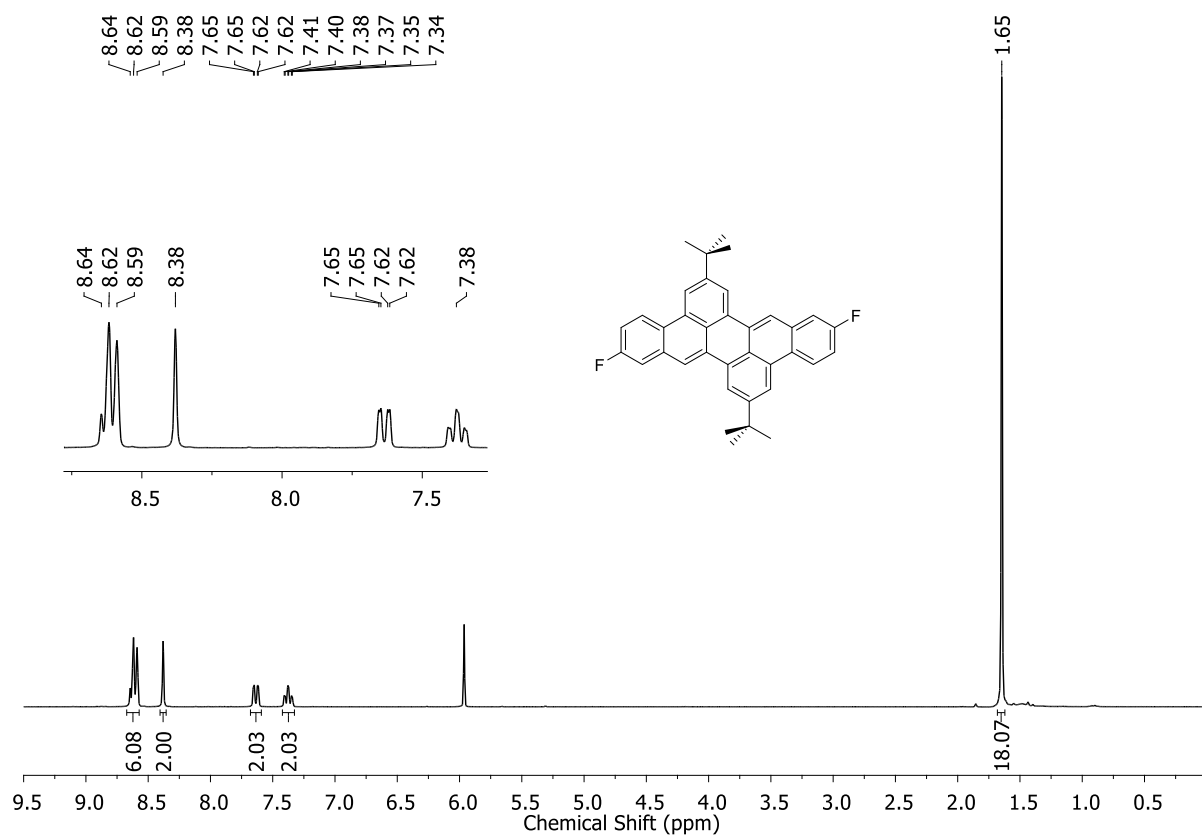


Figure S51. ^1H NMR spectrum ($\text{C}_2\text{D}_2\text{Cl}_4$, 300MHz, 373 K) of **6b**.

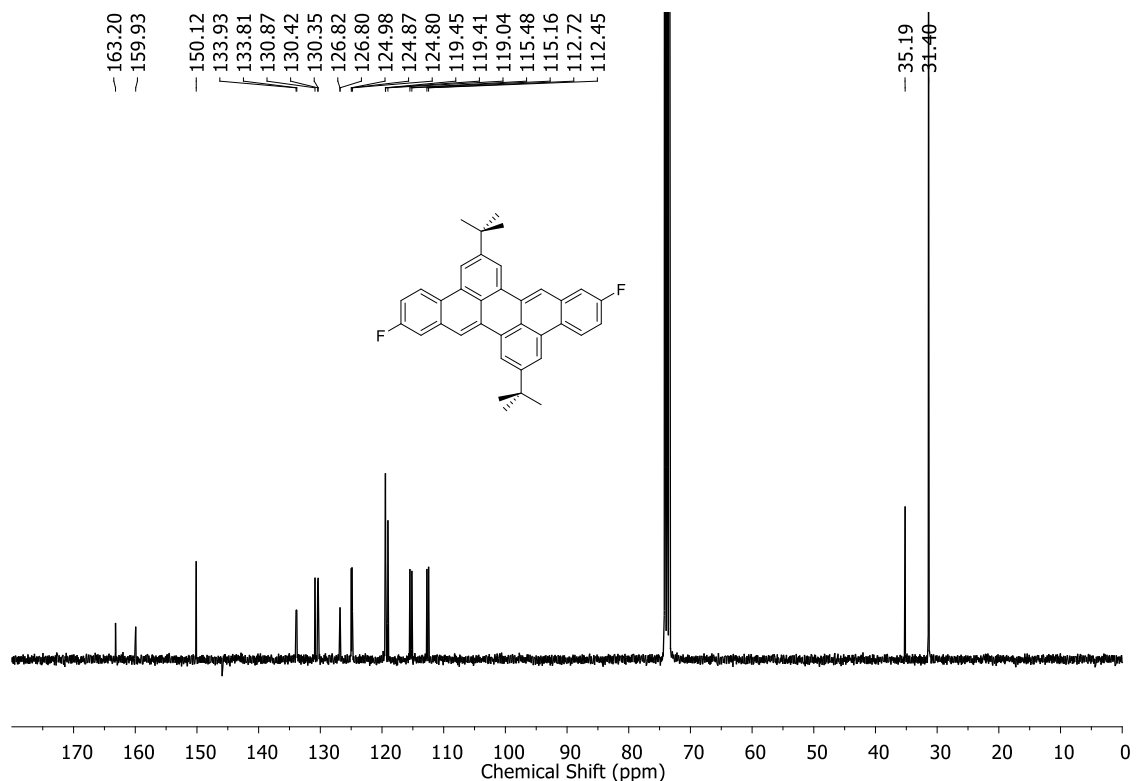


Figure S52. ^{13}C NMR spectrum ($\text{C}_2\text{D}_2\text{Cl}_4$, 75MHz, 373K) of **6b**.

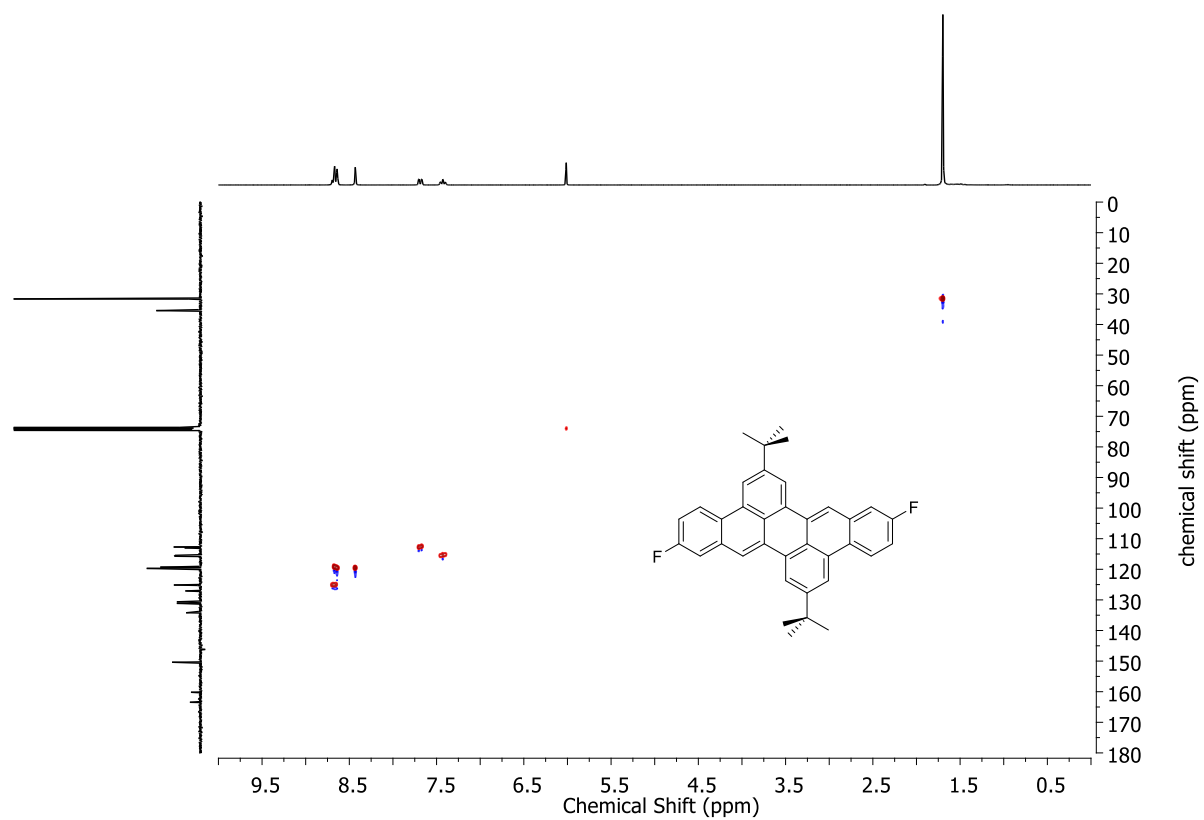


Figure S53. HSQC NMR spectrum of **6b**.

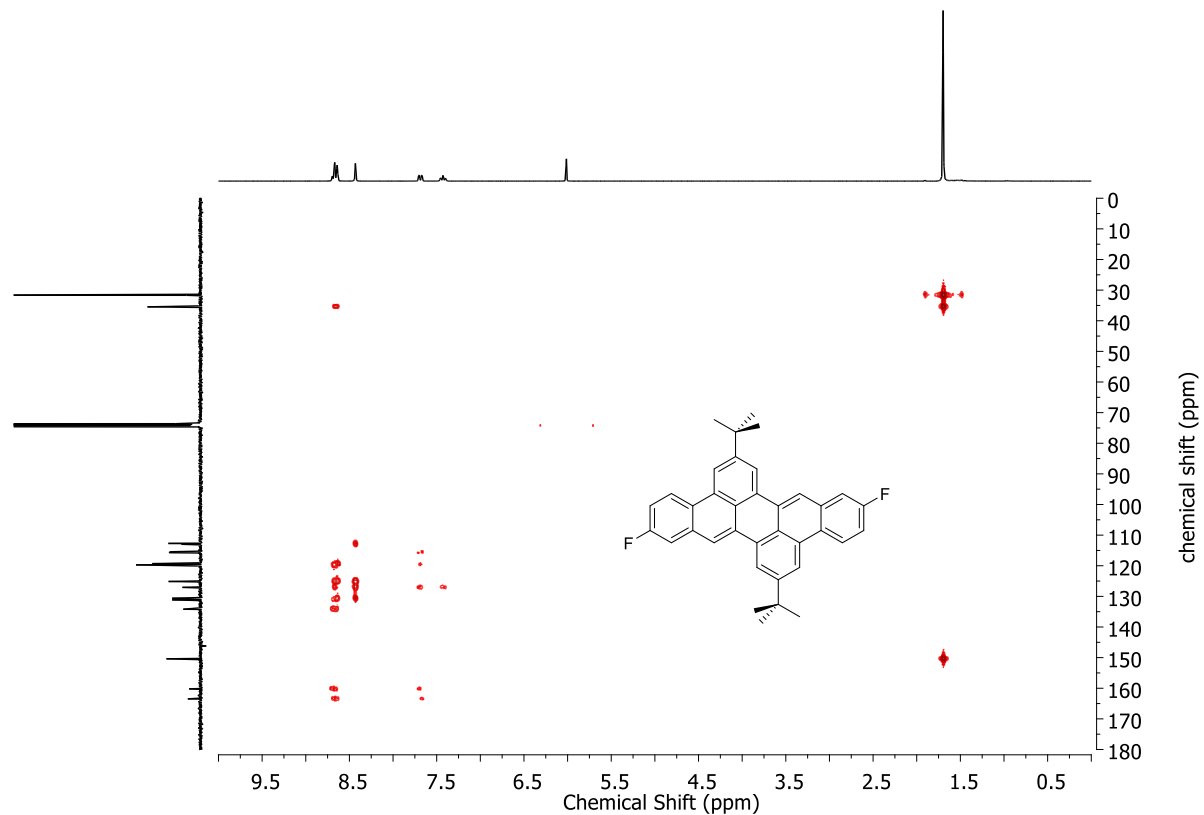


Figure S54. HMBC NMR spectrum of **6b**.

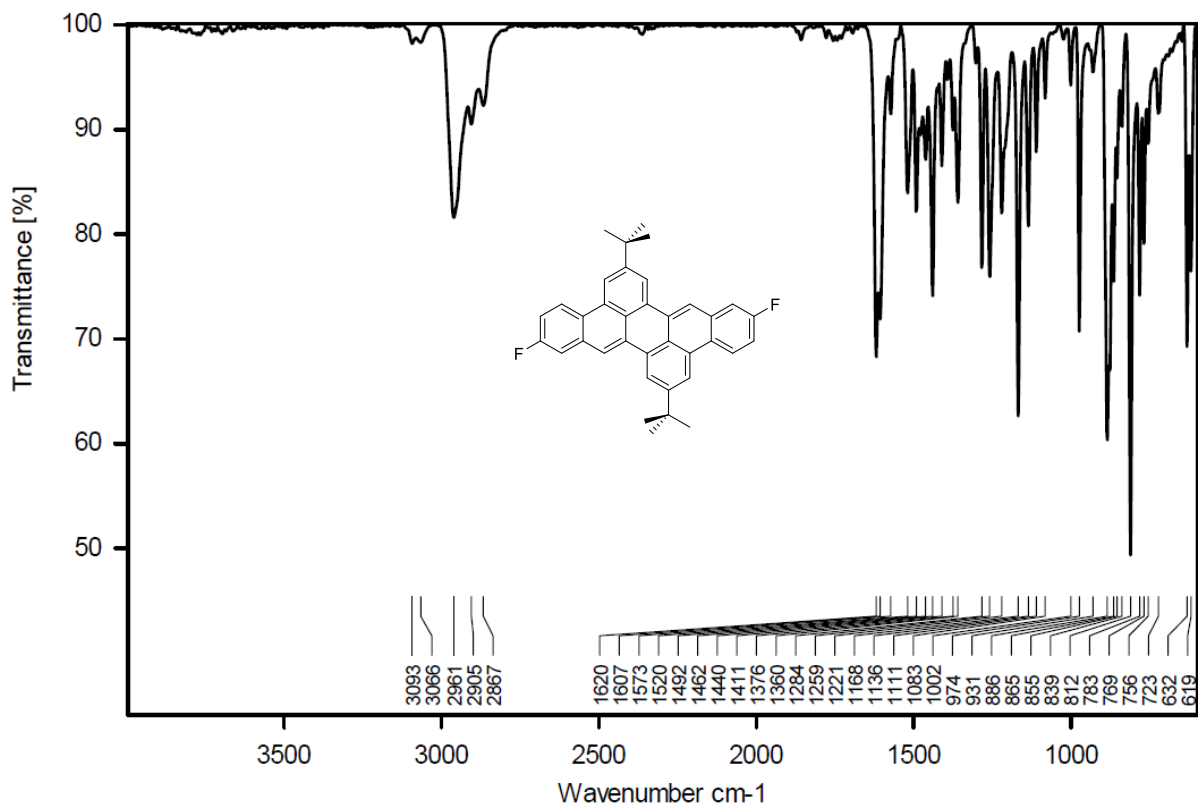


Figure S55. FT-IR spectrum (ATR) of **6b**.

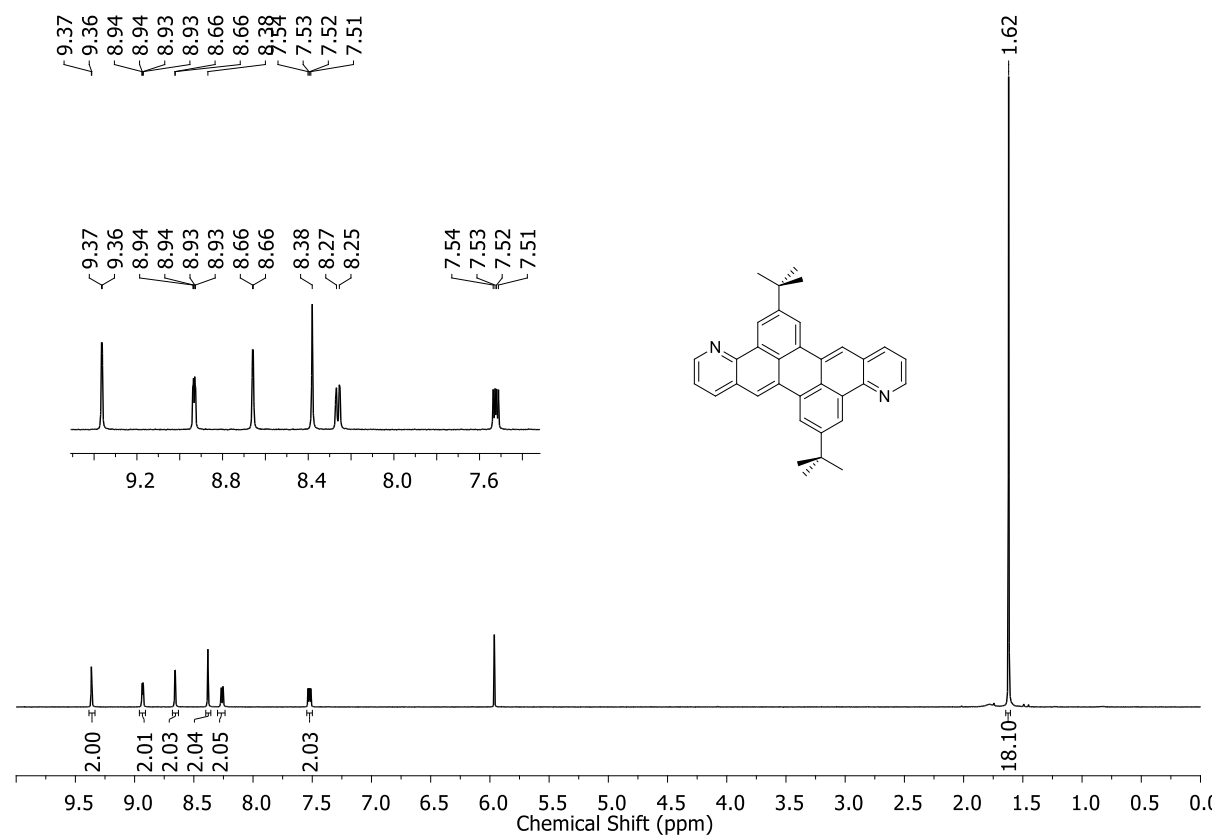


Figure S56. ^1H NMR spectrum (CDCl_3 , 500MHz) of **6c**.

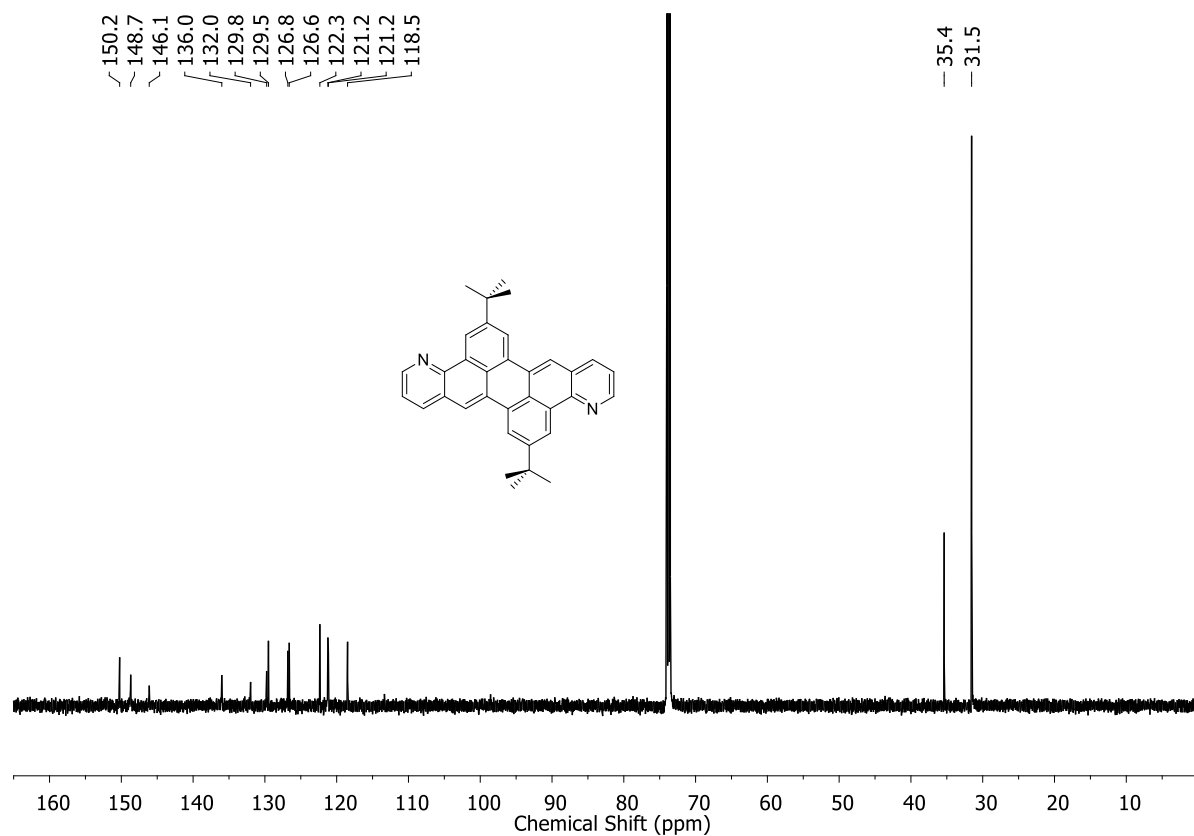


Figure S57. ^{13}C NMR spectrum (CDCl_3 , 125MHz) of **6c**.

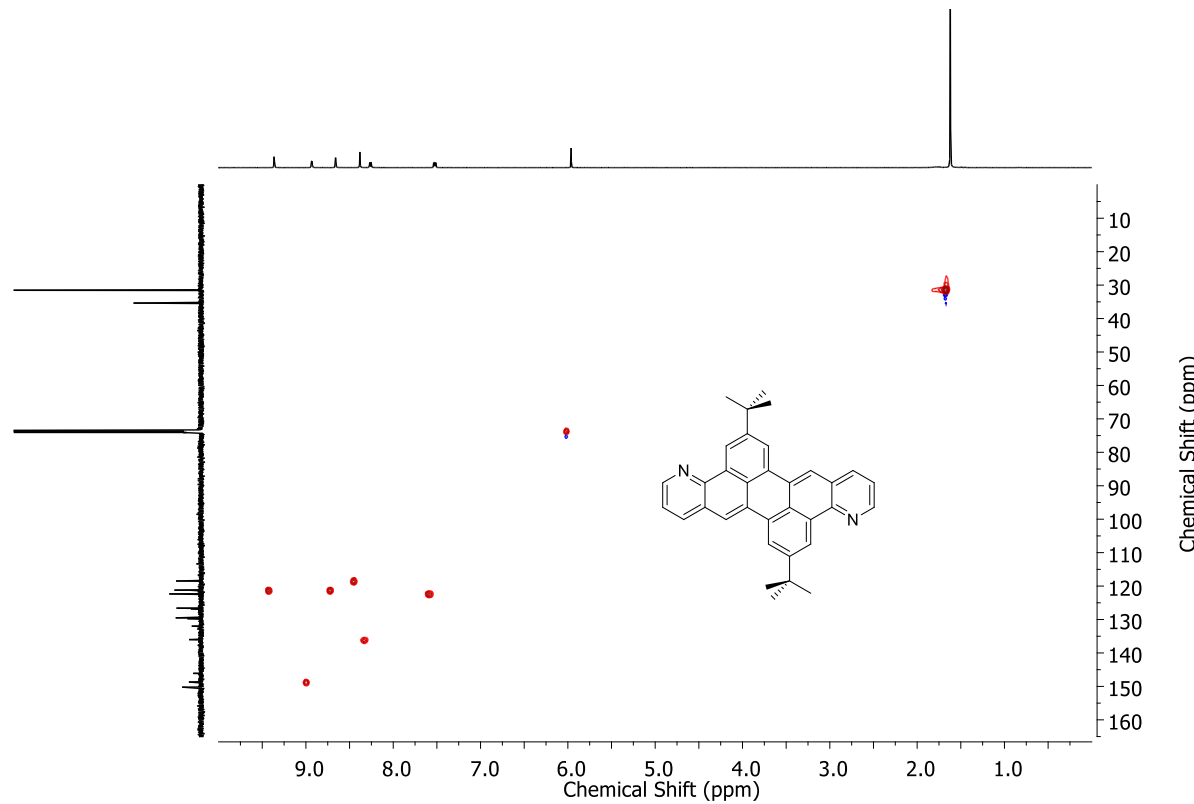


Figure S58. HSQC NMR spectrum of **6c**.

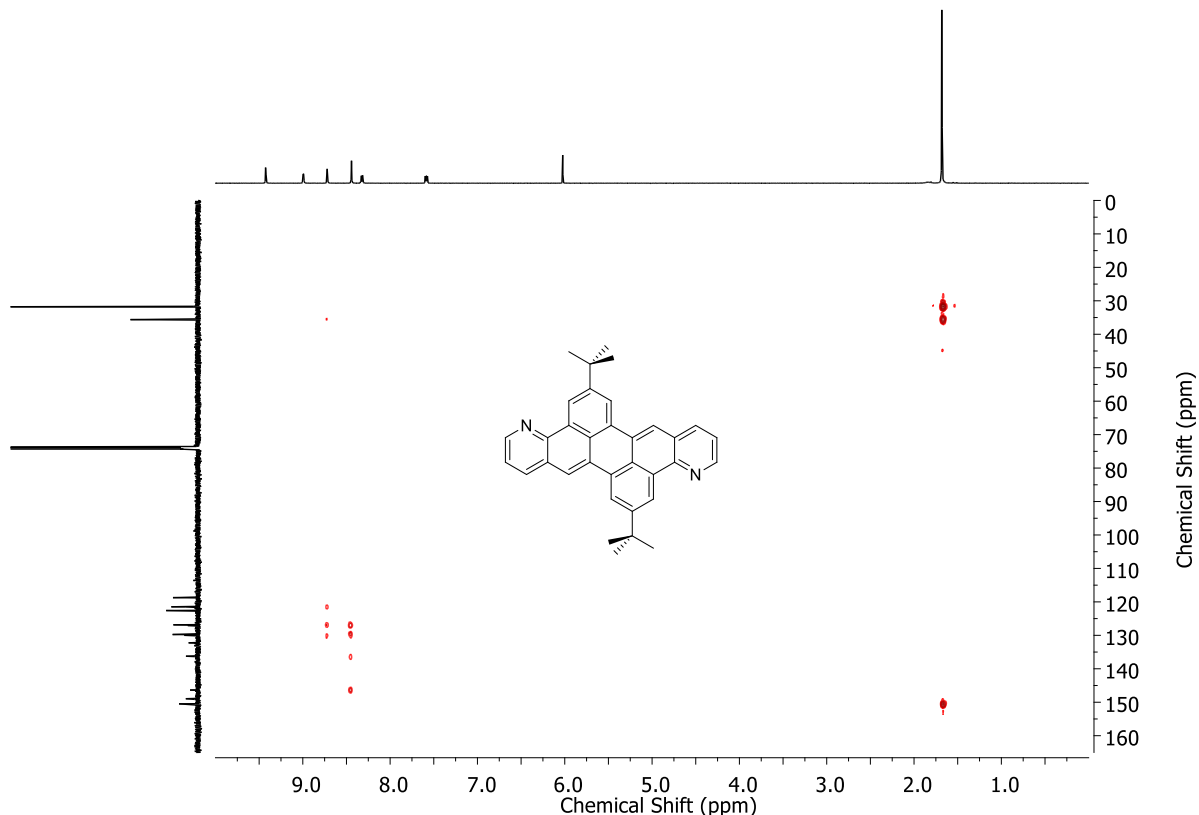


Figure S59. HMBC NMR spectrum of **6c**.

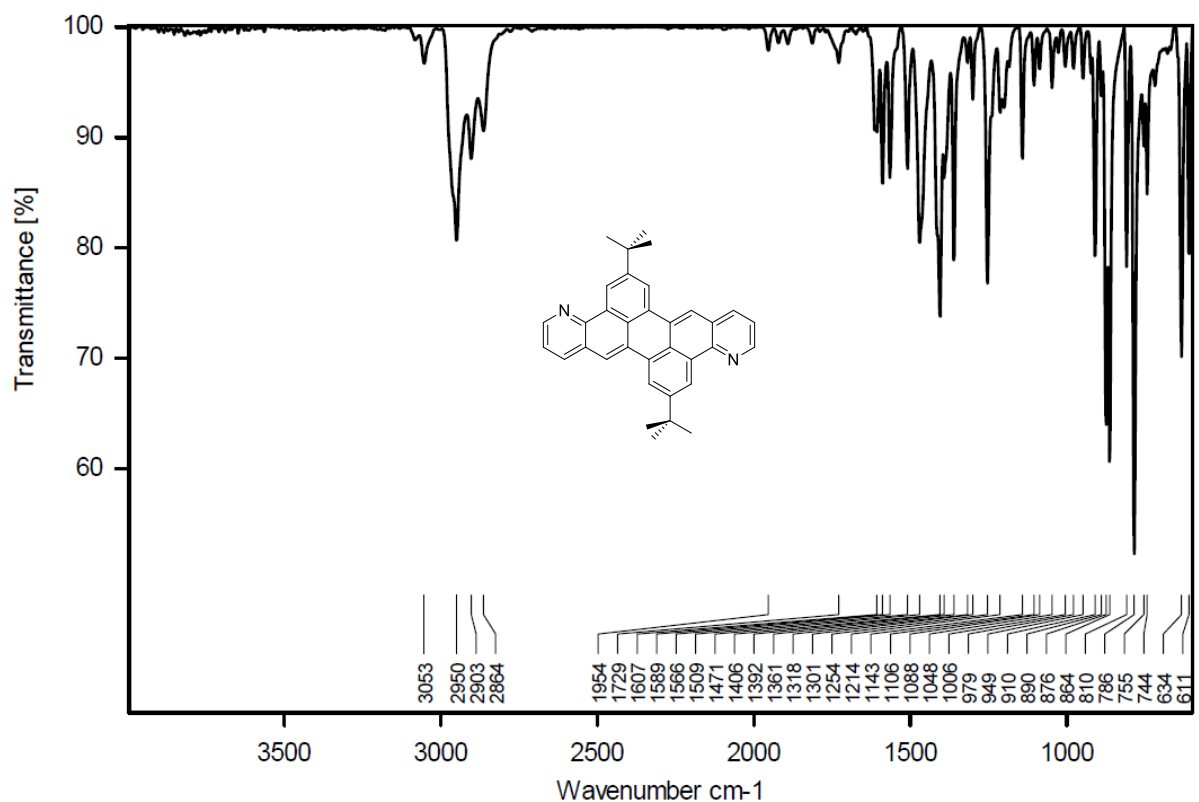


Figure S60. FT-IR spectrum (ATR) of **6c**.

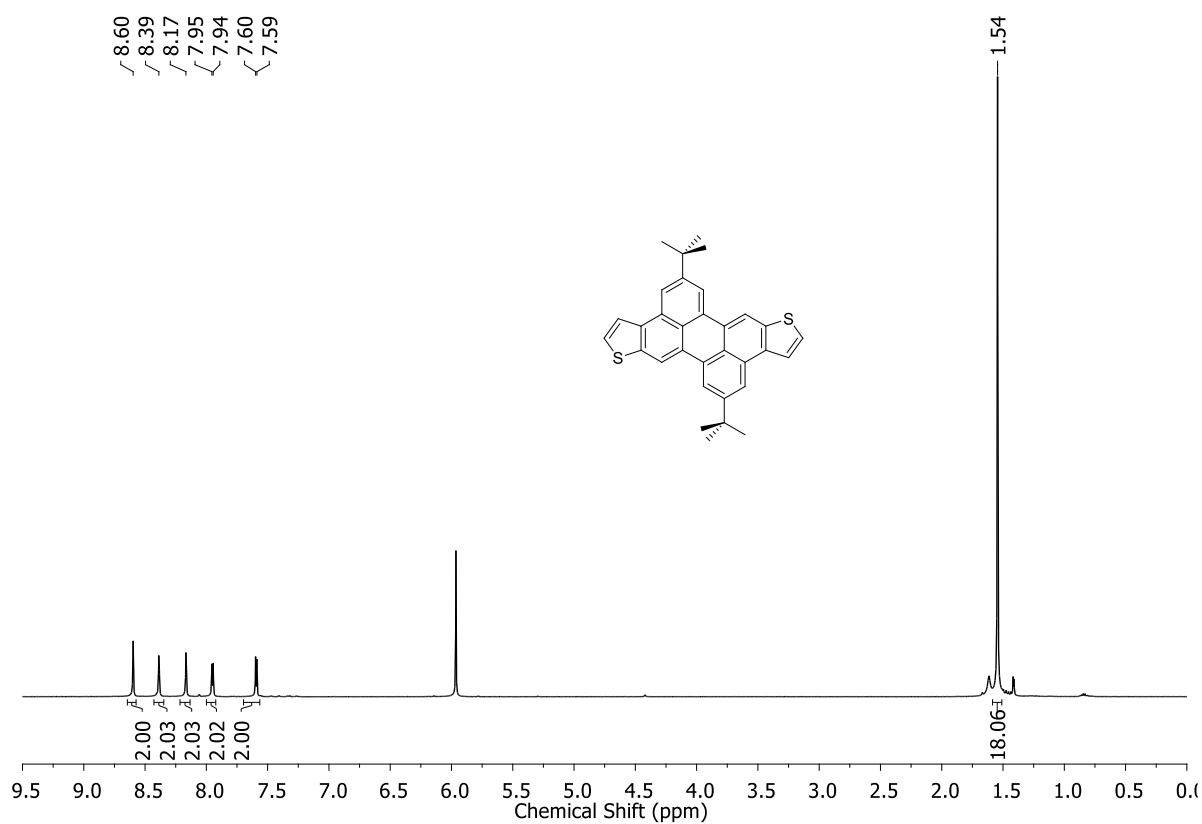


Figure S61.¹H NMR spectrum (C₂D₂Cl₄, 500MHz) of **6d**.

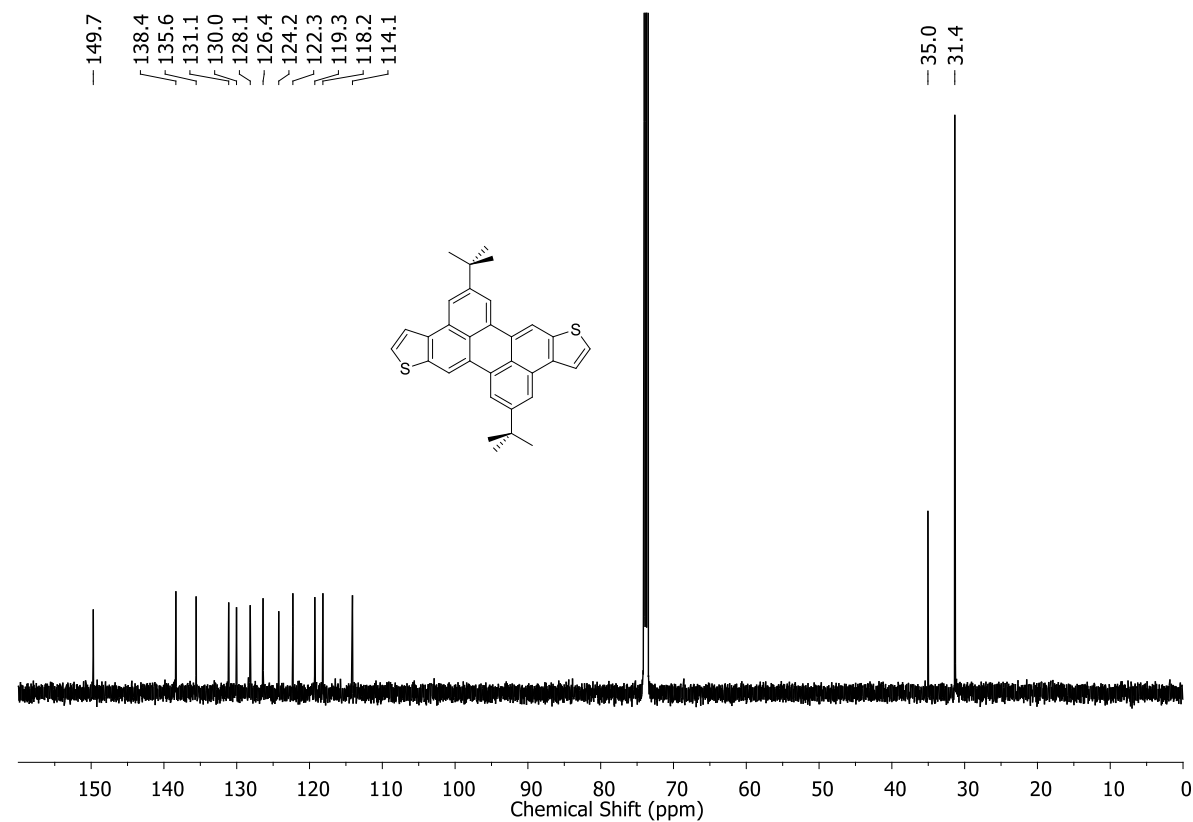


Figure S62. ^{13}C NMR spectrum ($\text{C}_2\text{D}_2\text{Cl}_4$, 125MHz) of **6d**.

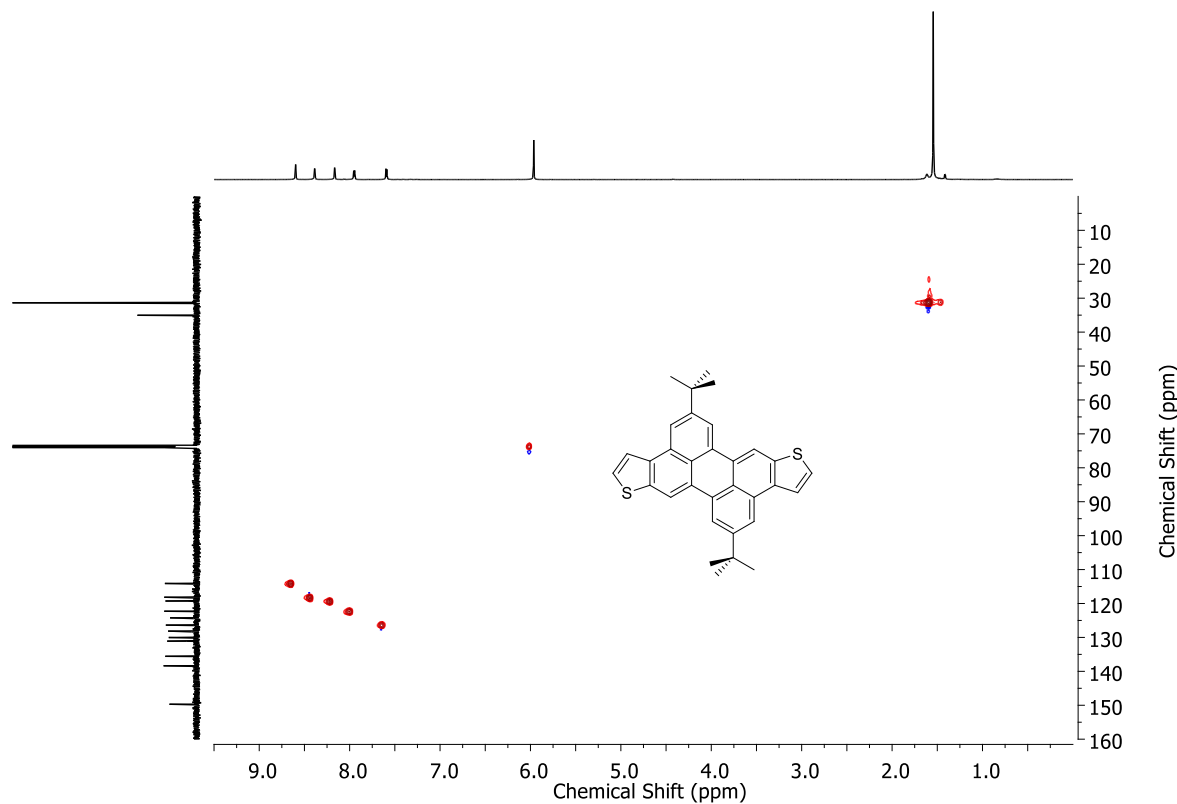


Figure S63. HSQC NMR spectrum of **6d**.

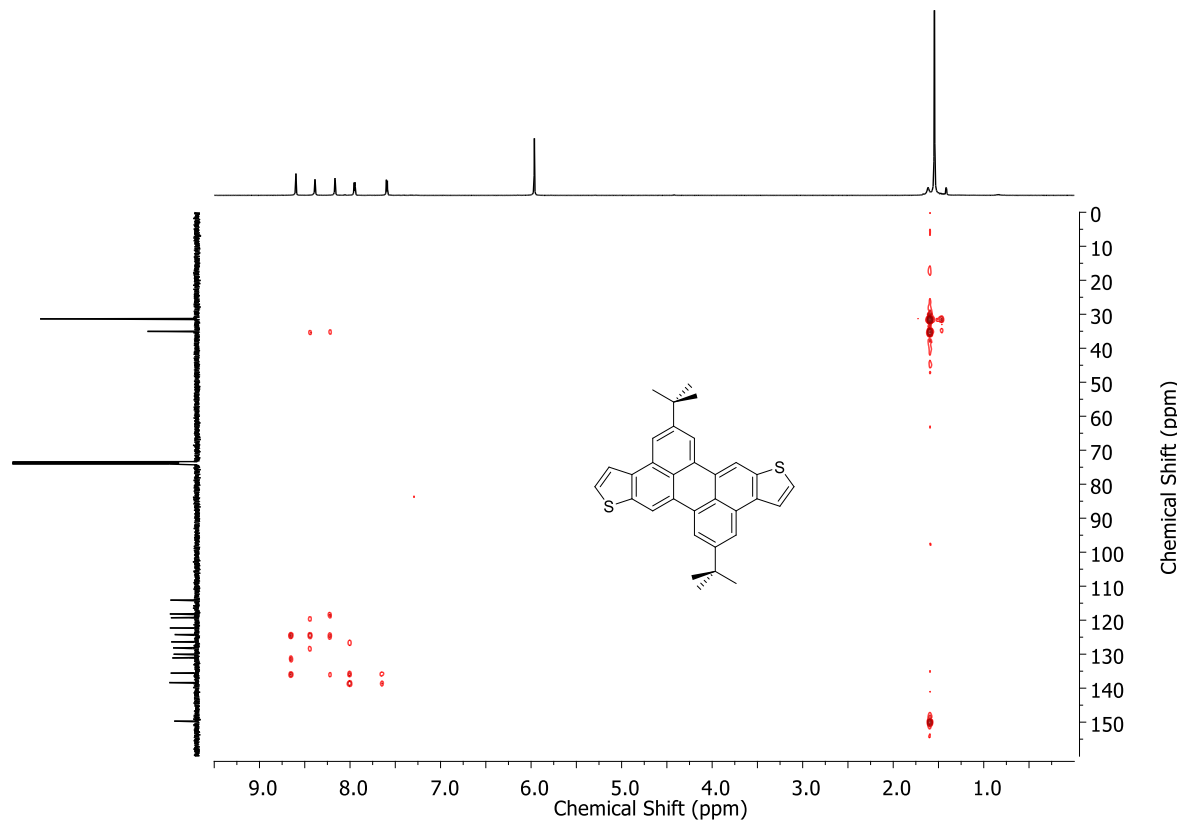


Figure S64. HMBC NMR spectrum of **6d**.

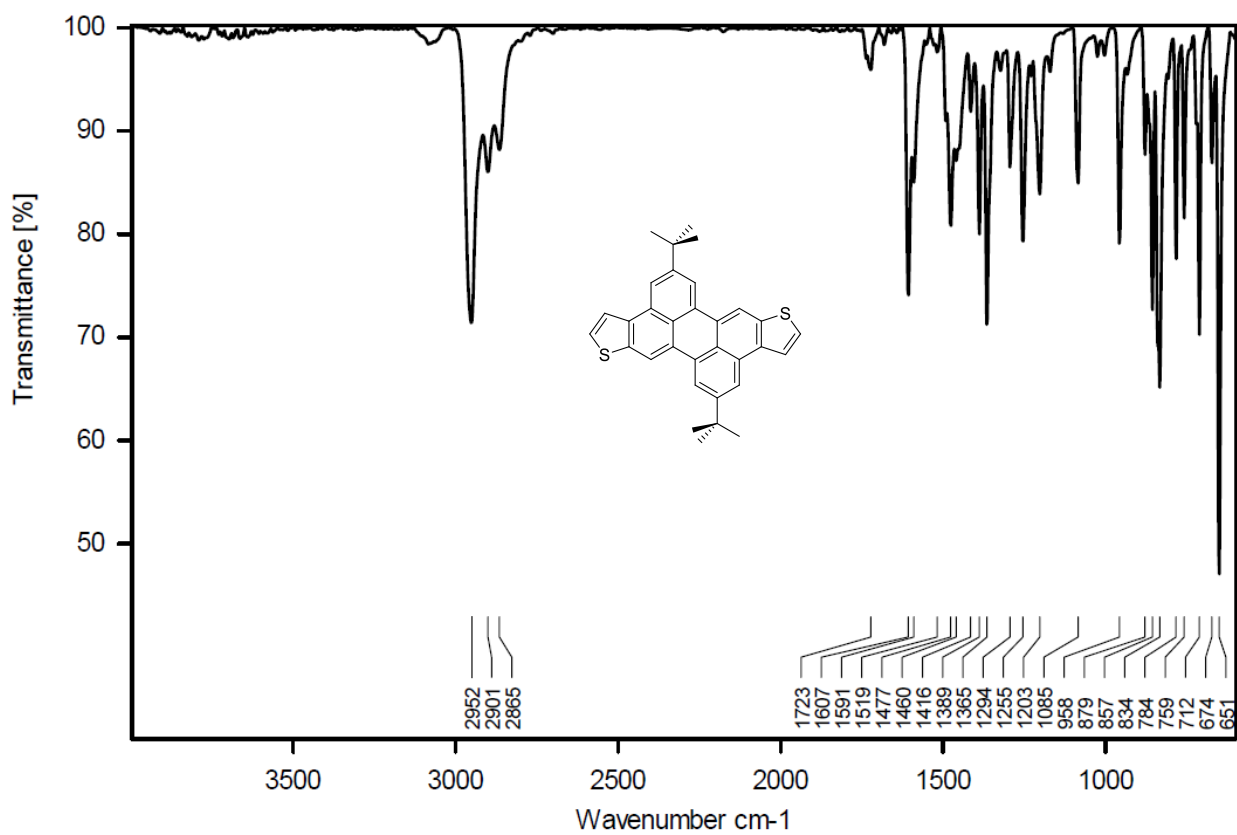


Figure S65. FT-IR spectrum (ATR) of **6d**.

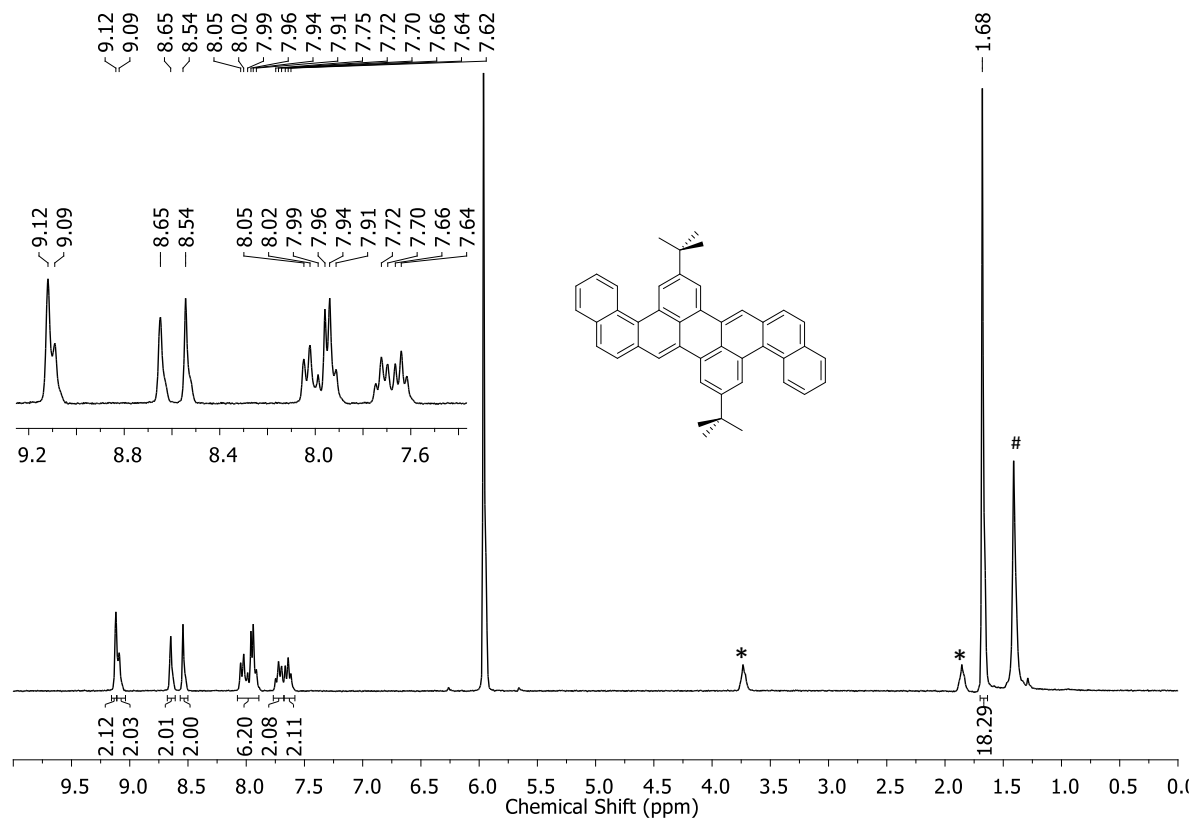


Figure S66. ^1H NMR spectrum ($\text{C}_2\text{D}_2\text{Cl}_4$, 300MHz, 403K) of **6e**. * residual THF; # water.

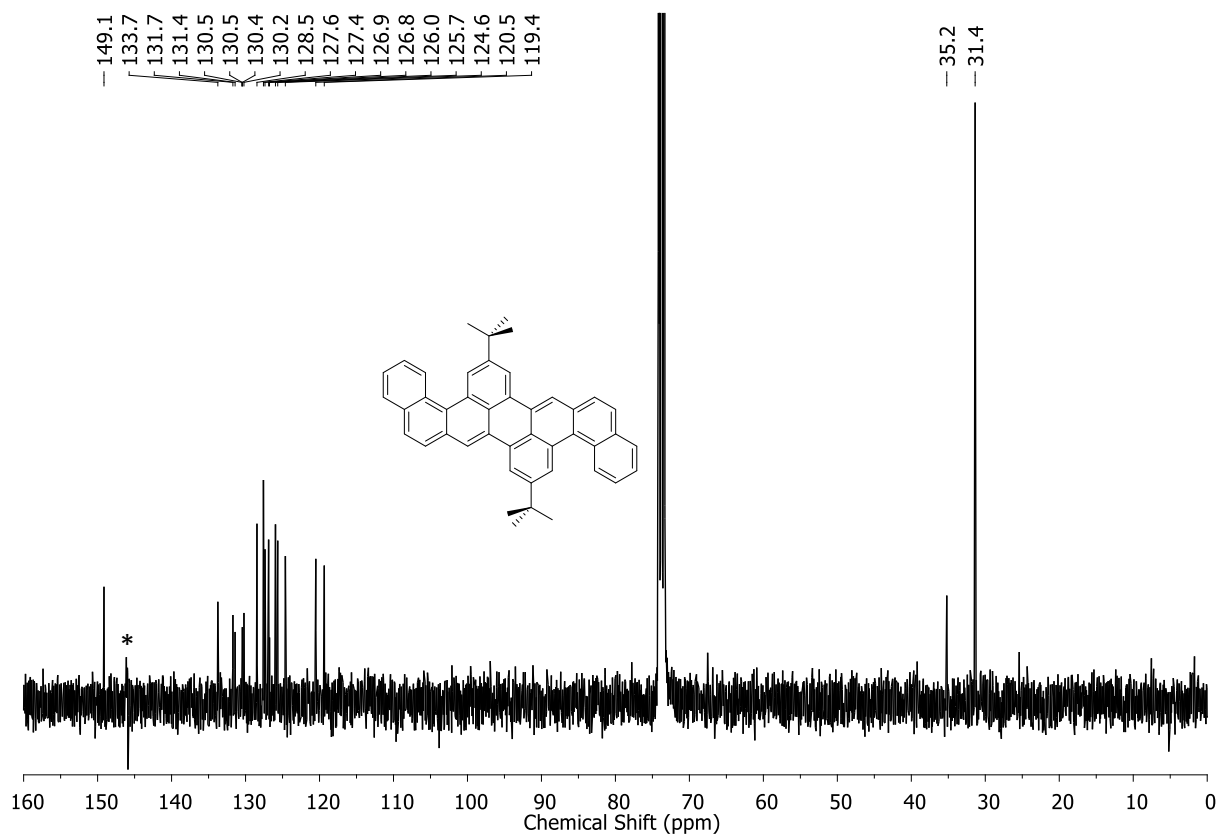


Figure S67. ^{13}C NMR spectrum ($\text{C}_2\text{D}_2\text{Cl}_4$, 75MHz, 403K) of **6e**. * noise.

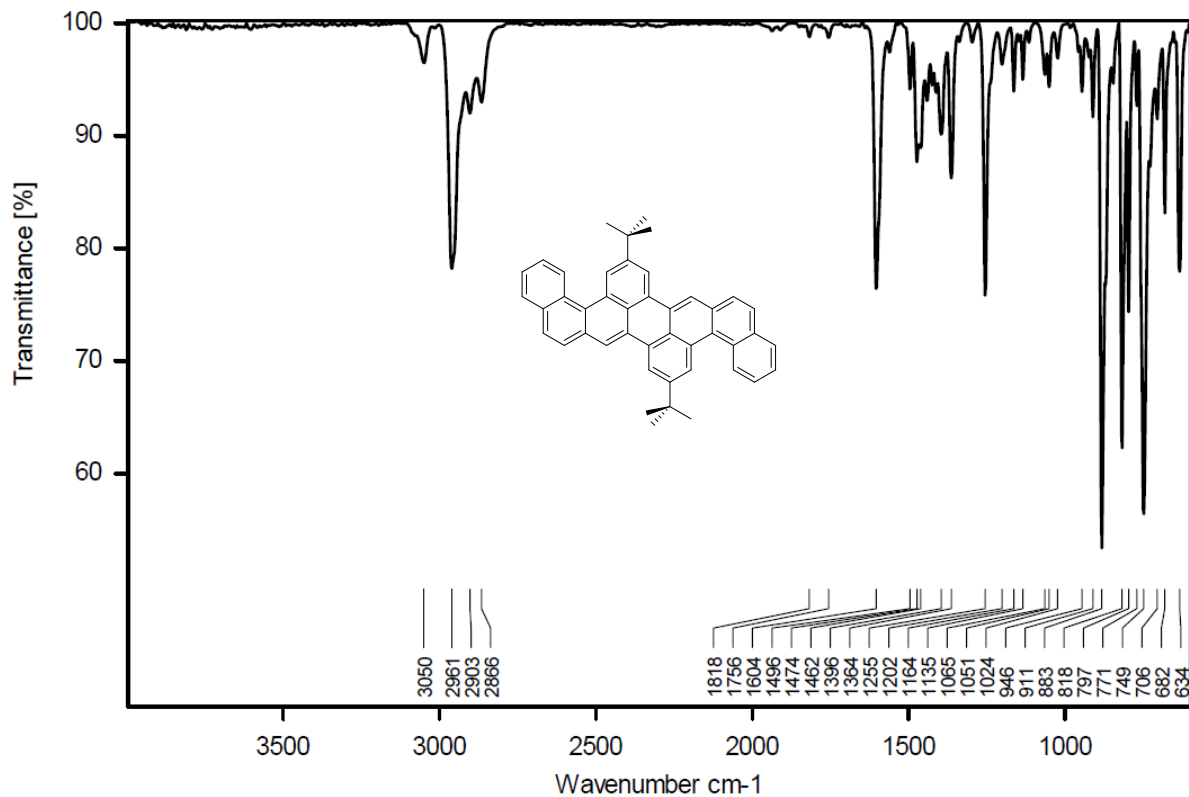


Figure S68. FT-IR spectrum (ATR) of **6e**.

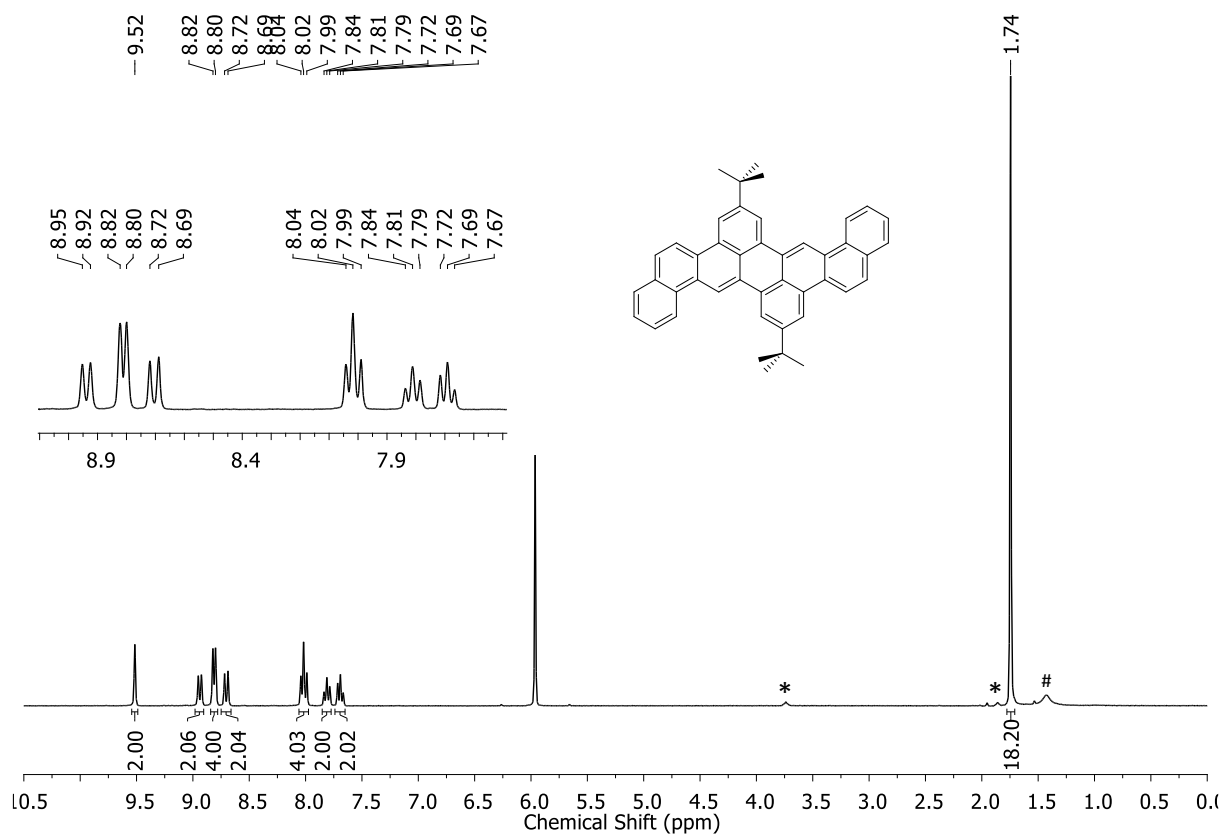


Figure S69. ^1H NMR spectrum ($\text{C}_2\text{D}_2\text{Cl}_4$, 300MHz, 403 K) of **6f**. * residual THF; # water.

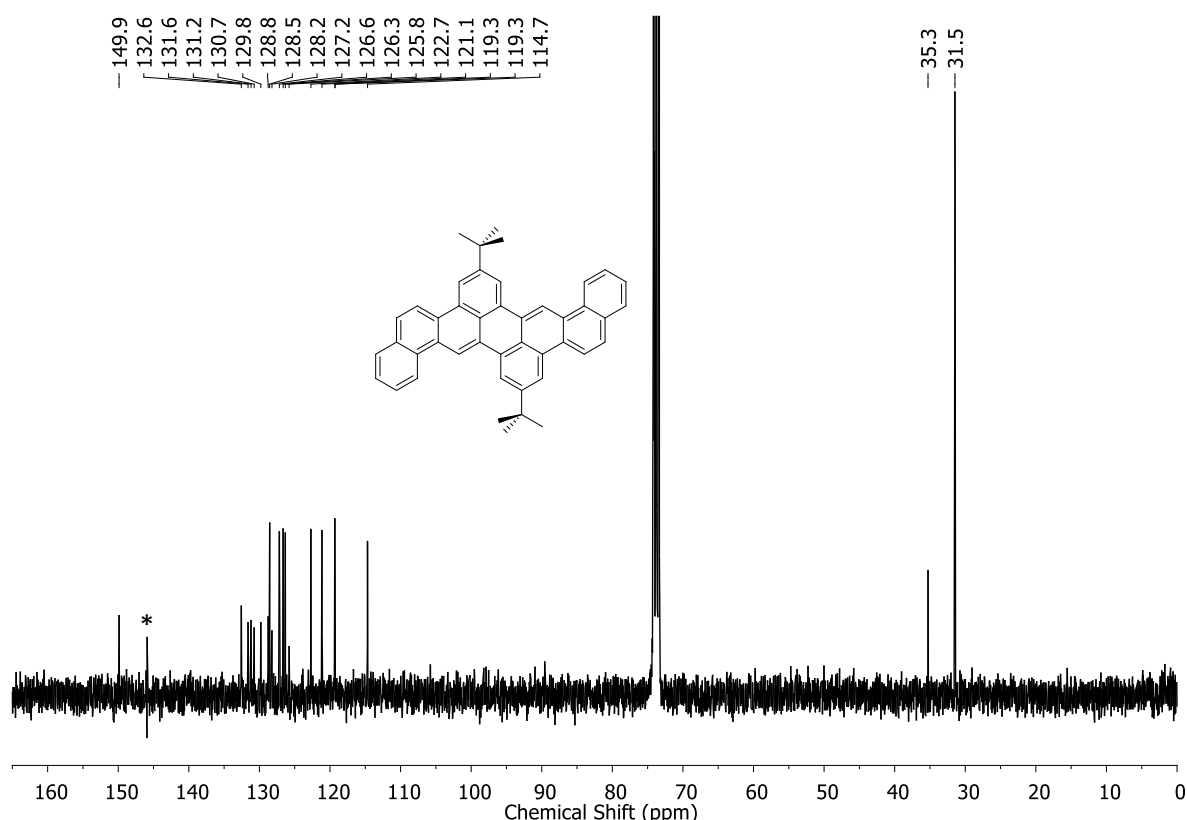


Figure S70. ^{13}C NMR spectrum ($\text{C}_2\text{D}_2\text{Cl}_4$, 75MHz, 403 K) of **6f**. * noise.

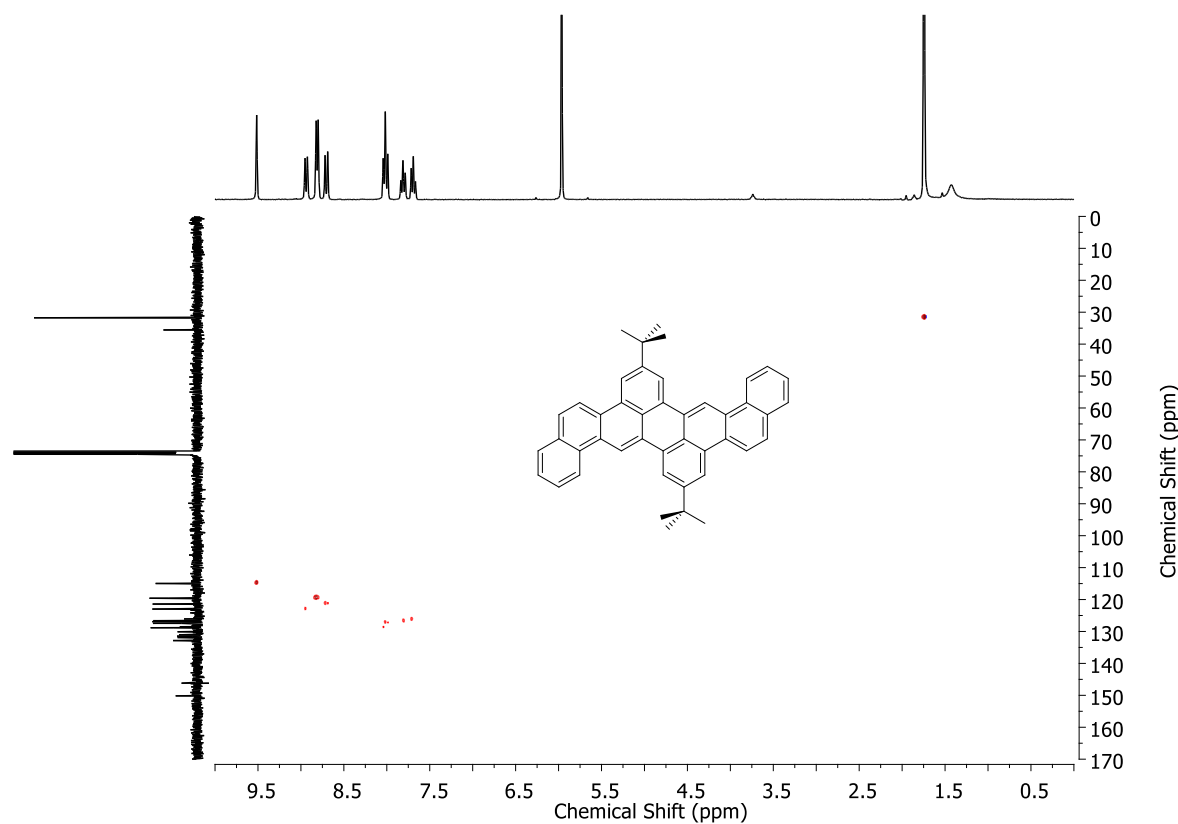


Figure S71. HSQC NMR spectrum of **6f**.

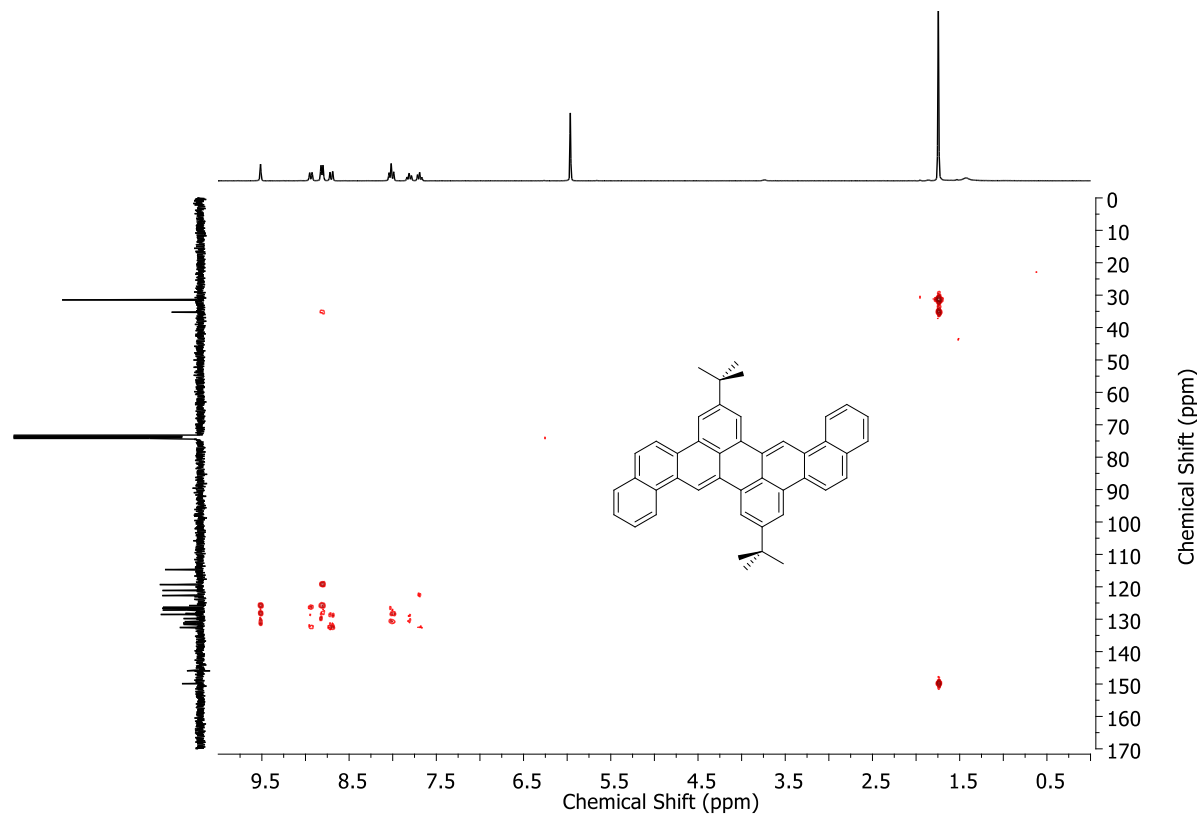


Figure S72. HMBC NMR spectrum of **6f**.

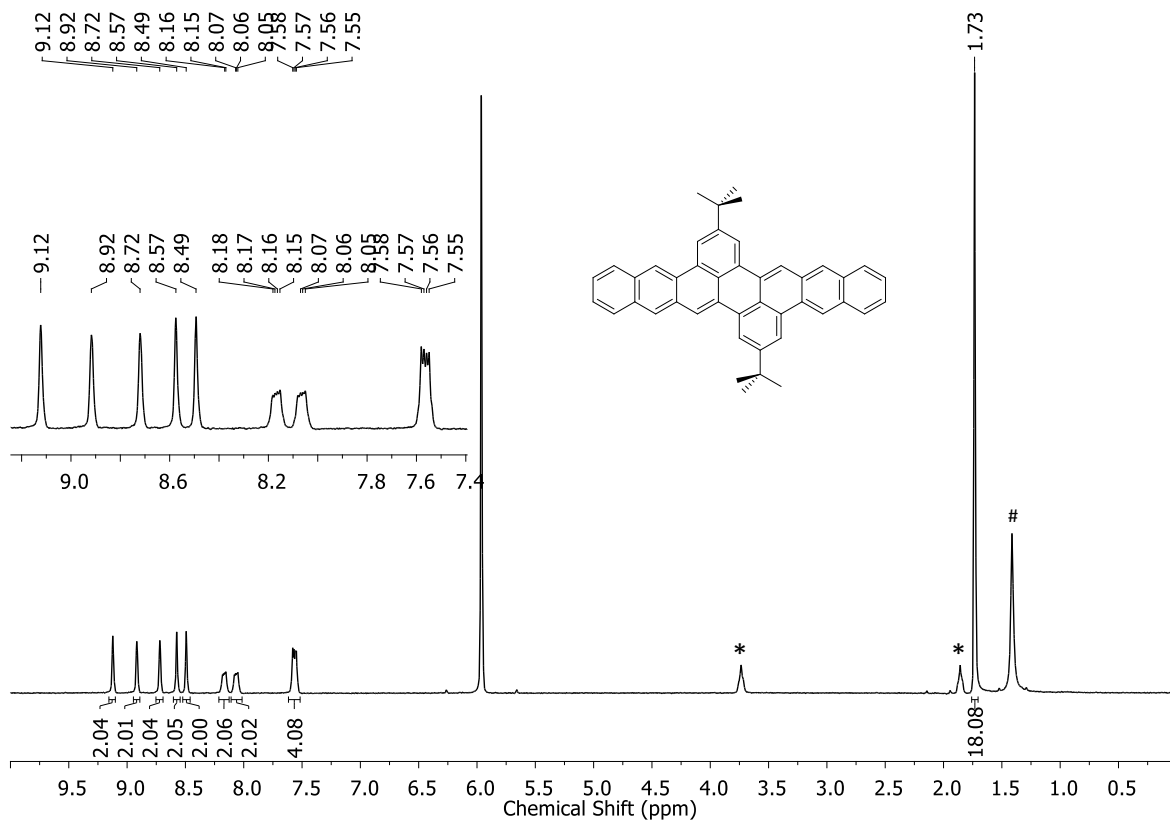


Figure S73.¹H NMR spectrum (C₂D₂Cl₄, 300MHz, 403K) of **6g**. * residual THF; # water.

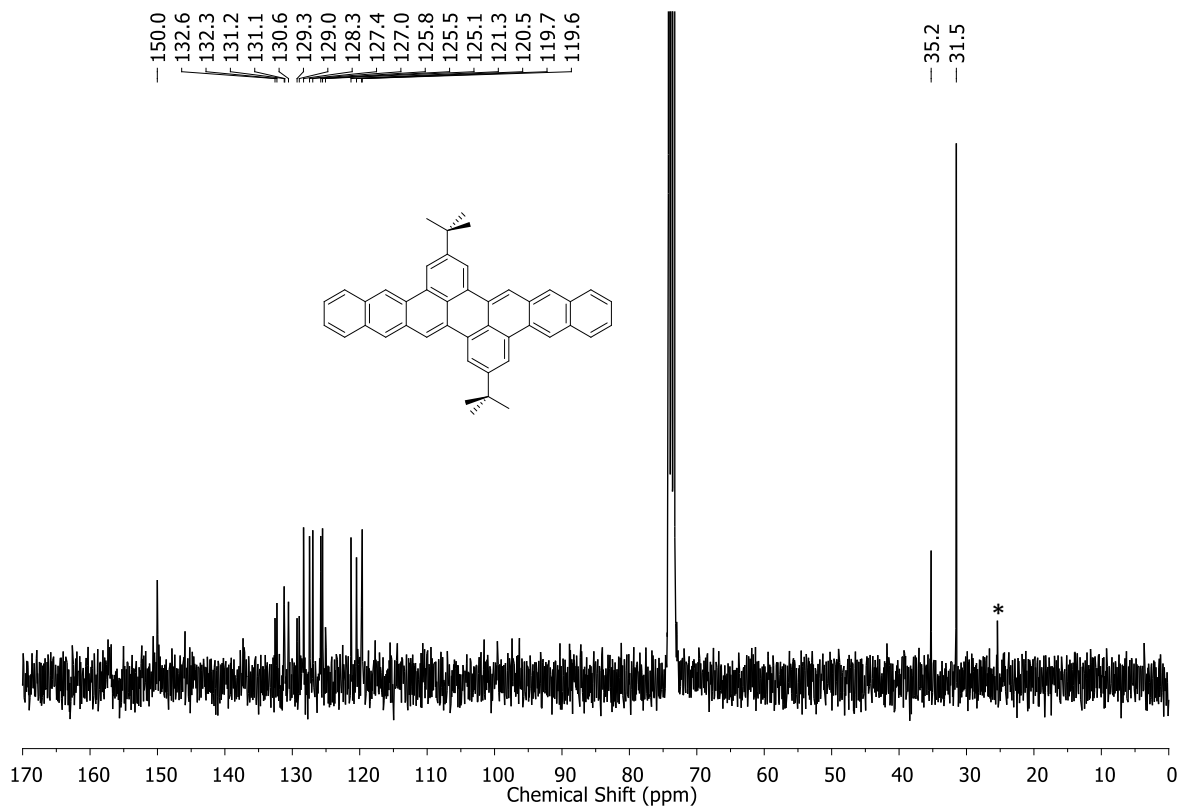


Figure S74. ^{13}C NMR spectrum ($\text{C}_2\text{D}_2\text{Cl}_4$, 75MHz, 403K) of **6g**. * residual THF.

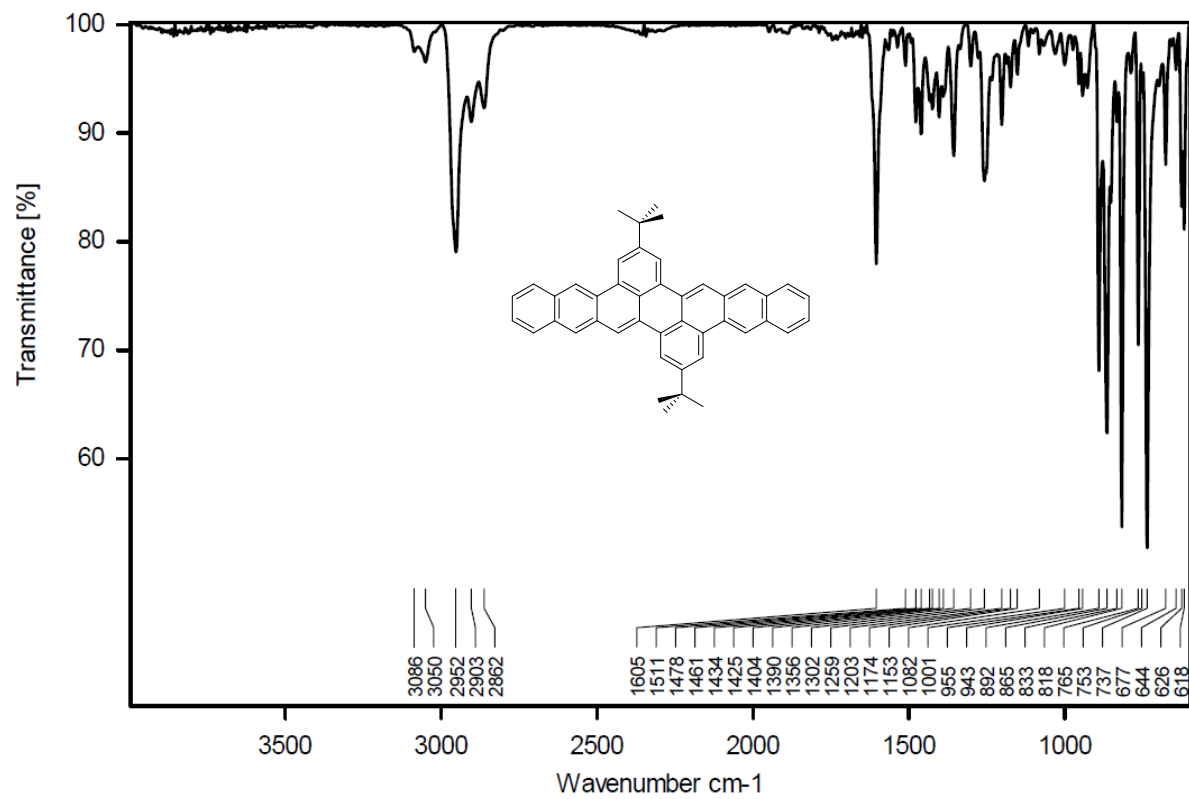


Figure S75. FT-IR spectrum (ATR) of **6g**.

5. UV-vis and fluorescence spectra

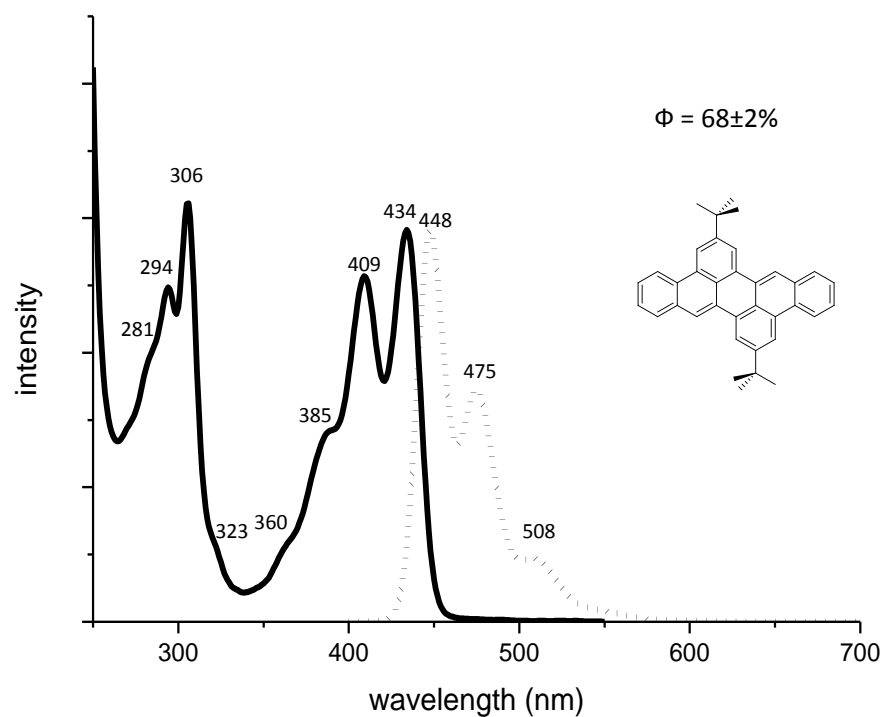


Figure S76. UV/Vis and emission (Ex 434 nm) spectra and quantum yield of compound **6a** measured in CHCl_3 at room temperature.

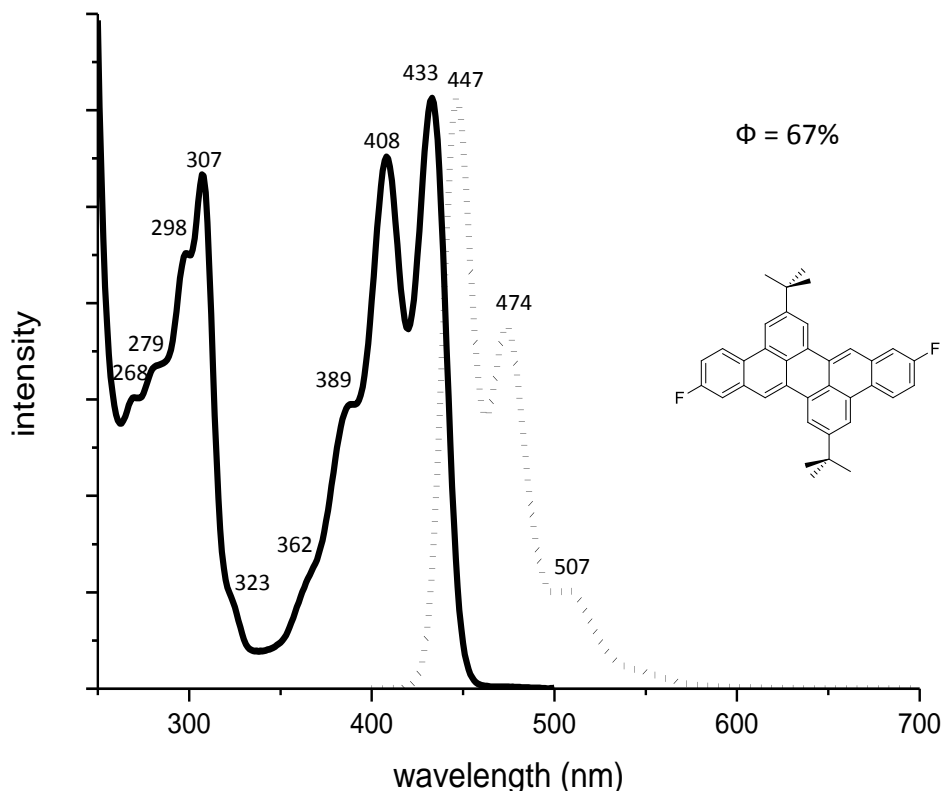


Figure S77. UV/Vis and emission (Ex 433 nm) spectra and quantum yield of compound **6b** measured in CHCl_3 at room temperature.

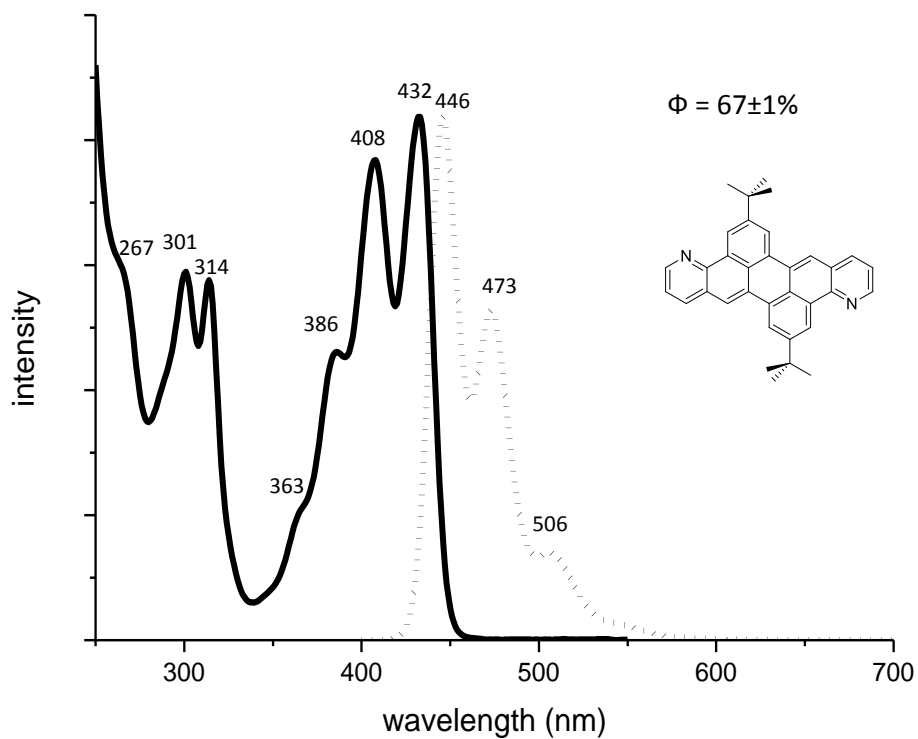


Figure S78. UV/Vis and emission (Ex 432 nm) spectra and quantum yield of compound **6c** measured in CHCl₃ at room temperature.

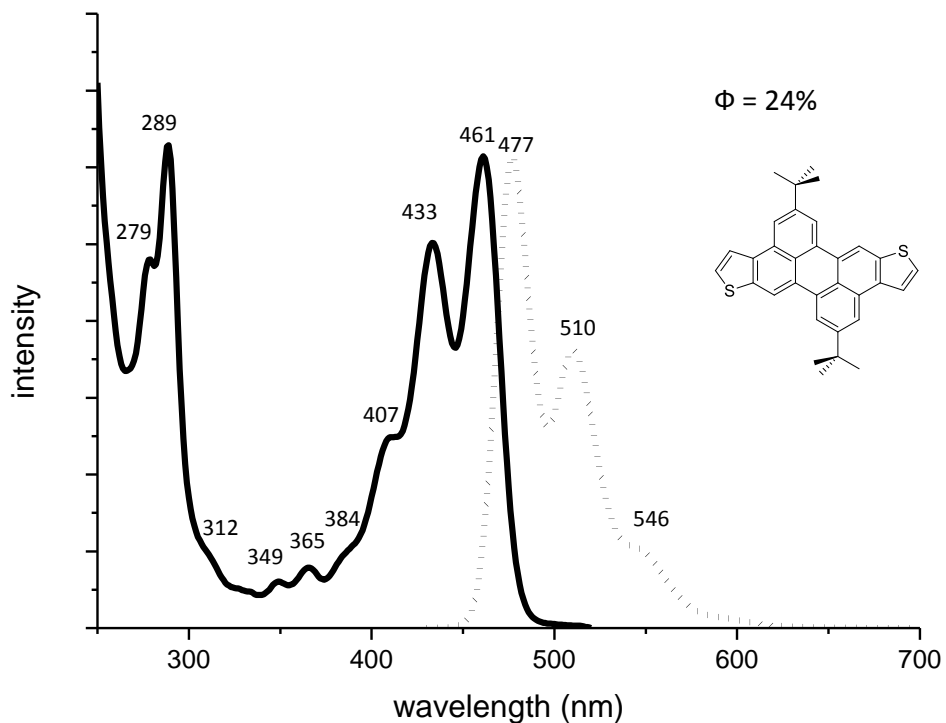


Figure S79. UV/Vis and emission (Ex 461 nm) spectra and quantum yield of compound **6d** measured in CHCl₃ at room temperature.

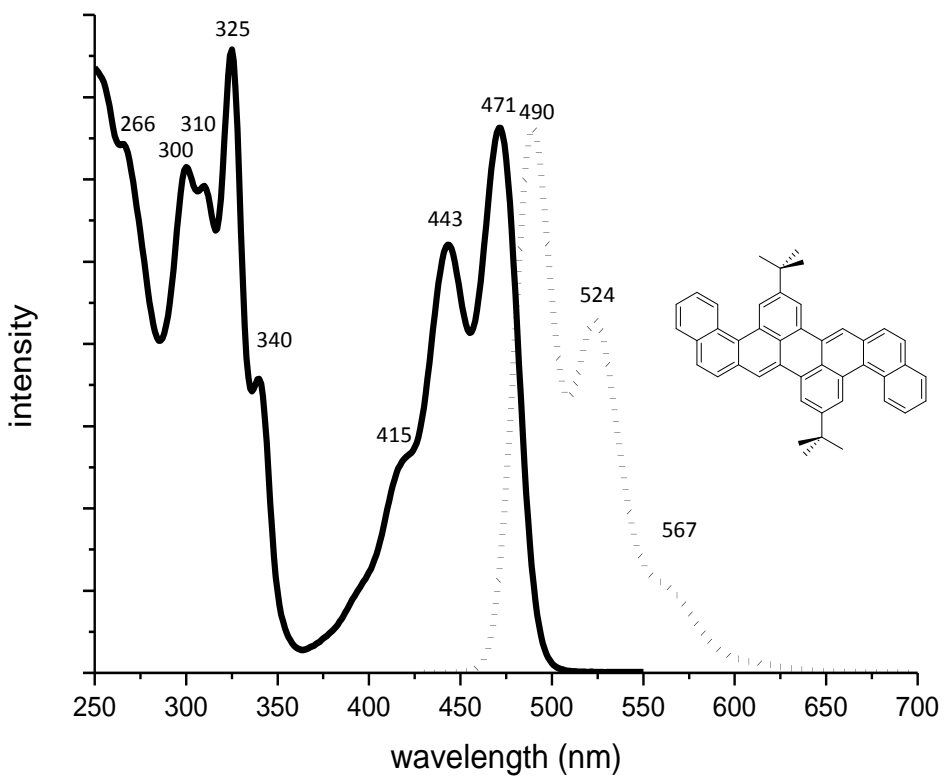


Figure S80. UV/Vis and emission (Ex 471 nm) spectra and quantum yield of compound **6e** measured in CHCl₃ at room temperature.

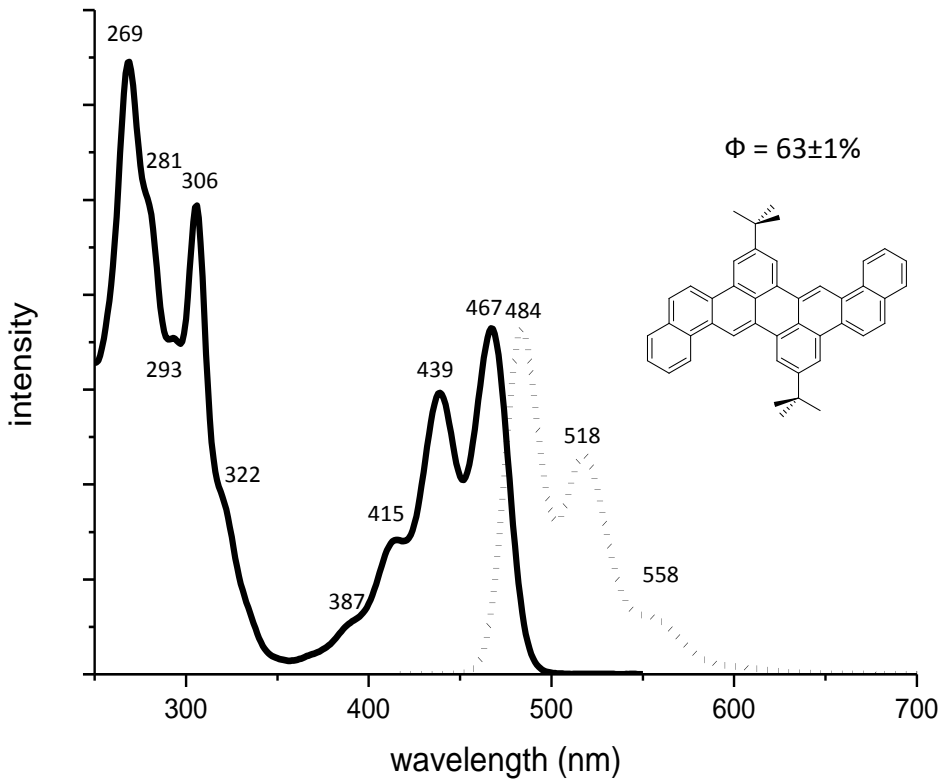


Figure S81. UV/Vis and emission (Ex 467 nm) spectra and quantum yield of compound **6f** measured in CHCl₃ at room temperature.

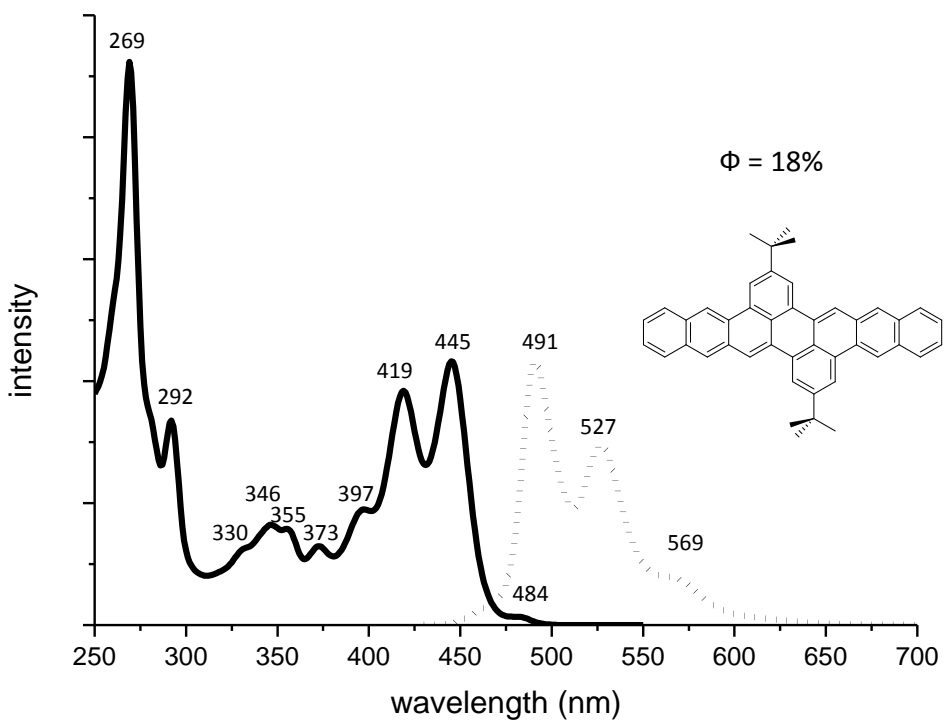


Figure S82. UV/Vis and emission (Ex 445 nm) spectra of compound **6g** measured in CHCl₃ at room temperature.

6. DFT calculations

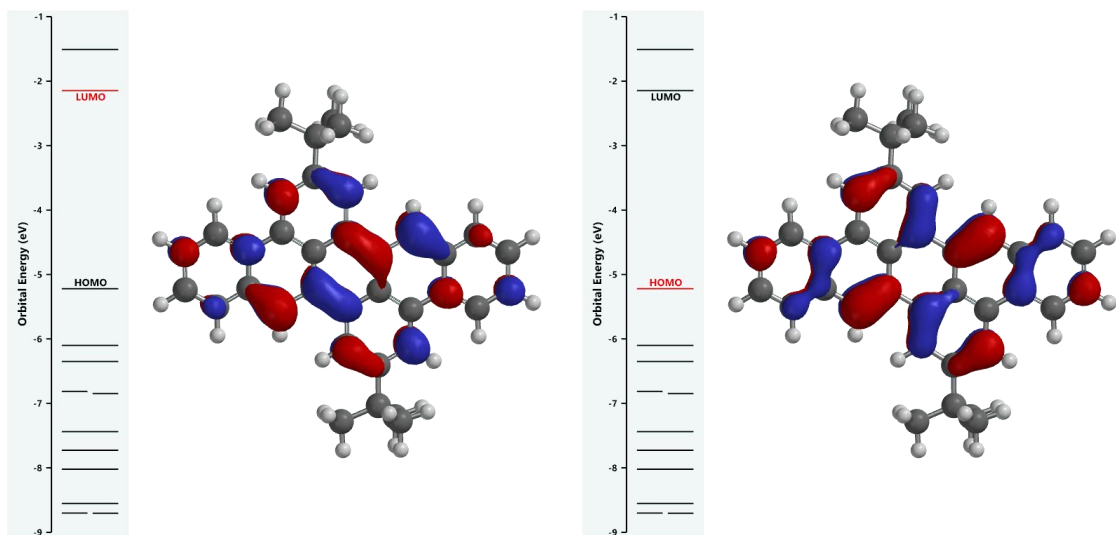


Figure S83. Calculated LUMO (left) and HOMO (right) energy levels of **6a**.

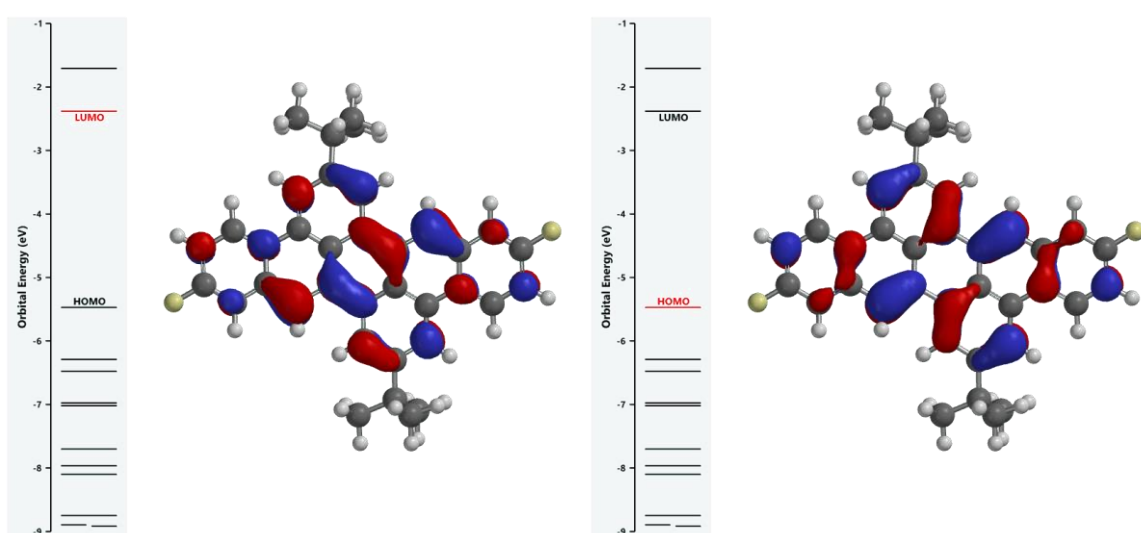


Figure S84. Calculated LUMO (left) and HOMO (right) energy levels of **6b**.

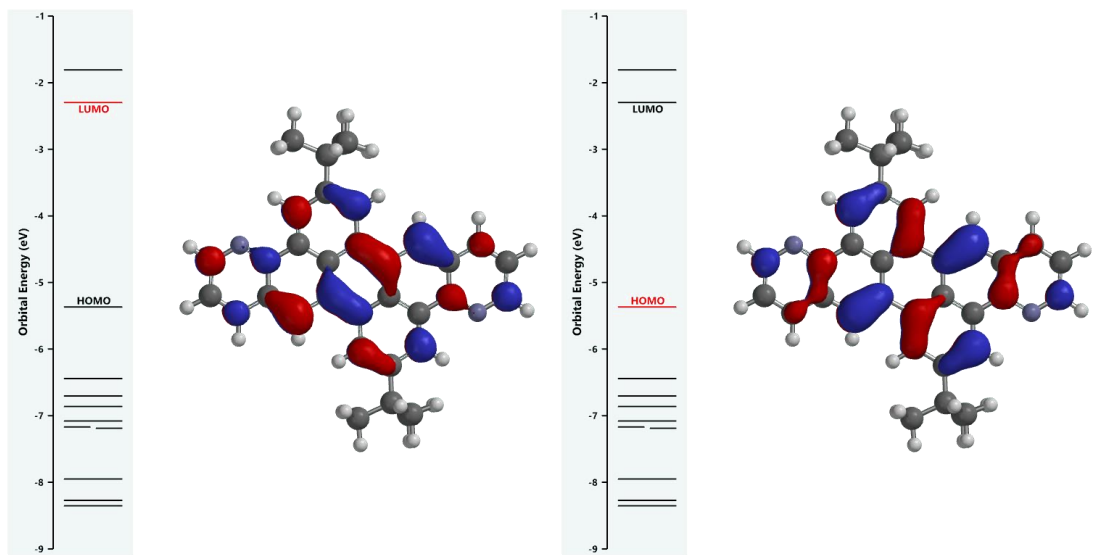


Figure S85. Calculated LUMO (left) and HOMO (right) energy levels of **6c**.

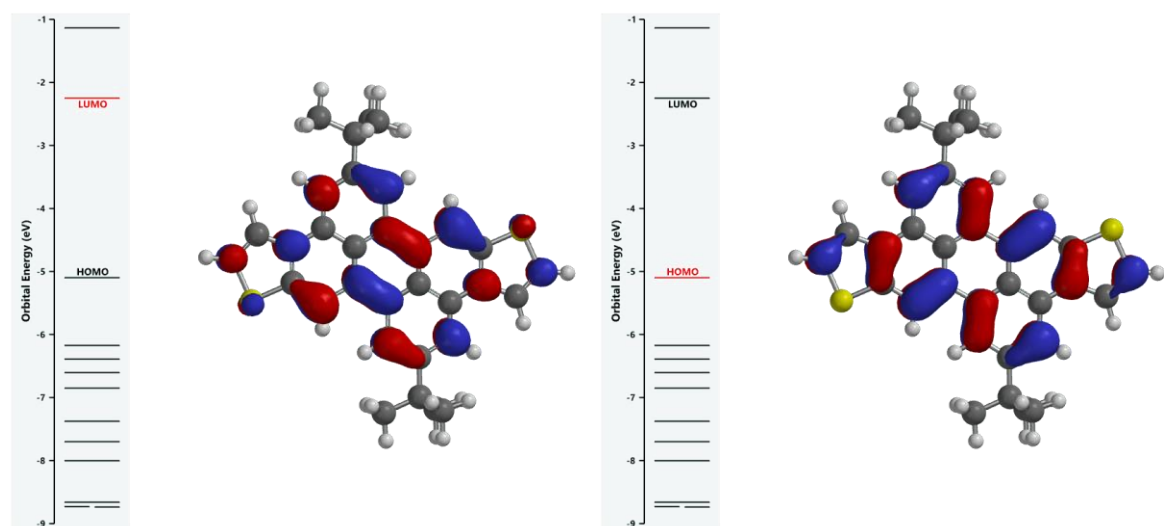


Figure S86. Calculated LUMO (left) and HOMO (right) energy levels of **6d**.

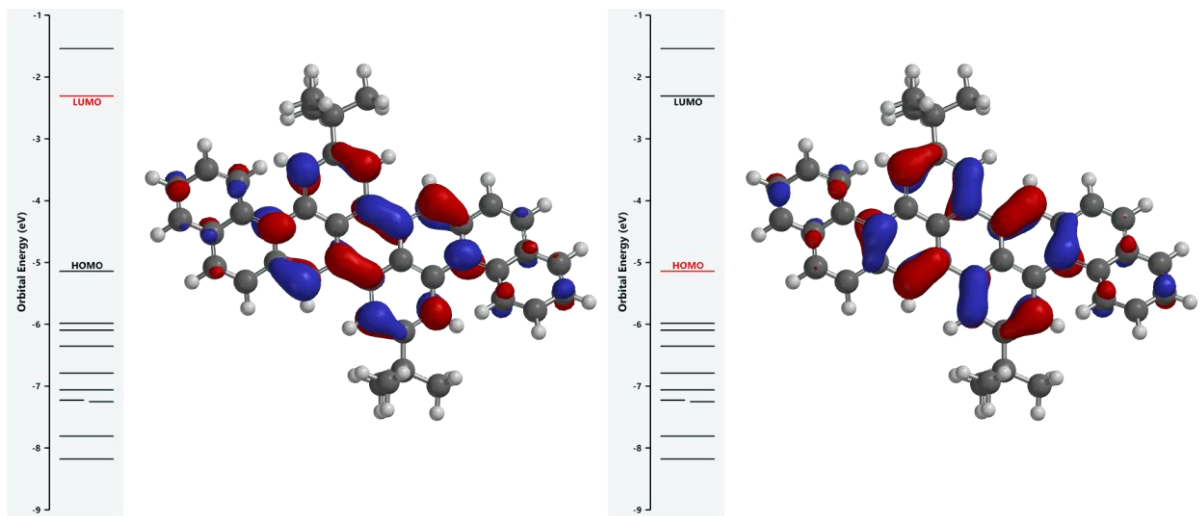


Figure S87. Calculated LUMO (left) and HOMO (right) energy levels of **6e**.

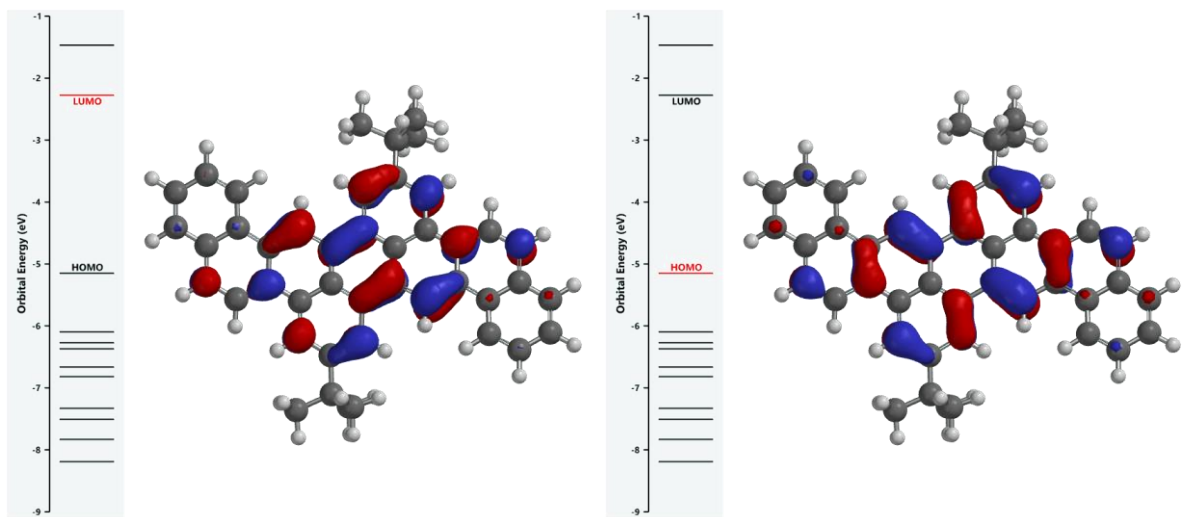


Figure S88. Calculated LUMO (left) and HOMO (right) energy levels of **6f**.

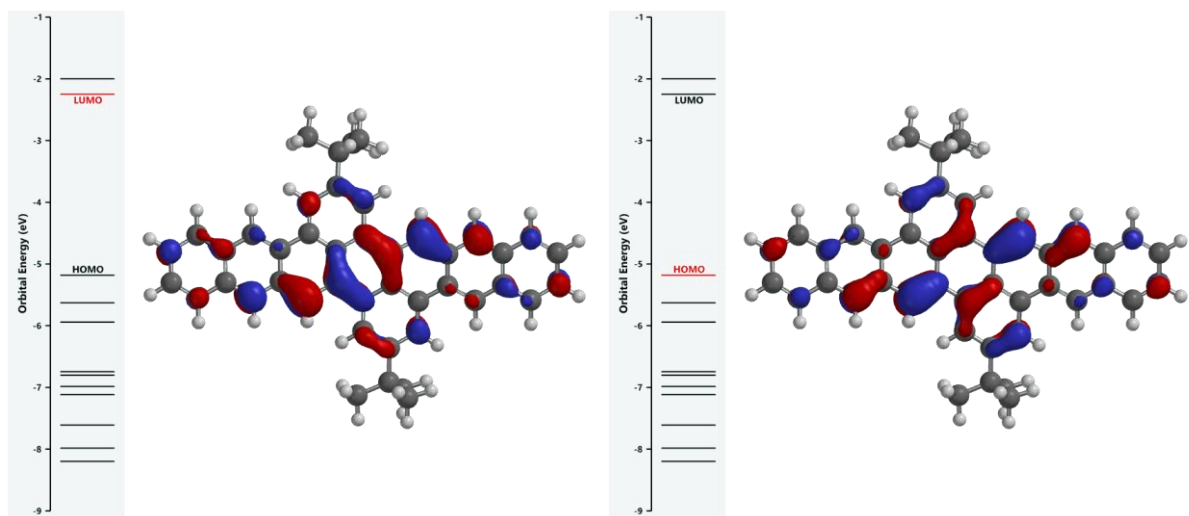


Figure S89. Calculated LUMO (left) and HOMO (right) energy levels of **6g**.

7. Cyclovoltammograms

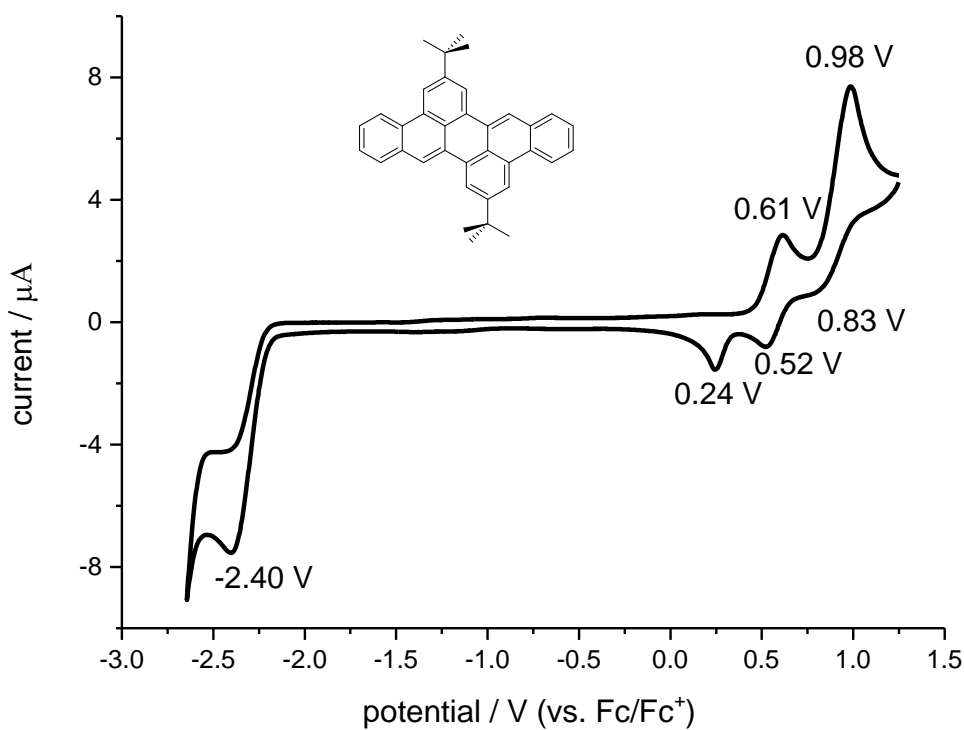


Figure S90. Cyclic voltammogram of compound **6a** measured in 0.1 M Bu_4NClO_4 in DCM at room temperature. The scan speed was 100 mV/s, and ferrocene/ferrocenium (Fc/Fc⁺) was used as internal reference.

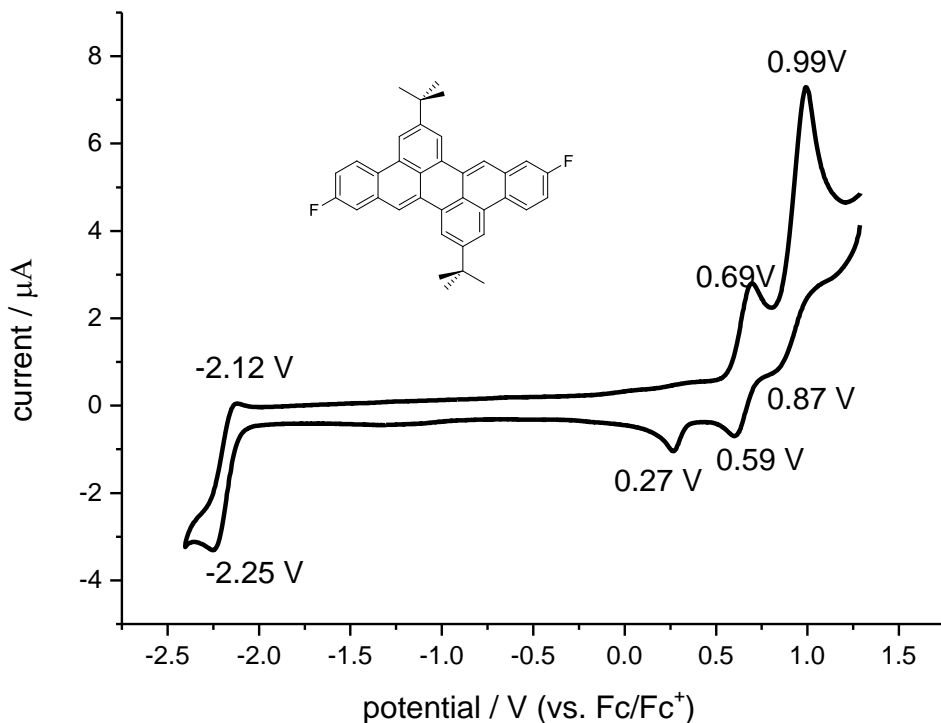


Figure S91. Cyclic voltammogram of compound **6b** measured in 0.1 M Bu_4NClO_4 in DCM at room temperature. The scan speed was 100 mV/s, and ferrocene/ferrocenium (Fc/Fc⁺) was used as internal reference.

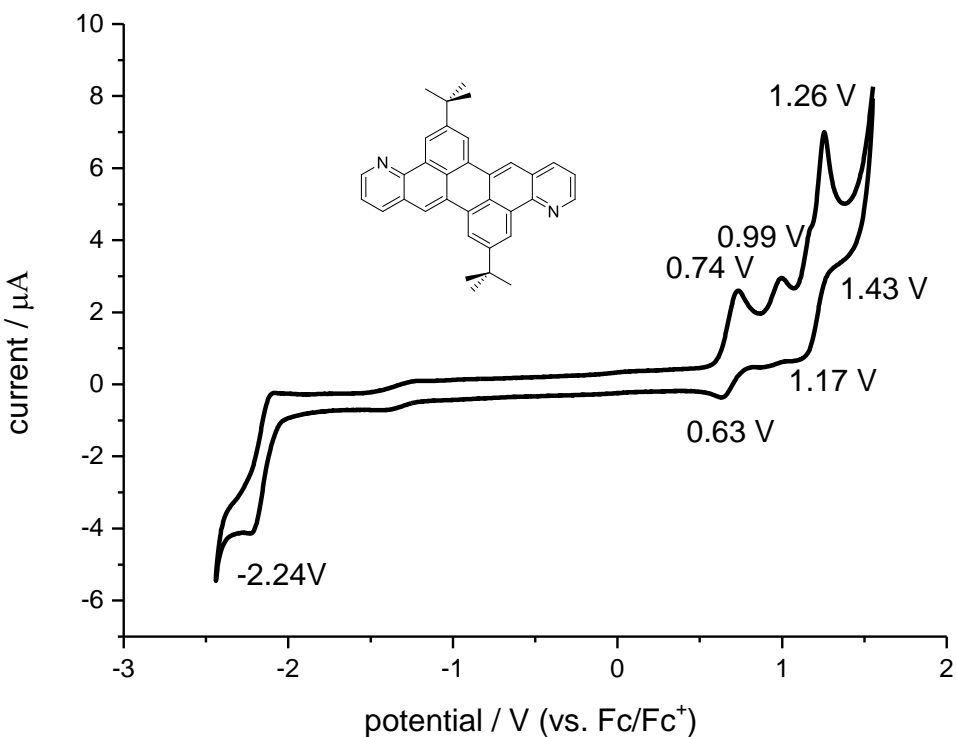


Figure S92. Cyclic voltammogram of compound **6c** measured in 0.1 M Bu₄NClO₄ in DCM at room temperature. The scan speed was 100 mV/s, and ferrocene/ferrocenium (Fc/Fc⁺) was used as internal reference.

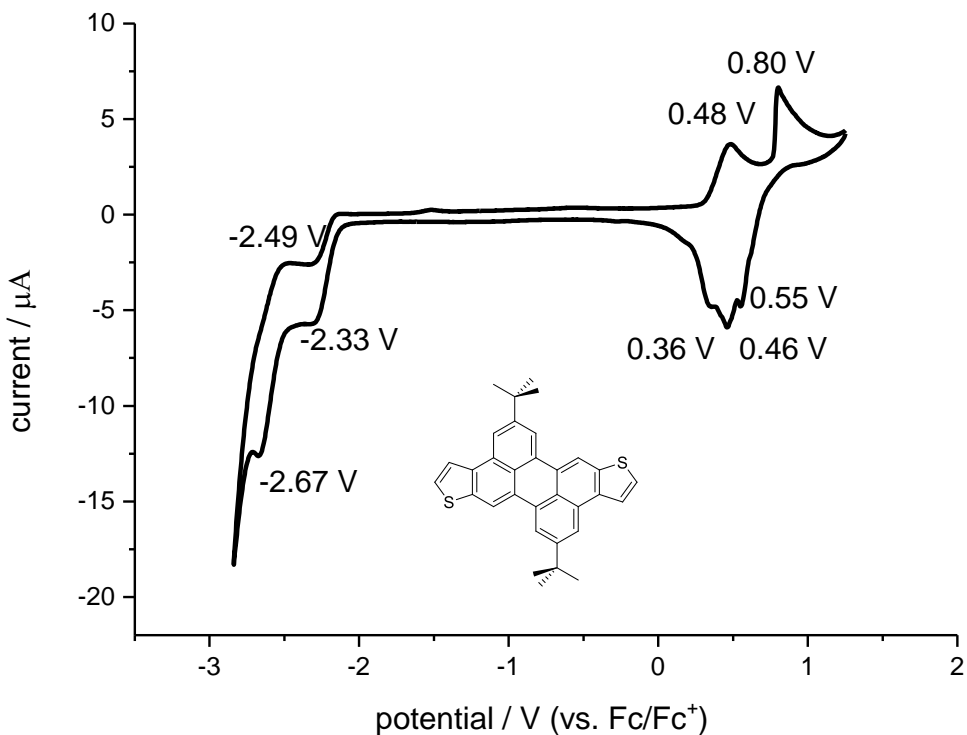


Figure S93. Cyclic voltammogram of compound **6d** measured in 0.1 M Bu₄NClO₄ in DCM at room temperature. The scan speed was 100 mV/s, and ferrocene/ferrocenium (Fc/Fc⁺) was used as internal reference.

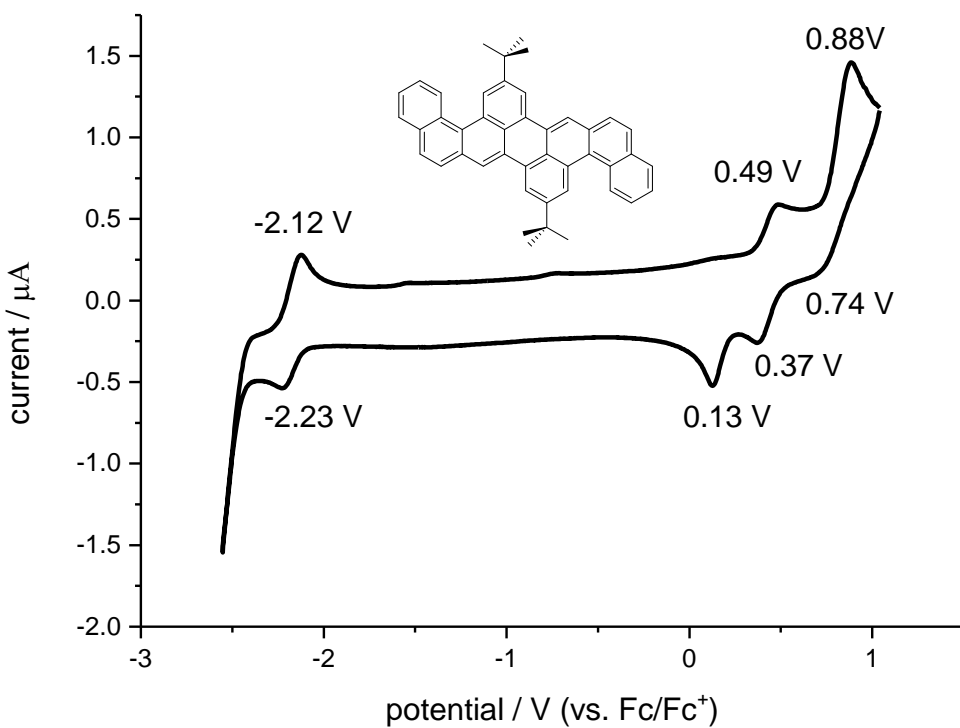


Figure S94. Cyclic voltammogram of compound **6e** measured in 0.1 M Bu₄NClO₄ in *o*DCB at room temperature. The scan speed was 100 mV/s, and ferrocene/ferrocenium (Fc/Fc⁺) was used as internal reference.

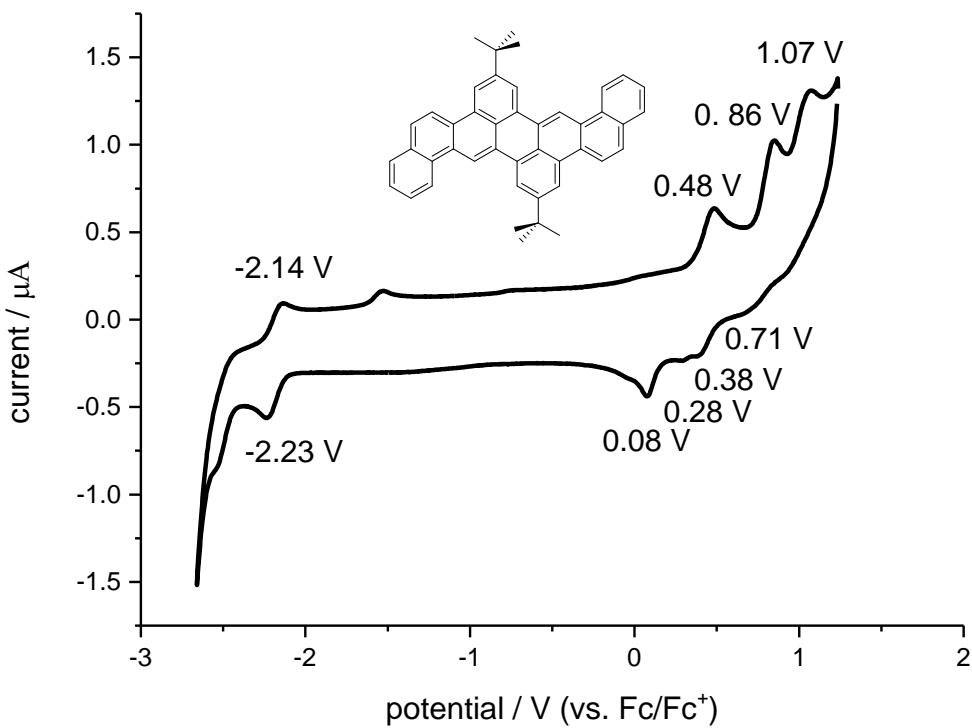


Figure S95. Cyclic voltammogram of compound **6f** measured in 0.1 M Bu₄NClO₄ in *o*DCB at room temperature. The scan speed was 100 mV/s, and ferrocene/ferrocenium (Fc/Fc⁺) was used as internal reference.

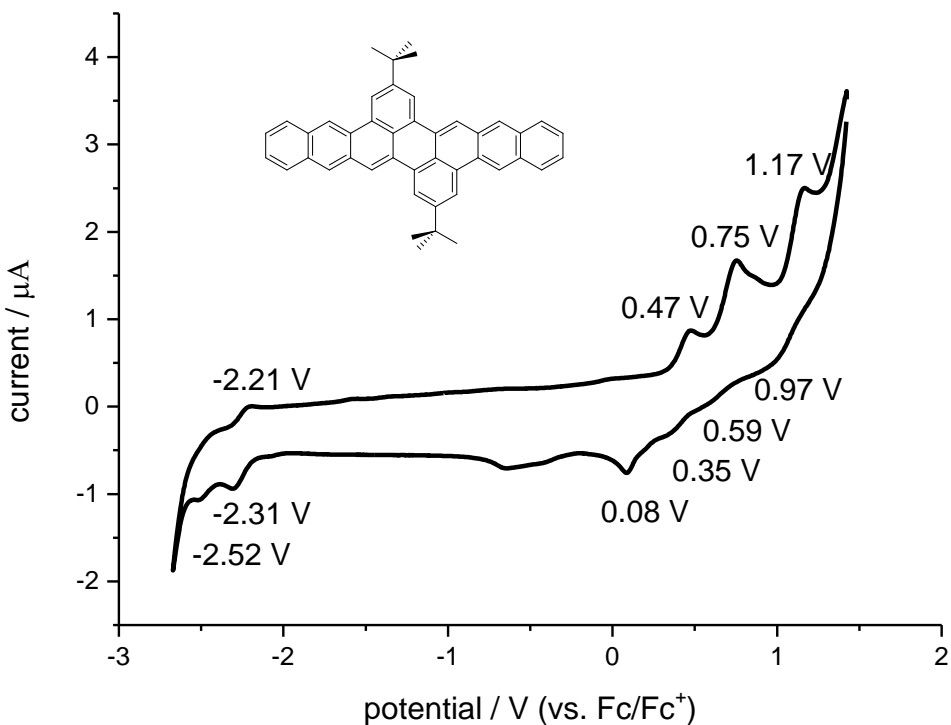


Figure S96. Cyclic voltammogram of compound **6g** measured in 0.1 M Bu₄NClO₄ in *o*DCB at room temperature. The scan speed was 100 mV/s, and ferrocene/ferrocenium (Fc/Fc⁺) was used as internal reference.

8. Fabrication and characterization of organic thin-film transistors

Organic thin-film transistors (TFTs) were fabricated on heavily doped silicon that serves both as the substrate and as the gate electrode of the TFTs. The gate dielectric is a combination of a 100-nm-thick layer of thermally grown silicon dioxide (SiO_2), an 8-nm-thick layer of Al_2O_3 (deposited by atomic layer deposition, ALD), and a self-assembled monolayer of either 12,12,13,13,14,14,15,15,16,16,17,17,18,18,18-pentadecylfluorooctadecylphosphonic acid (F-SAM; kindly provided by Matthias Schlörholz) or *n*-tetradecylphosphonic acid (H-SAM; Alfa Aesar). A 30-nm-thick layer of the organic semiconductor was deposited by thermal sublimation in vacuum (10^{-6} mbar). During the deposition of the organic semiconductor, the substrate was held at an elevated temperature to promote molecular ordering. Finally, gold source and drain contacts were deposited by thermal evaporation in vacuum through a shadow mask. All TFTs have a channel length of 100 nm and a channel width of 200 μm . The current-voltage characteristics were measured in ambient air at room temperature.

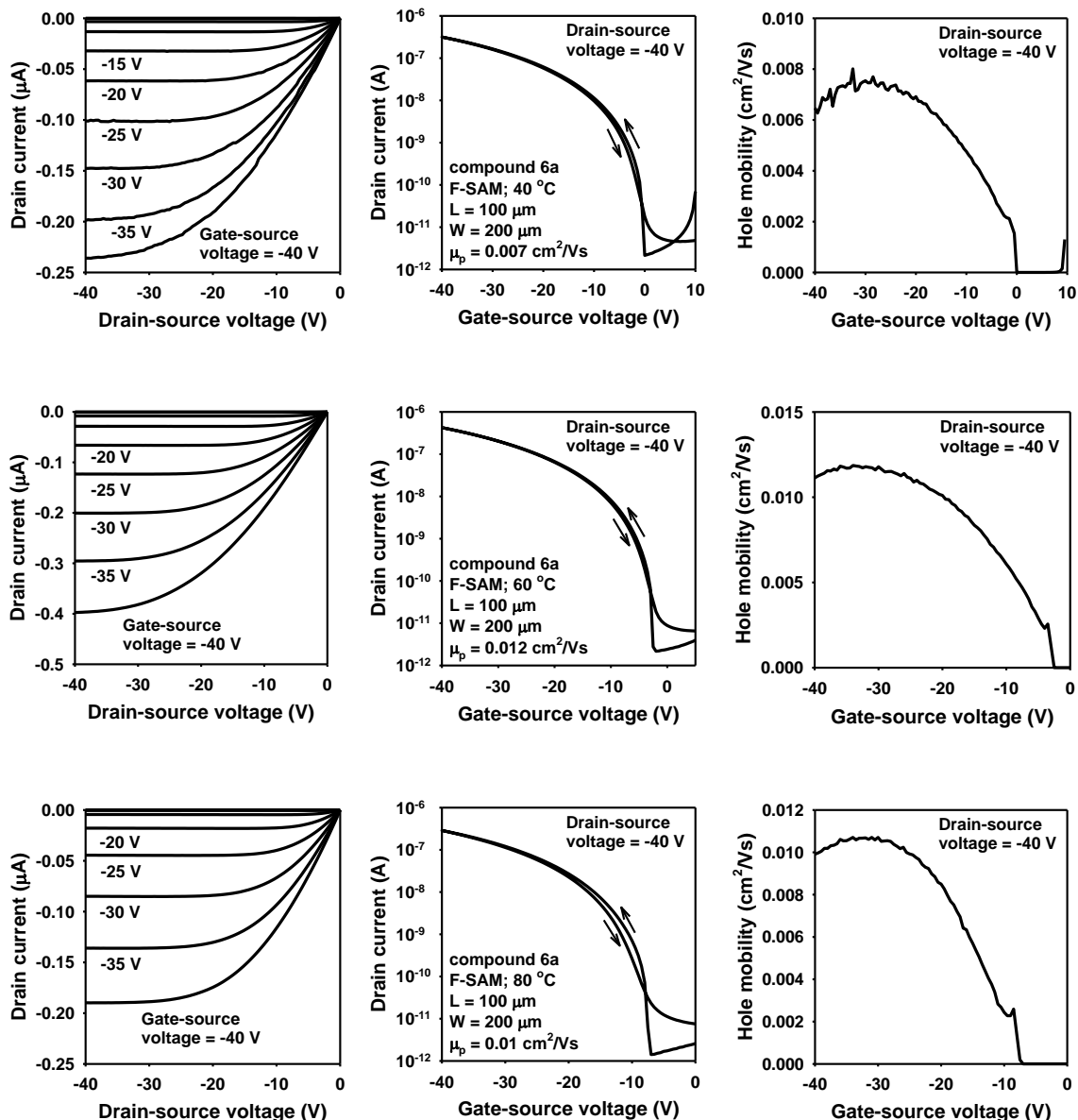


Figure S97. Current-voltage characteristics of TFTs based on compound **6a**. The $\text{SiO}_2/\text{Al}_2\text{O}_3$ gate dielectric was functionalized with a fluoroalkylphosphonic acid SAM. During the deposition of the organic semiconductor layer, the substrate was held at a temperature of 40, 60 or 80 °C.

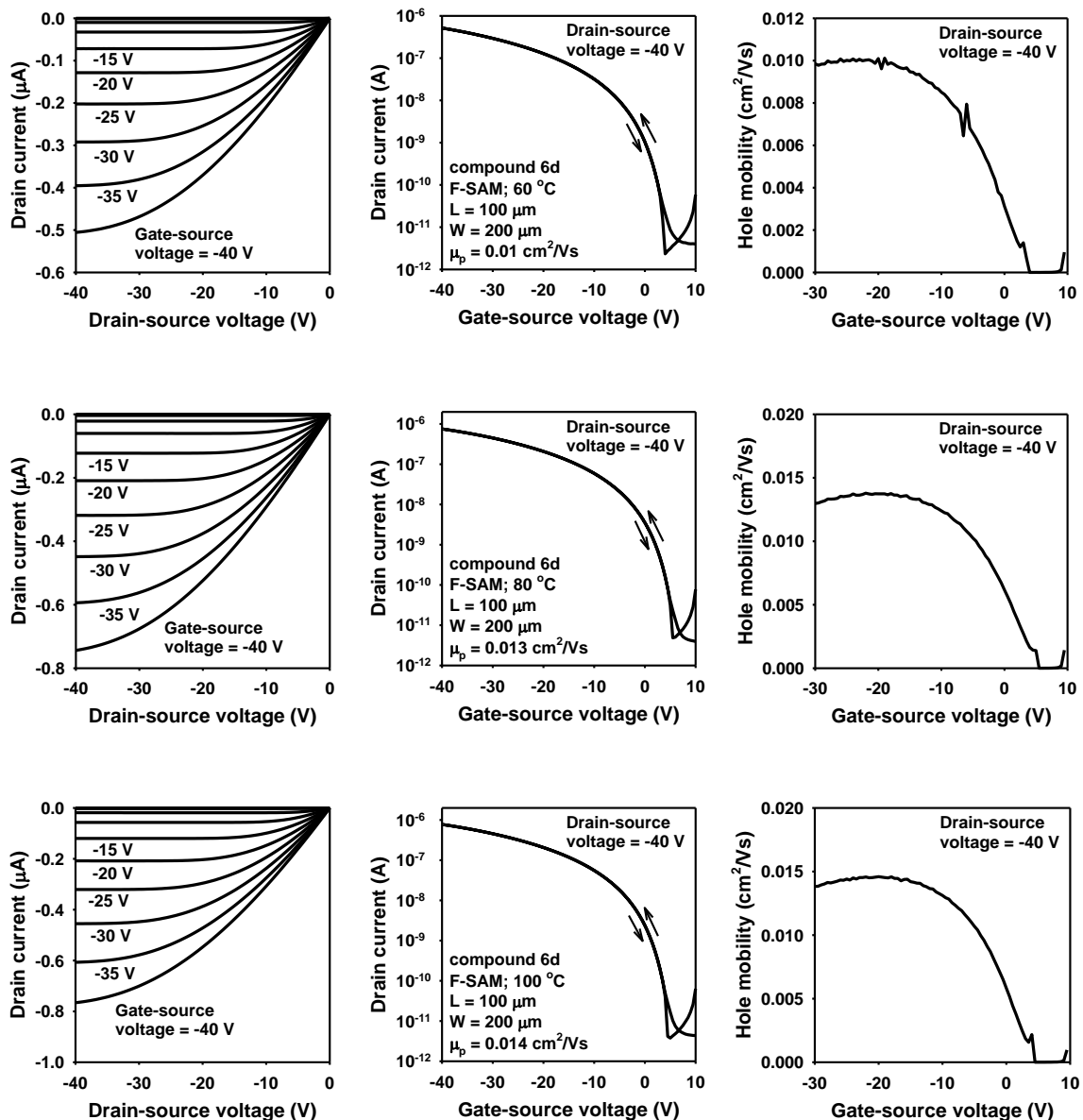


Figure S98. Current-voltage characteristics of TFTs based on compound **6d**. The $\text{SiO}_2/\text{Al}_2\text{O}_3$ gate dielectric was functionalized with a fluoroalkylphosphonic acid SAM. During the deposition of the organic semiconductor layer, the substrate was held at a temperature of 60, 80 or 100 °C.

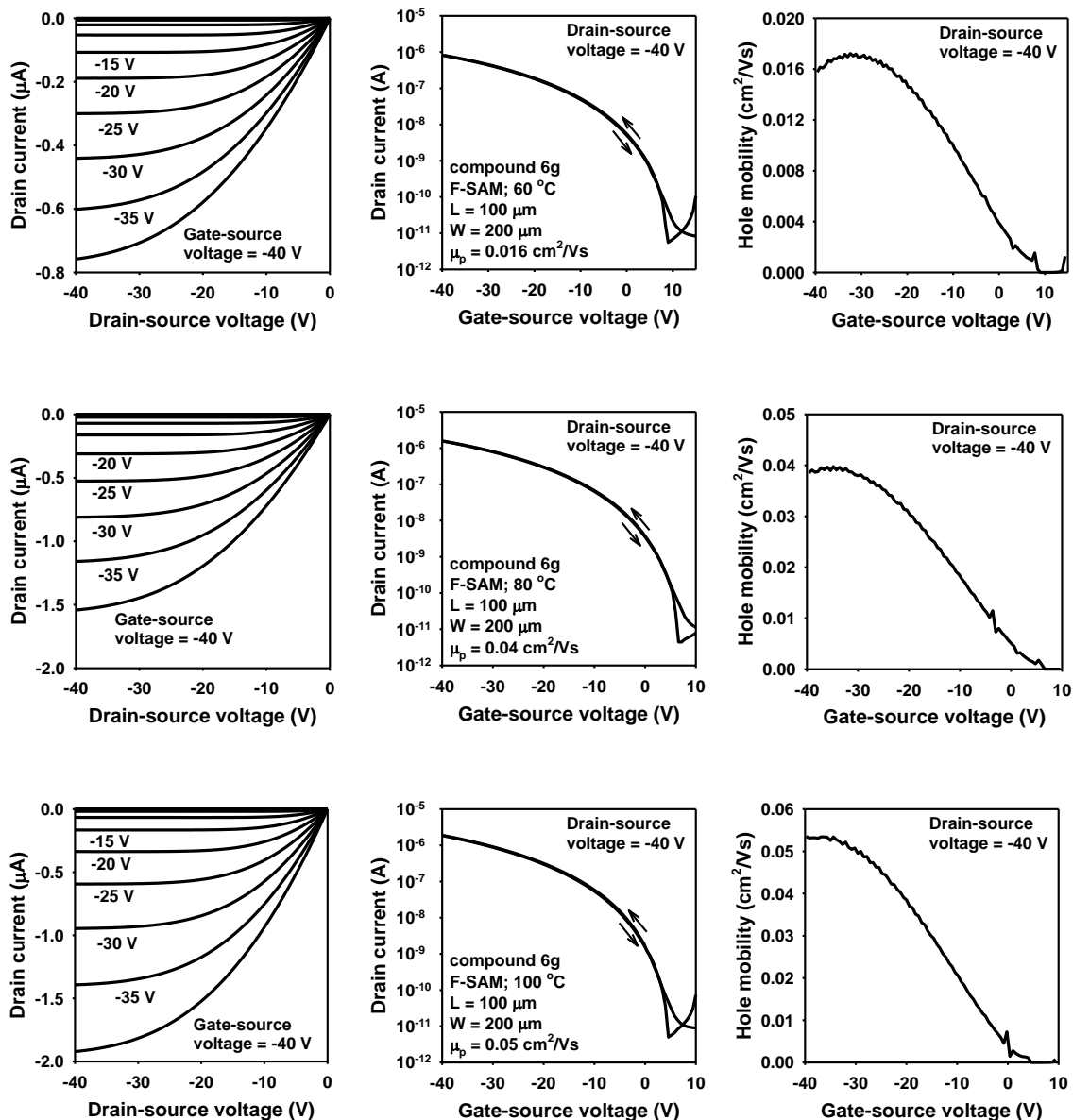


Figure S99. Current-voltage characteristics of TFTs based on compound **6g**. The $\text{SiO}_2/\text{Al}_2\text{O}_3$ gate dielectric was functionalized with a fluoroalkylphosphonic acid SAM.. During the deposition of the organic semiconductor layer, the substrate was held at a temperature of 60, 80 or 100 °C.

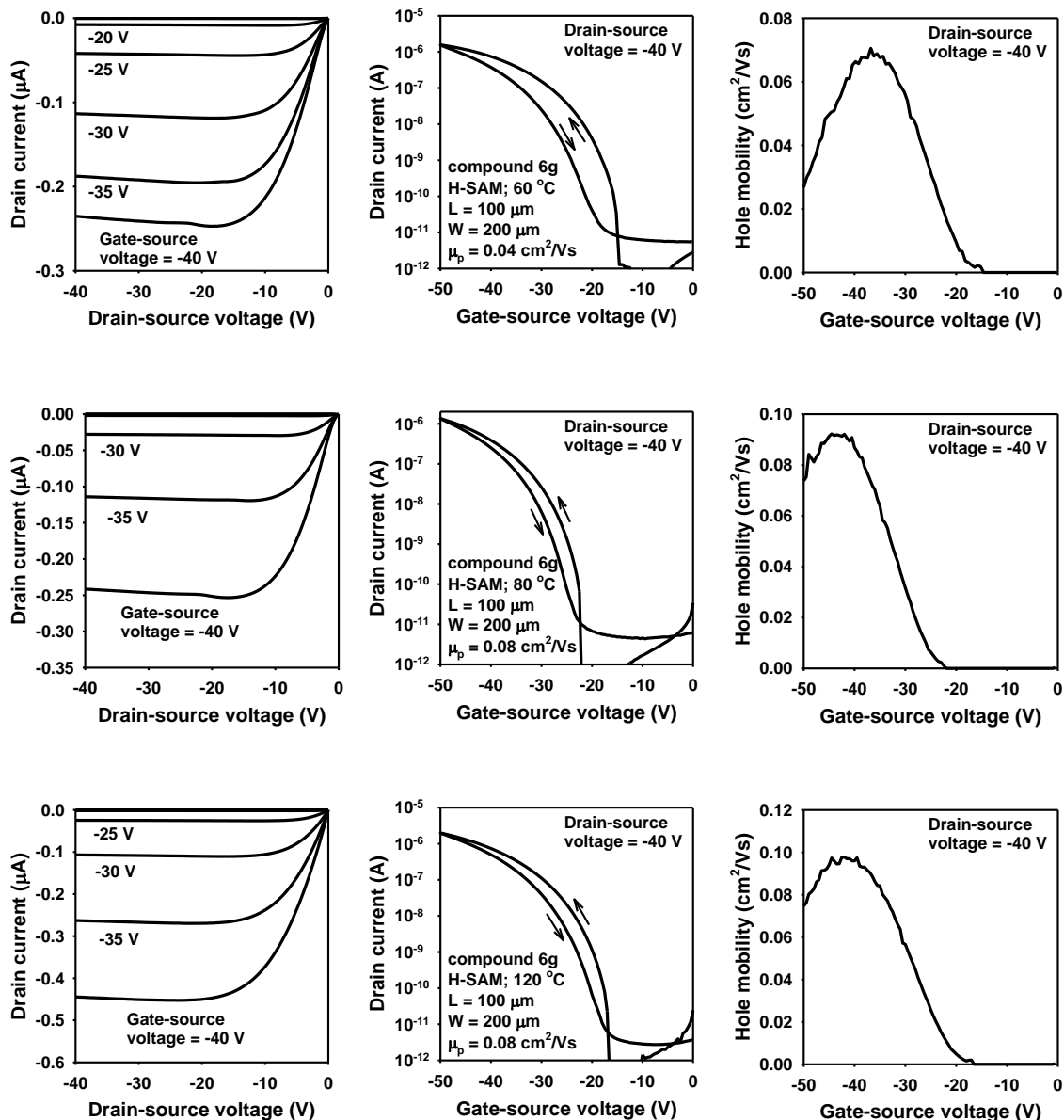


Figure S100. Current-voltage characteristics of TFTs based on compound **6g**. The $\text{SiO}_2/\text{Al}_2\text{O}_3$ gate dielectric was functionalized with an alkylphosphonic acid SAM. During the deposition of the organic semiconductor layer, the substrate was held at a temperature of 60 , 80 or 120 $^\circ\text{C}$.

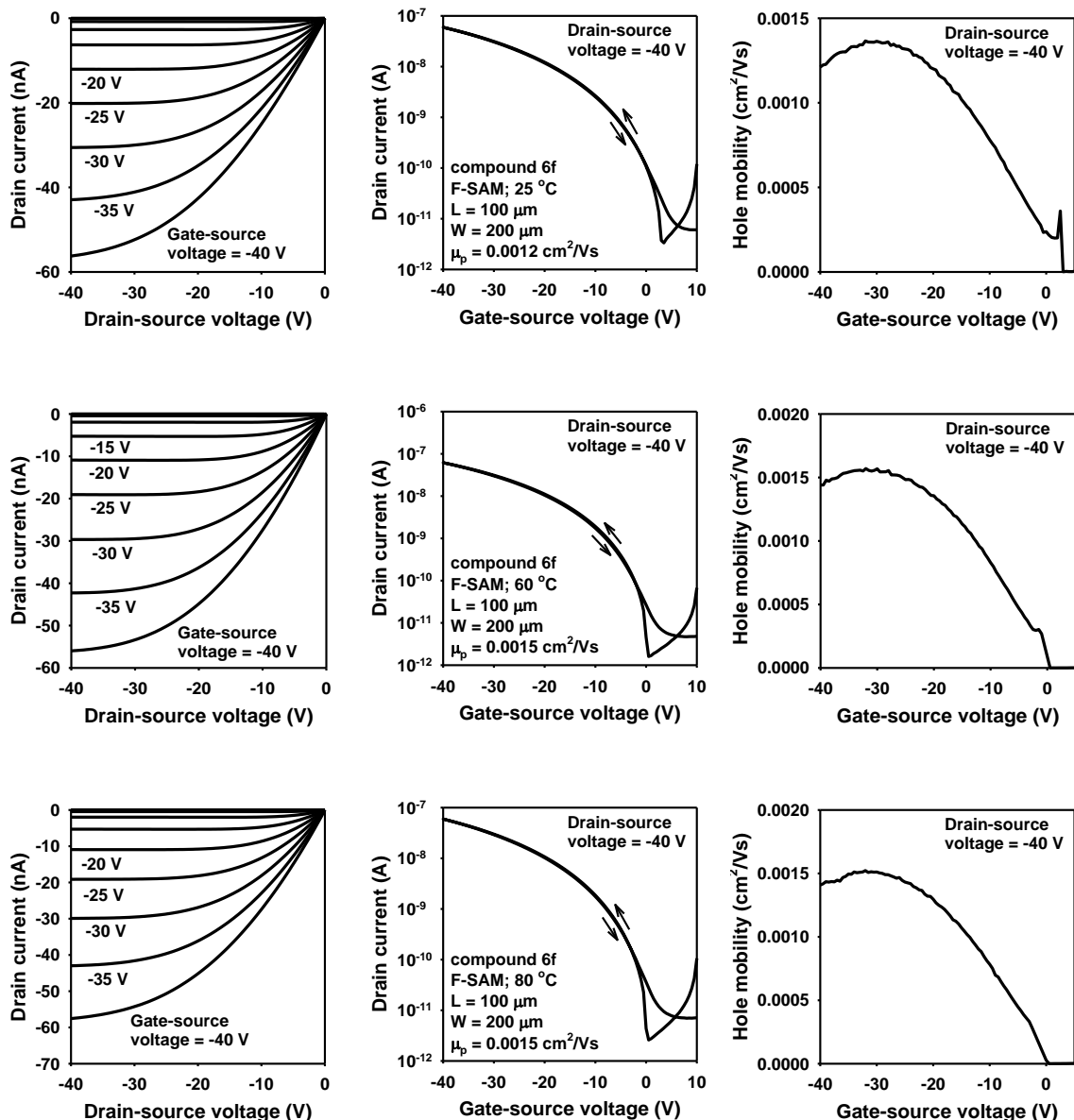


Figure S101. Current-voltage characteristics of TFTs based on compound **6f**. The $\text{SiO}_2/\text{Al}_2\text{O}_3$ gate dielectric was functionalized with a fluoroalkylphosphonic acid SAM. During the deposition of the organic semiconductor layer, the substrate was held at a temperature of 25, 60 or 80 °C.

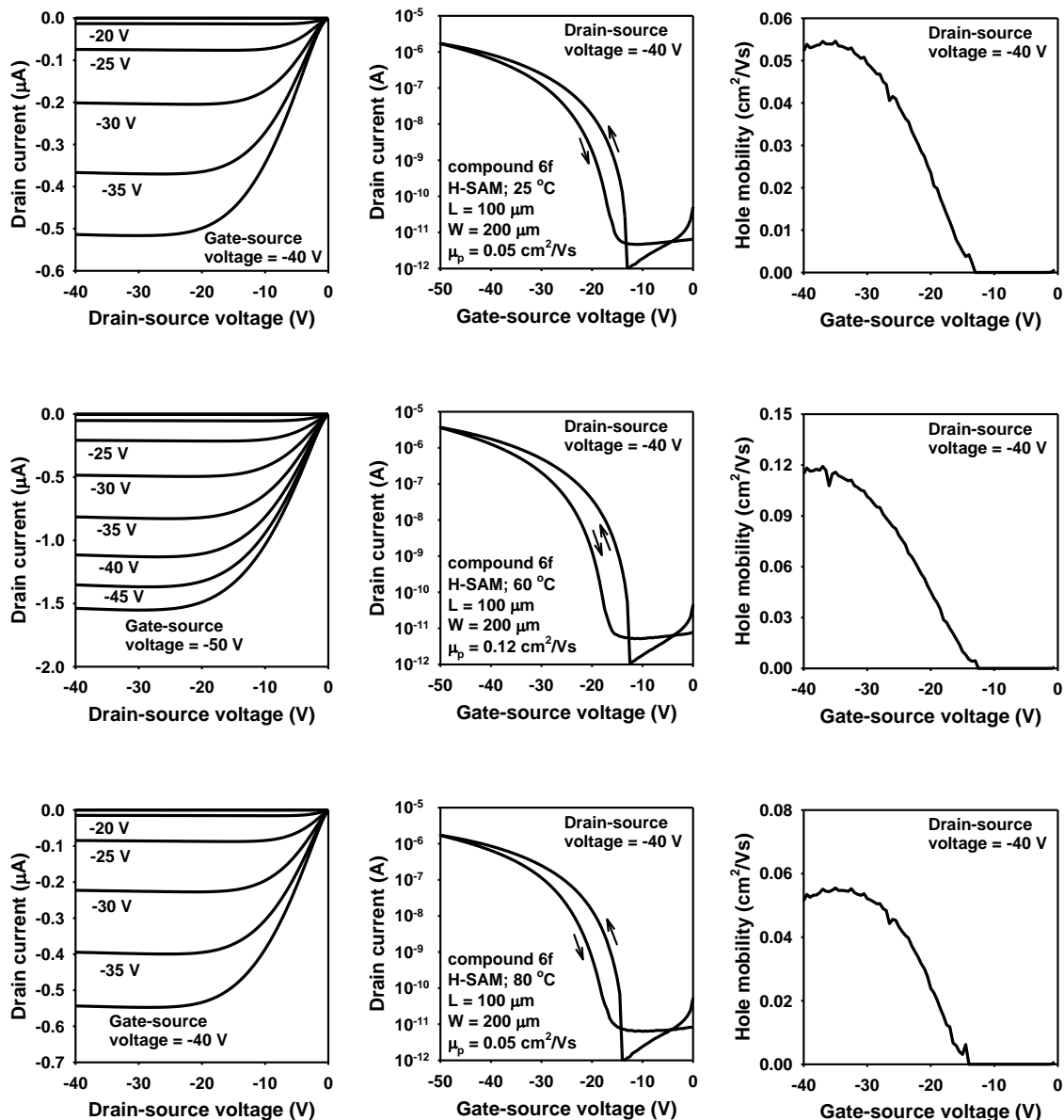


Figure S102. Current-voltage characteristics of TFTs based on compound **6f**. The $\text{SiO}_2/\text{Al}_2\text{O}_3$ gate dielectric was functionalized with an alkylphosphonic acid SAM. During the deposition of the organic semiconductor layer, the substrate was held at a temperature of 25, 60 or 80 °C.

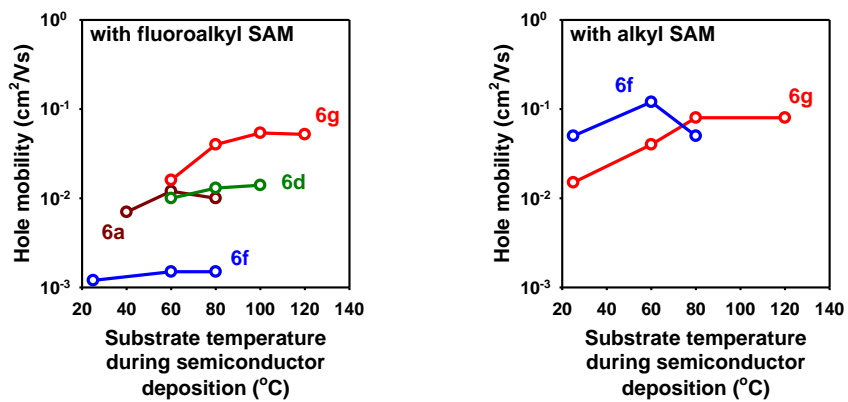


Figure S103. Influence of the substrate temperature during the deposition of the organic semiconductor layer on the field-effect mobility of the thin-film transistors. The $\text{SiO}_2/\text{Al}_2\text{O}_3$ gate dielectric was functionalized either with a self-assembled monolayer of pentadecylfluorooctadecylphosphonic acid (fluoroalkyl SAM) or *n*-tetradecylphosphonic acid (alkyl SAM).

Table S9. Summary of the charge-carrier field-effect mobilities of the thin-film transistors.

compound	SAM	substrate temperature during semiconductor deposition					
		25 °C	40 °C	60 °C	80 °C	100 °C	120 °C
6a	fluoroalkyl SAM		0.007	0.012	0.010		
	alkyl SAM			no useful characteristics			
6c	fluoroalkyl SAM			no field effect			
	alkyl SAM			no field effect			
6d	fluoroalkyl SAM			0.010	0.013	0.014	
	alkyl SAM			no useful characteristics			
6f	fluoroalkyl SAM	0.0012		0.0015	0.0015		
	alkyl SAM	0.05		0.12	0.05		
6g	fluoroalkyl SAM	3×10^{-4}		0.016	0.04	0.05	0.05
	alkyl SAM	0.015		0.04	0.08		0.08

9. References

- [S1] J.-F. Lee, Y.-C. Chen, J.-T. Lin, C.-C. Wu, C.-Y. Chen, C.-A. Dai, C.-Y. Chao, H.-L. Chen, W.-B. Liau, *Tetrahedron* **2011**, *67*, 1696.
- [S2] S. Paul, S. Samanta, J. K. Ray, *Tetrahedron Lett.* **2010**, *51*, 5604-5608.
- [S3] T. K. Wood, w. E. Piers, B. A. Keay, M. Parvez, *Chem. Eur. J.* **2010**, *16*, 12199.